Wearable Sensors and Machine Learning based Human Movement Analysis

– Applications in Sports and Medicine –

Zur Erlangung des akademischen Grades eines
DOKTORS DER PHILOSOPHIE (Dr. phil.)

von der KIT-Fakultät für Geistes- und Sozialwissenschaften des
Karlsruher Instituts für Technologie (KIT)
angenommene

DISSERTATION

von
Bernd Josef Stetter

Dekan: Prof. Dr. Michael Schefczyk

1. Gutachter: Prof. Dr. Stefan Sell

2. Gutachter: Prof. Dr. Thorsten Stein

Tag der mündlichen Prüfung: 26. Februar 2021

Acknowledgements

This work would not have been possible without the combined support of many people. First, I would like to thank my supervisors, Prof. Dr. Stefan Sell and Prof. Dr. Thorsten Stein, for their continuous support and dedication, and for all the inspiring new ideas and discussions. This guidance helped me to grow tremendously as a researcher.

Further, a special thank goes to Dr. Frieder C. Krafft, Dr. Steffen Ringhof, Dr. Gunther Kurz, Marian Hoffmann, Felix Möhler and all team members of the working division Sports Orthopedics and the BioMotion Center. I really enjoy working with you and the open exchange of ideas.

I would also like to thank Dr. Benno M. Nigg, Dr. Vincent von Tscharner, Sandro Nigg and the Biomechanigg group in Calgary for a great collaboration on ice hockey research. During this time I learned many skills helping me using modern data science methods in biomechanics.

I am very grateful to my brother Christian for proofreading this thesis.

Finally, a big thank you goes to Verena for her permanent support and encouragement as well as my family for supporting me during this doctoral project and all the years before.

Summary

In recent years, human movement analysis in real-life settings outside the laboratory has experienced increasing attention in sports and medical applications. At the same time, wearable sensors have been evolved as valuable tools. This has allowed to acquire large-scale human movement data that are typically complex, heterogeneous, and noisy. In this context, modeling approaches are required, as the measured quantities often do not directly reflect meaningful biomechanical variables. More recently, machine learning methods have emerged as promising modeling tools that exploit unstructured data for estimating relevant target variables, such as joint kinematics and dynamics.

Although research in this field is still in its initial phase, there is a great potential not only to enlarge the range of numerous applications in sports but also to obtain biomechanical measures used to infer the load on body structures, such as joint forces. This applies in particular to unique sports such as ice hockey skating. Furthermore, little research has been conducted with respect to the direct estimation of biomechanical surrogate measures for knee joint load (i.e., joint dynamics) using wearable technology. This is of paramount importance, as ambulatory joint load assessment can improve health diagnostics and rehabilitation of injuries as well as musculoskeletal diseases.

The overall aim of this thesis is to assess how, and to what extent, wearable sensors and machine learning techniques can biomechanically quantify sports performance and the load on body structures during the execution of everyday and sport movements.

This thesis is based on four studies that are published in international peer-reviewed journals. The first two studies focus on the automated event detection and mobile performance analysis during ice hockey skating. The other two studies present the outcome of an artificial neural network (ANN) approach to estimate knee joint forces during sport movements and for the ambulatory assessment of joint loading in knee osteoarthritis using wearable sensors.

Study I provides a precise, efficient, and simple way to perform temporal analy-

ses in ice hockey skating by means of a skate-mounted accelerometer. Validation of this novel approach is performed based on plantar pressure data. Accuracies of both data acquisition methods vary in less than one millisecond for contact and stride time.

Study II highlights the potential of accelerometers for assessing skating technique elements as well as elements characterizing the propulsive power of skating strides. Discriminating effects across skill levels and sprint phases are shown for contact time and stride propulsion. The highest strength of association with the sprint performance is shown for stride propulsion.

In study III, an ANN is trained to estimate three-dimensional knee joint forces based on two wearable sensors integrated in a knee sleeve. The examination is performed across a variety of movements, including linear motions, changes of direction, and jumps. The ANN-estimated knee joint forces show good agreement with inverse dynamics-calculated reference data for most of the investigated movements, except for the medio-lateral force component.

Finally, in study IV, the developed approach for an ambulatory assessment of joint loading in knee osteoarthritis displays a strong agreement between the ANN-estimated knee flexion moments and reference data for the majority of analyzed locomotion tasks. The ANN-estimated knee adduction moment shows a lower conformity in comparison to the knee flexion moment, ranging from weak in cutting and fast running to strong for walking straight. As a consequence, cautious interpretation is required with respect to the ANN-based estimation of the knee joint loading by way of the ambulatory minimal body-worn sensor setup.

The findings of study I and study II help to overcome limitations in the assessment of ice hockey skating and open new possibilities for in-field performance diagnosis. Thus, the training quality and player development can substantially benefit from wearable performance sensors. Since estimating meaningful biomechanical quantities from wearable sensor data is not a trivial task, the methodological steps and findings of study III and study IV pave the way for the development of novel health technologies. Looking ahead, wearable sensors could serve as a smart monitoring device for human movement analysis in real-world settings.

Ultimately, wearable human movement analysis can facilitate sports performance diagnosis, improve health diagnostics and rehabilitation of injuries as well as musculoskeletal diseases.

Zusammenfassung

Die Analyse menschlicher Bewegung außerhalb des Labors unter realen Bedingungen ist in den letzten Jahren sowohl in sportlichen als auch in medizinischen Anwendungen zunehmend bedeutender geworden. Mobile Sensoren, welche am Körper getragen werden, haben sich in diesem Zusammenhang als wertvolle Messinstrumente etabliert. Auf Grund des Umfangs, der Komplexität, der Heterogenität und der Störanfälligkeit der Daten werden vielseitige Analysemethoden eingesetzt, um die Daten zu verarbeiten und auszuwerten. Zudem sind häufig Modellierungsansätze notwendig, da die gemessenen Größen nicht auf direktem Weg aussagekräftige biomechanische Variablen liefern. Seit wenigen Jahren haben sich hierfür Methoden des maschinellen Lernens als vielversprechende Instrumente zur Ermittlung von Zielvariablen, wie beispielsweise der Gelenkwinkel, herausgestellt.

Aktuell befindet sich die Forschung an der Schnittstelle aus Biomechanik, mobiler Sensoren und maschinellem Lernen noch am Anfang. Der Bereich birgt grundsätzlich ein erhebliches Potenzial, um einerseits das Spektrum an mobilen Anwendungen im Sport, insbesondere in Sportarten mit komplexen Bewegungsanforderungen, wie beispielsweise dem Eishockey, zu erweitern. Andererseits können Methoden des maschinellen Lernens zur Abschätzung von Belastungen auf Körperstrukturen mittels mobiler Sensordaten genutzt werden. Vor allem die Anwendung mobiler Sensoren in Kombination mit Prädiktionsmodellen zur Ermittlung der Kniegelenkbelastung, wie beispielsweise der Gelenkmomente, wurde bisher nur unzureichend erforscht. Gleichwohl kommt der mobilen Erfassung von Gelenkbelastungen in der Diagnostik und Rehabilitation von Verletzungen sowie Muskel-Skelett-Erkrankungen eine zentrale Bedeutung zu.

Das übergeordnete Ziel dieser Dissertation ist es, festzustellen inwieweit tragbare Sensoren und Verfahren des maschinellen Lernens zur Quantifizierung sportlicher Bewegungsmerkmale sowie zur Ermittlung der Belastung von Körperstrukturen bei der Ausführung von Alltags- und Sportbewegungen eingesetzt werden können.

Die Dissertation basiert auf vier Studien, welche in internationalen Fachzeitschriften mit Peer-Review-Prozess erschienen sind. Die ersten beiden Studien konzentrieren sich zum einen auf die automatisierte Erkennung von zeitlichen Events und zum anderen auf die mobile Leistungsanalyse während des Schlittschuhlaufens im Eishockey. Die beiden weiteren Studien präsentieren jeweils einen neuartigen Ansatz zur Schätzung von Belastungen im Kniegelenk mittels künstlich neuronalen Netzen. Zwei mobile Sensoren, welche in eine Kniebandage integriert sind, dienen hierbei als Datenbasis zur Ermittlung von Kniegelenkskräften während unterschiedlicher Sportbewegungen sowie von Kniegelenksmomenten während verschiedener Lokomotionsaufgaben.

Studie I zeigt eine präzise, effiziente und einfache Methode zur zeitlichen Analyse des Schlittschuhlaufens im Eishockey mittels einem am Schlittschuh befestigten Beschleunigungssensor. Die Validierung des neuartigen Ansatzes erfolgt anhand synchroner Messungen des plantaren Fußdrucks. Der mittlere Unterschied zwischen den beiden Erfassungsmethoden liegt sowohl für die Standphasendauer als auch der Gangzyklusdauer unter einer Millisekunde.

Studie II zeigt das Potenzial von Beschleunigungssensoren zur Technik- und Leistungsanalyse des Schlittschuhlaufens im Eishockey. Die Ergebnisse zeigen für die Standphasendauer und Schrittintensität sowohl Unterschiede zwischen beschleunigenden Schritten und Schritten bei konstanter Geschwindigkeit als auch zwischen Teilnehmern unterschiedlichen Leistungsniveaus. Eine Korrelationsanalyse offenbart, insbesondere für die Schrittintensität, einen starken Zusammenhang mit der sportlichen Leistung des Schlittschuhlaufens im Sinne einer verkürzten Sprintzeit.

Studie III präsentiert ein tragbares System zur Erfassung von Belastungen im Kniegelenk bei verschiedenen sportlichen Bewegungen auf Basis zweier mobiler Sensoren. Im Speziellen werden unterschiedliche lineare Bewegungen, Richtungswechsel und Sprünge betrachtet. Die mittels künstlich neuronalem Netz ermittelten dreidimensionalen Kniegelenkskräfte zeigen, mit Ausnahme der mediolateralen Kraftkomponente, für die meisten analysierten Bewegungen eine gute Übereinstimmung mit invers-dynamisch berechneten Referenzdaten.

Die abschließende Studie IV stellt eine Erweiterung des in Studie III entwickelten tragbaren Systems zur Ermittlung von Belastungen im Kniegelenk dar. Die ambulante Beurteilung der Gelenkbelastung bei Kniearthrose steht hierbei im Fokus. Die entwickelten Prädiktionsmodelle zeigen für das Knieflexionsmoment

eine gute Übereinstimmung mit invers-dynamisch berechneten Referenzdaten für den Großteil der analysierten Bewegungen. Demgegenüber ist bei der Ermittlung des Knieadduktionsmoments mittels künstlichen neuronalen Netzen Vorsicht geboten. Je nach Bewegung, kommt es zu einer schwachen bis starken Übereinstimmung zwischen der mittels Prädiktionsmodell bestimmten Belastung und dem Referenzwert.

Zusammenfassend tragen die Ergebnisse von Studie I und Studie II zur sportartspezifischen Leistungsanalyse im Eishockey bei. Zukünftig können sowohl die Trainingsqualität als auch die gezielte Verbesserung sportlicher Leistung durch den Einsatz von am Körper getragener Sensoren in hohem Maße profitieren. Die methodischen Neuerungen und Erkenntnisse aus Studie III und Studie IV ebnen den Weg für die Entwicklung neuartiger Technologien im Gesundheitsbereich. Mit Blick in die Zukunft können mobile Sensoren zur intelligenten Analyse menschlicher Bewegungen sinnvoll eingesetzt werden.

Die vorliegende Dissertation zeigt, dass die mobile Bewegungsanalyse zur Erleichterung der sportartspezifischen Leistungsdiagnostik unter Feldbedingungen beiträgt. Zudem zeigt die Arbeit, dass die mobile Bewegungsanalyse einen wichtigen Beitrag zur Verbesserung der Gesundheitsdiagnostik und Rehabilitation nach akuten Verletzungen oder bei chronischen muskuloskelettalen Erkrankungen leistet.

Table of contents

List of figures

List of tables

Abbreviations

ANN Artificial Neural Network
ANOVA Analysis of Variance
BO Blade-Off
CoM Center of Mass
CT Contact Time
GRF Ground Reaction Force
IMU Inertial Measurement Unit
IC Initial Contact
KAM Knee Adduction Moment
KFM Knee Flexion Moment
KJF Knee Joint Force
KOA Knee Osteoarthritis
LoA Limits of Agreement
MIMU Magnetic and Inertial Measurement Unit
MEMS Micro-Electro-Mechanical Systems
nPVI normalized Pairwise Variability Index
OLJ One-Leg horizontal Jump
r Pearson's correlation coefficient
%Diff Percent Differences
rRMSE relative Root-Mean-Squared Error
RMSE Root-Mean-Squared Error
SP Stride Propulsion
ST Stride Time
3D three-dimensional
TST Total Sprint Time

1 Introduction

1.1 Motivation

Movement is an important aspect of human life, which basically enables us to interact with the world. Therefore, the analysis of movement is an interesting and active area in sports and medicine research, as it can help people to perform their everyday activities and sports in an adequate manner. The acquisition of objective biomechanical measures related to human movement by integrating wearable sensors (e.g., accelerometers) in sports equipment (e.g., shoes), orthopedic aids (e.g., knee sleeves), as well as fixed to the body has become increasingly popular during the last decades. Such mobile movement analyses open a broad range of applications in sports and medicine. Adequate use can aid in minimizing the risk of injuries (Verheul et al., 2020; Adesida et al., 2019), in decelerating the progression of diseases like osteoarthritis (Díaz et al., 2020; Richards et al., 2017), and in improving sports performance (Camomilla et al., 2018).

In spite of increasing research efforts, many fields of application, and techniques to extract meaningful information from acquired signals have not yet gained considerable attention. In particular, sports with unique conditions, such as ice hockey, have received little consideration. However, wearable systems could serve as a coaching and monitoring tool to support ice hockey players in their training and to capture athletes' progress (Buckeridge et al., 2015; Adesida et al., 2019). Furthermore, the estimation of biomechanical variables used to infer the load on body structures by means of wearable sensors has not yet been fully established, primarily due to the difficulty in assessing external forces (Camomilla et al., 2018; Shull et al., 2014). In this context, machine learning techniques such as Artificial Neural Networks (ANNs) can help to model the association between captured sensor signals and the biomechanical target measures, for example knee moments (Gurchiek et al., 2019; Halilaj et al., 2018).

To that end, this thesis investigates the feasibility of using wearable sensors and machine learning techniques to obtain meaningful biomechanical information in sport and medical applications. More precisely, temporal, performance, and

internal load related quantities are specifically considered in ice hockey skating as well as during various everyday and sport movements.

1.2 Outline of the thesis

The current thesis consists of six chapters. In this first chapter (chapter 1), theoretical and methodological fundamentals as well as the current state of research in the scientific area are presented. Additionally, the aims and the scope of the present thesis are introduced. Each of the four subsequent chapters (chapter 2, chapter 3, chapter 4 and chapter 5) represent an individual study considering an unresolved research issue in the field. The first two studies focus on applications in sports, while the latter two are more applicable in medicine. Each study has been published in an international peer-reviewed journal:

- Chapter 2: Study I – Automated gait event detection during ice hockey skating

  Stetter, B. J., Buckeridge, E., von Tscharner, V., Nigg, S. R. & Nigg, B. M. (2016). A novel approach to determine strides, ice contact, and swing phases during ice hockey skating using a single accelerometer. *Journal of Applied Biomechanics*, 32(1), 101–106.

- Chapter 3: Study II – Mobile ice hockey skating performance analysis

  Stetter, B. J., Buckeridge, E., Nigg, S. R., Sell, S. & Stein, T. (2019a). Towards a wearable monitoring tool for in-field ice hockey skating performance analysis. *European Journal of Sport Science*, 19(7), 893–901.

- Chapter 4: Study III – Estimation of knee joint forces in sport movements

  Stetter, B. J., Ringhof, S., Krafft, F. C., Sell, S. & Stein, T. (2019b). Estimation of knee joint forces in sport movements using wearable sensors and machine learning. *Sensors*, 10(8), 7772–7788.

- Chapter 5: Study IV – Estimation of joint loading in knee osteoarthritis

  Stetter, B. J., Krafft, F. C., Ringhof, S., Stein, T. & Sell, S. (2020). A machine learning and wearable sensor based approach to estimate external knee flexion and adduction moments during various locomotion tasks. *Frontiers in Bioengineering and Biotechnology*, 8, 9.

Finally, chapter 6 summarizes the main findings and gives an overall discussion of the presented research articles, provides implications and recommendations for future research and ends with a general conclusion.

1.3 Human movement analysis

Human movement analysis aims at gathering quantitative information about the mechanics during the execution of a motor task (Cappozzo et al., 2005) and has a long history, dating back to when the ancient Greeks (500-300 BC) depicted human movement (Andriacchi & Alexander, 2000; Nigg & Herzog, 2007). During this period, scientists developed basic abilities (i.a. mathematics, mechanics and medicine) to better describe movement and to develop underlying theories (Nigg & Herzog, 2007). Later on, during the scientific revolution, Newton's laws were established, which provided the impetus for the study of human movement and the tools to understand it (Nigg & Herzog, 2007). Experimentation became more and more an accepted approach to study human movement, and pioneers such as Jules Marey and Edweard Muybridge developed measuring methods to quantify kinematics and dynamics of movement. In the 1880s, Jules Marey and Edweard Muybridge became the first to use a sequential photograph method for quantifying patterns of animal locomotion and human movement (Andriacchi & Alexander, 2000; Nigg & Herzog, 2007). Photographs were soon replaced by motion film, and ever since, video analysis has prevailed to analyze human movement. Based on improvements in computing, three-dimensional (3D) studies have become increasingly common in biomechanics, and the whole process has become much quicker and more convenient (Whittle, 1996; Andriacchi & Alexander, 2000; Cappozzo et al., 2005). Therefore, multi-camera motion capture systems have become standard tools to study movement kinematics. In addition, external forces are measured using dynamometers, such as force plates, whereas electrical activity of muscles is recorded through electromyography (Nigg & Herzog, 2007; Cappozzo et al., 2005). Nowadays, biomechanical and musculoskeletal modeling are playing an important role in generating information that cannot be directly observed (e.g., load on internal body structures) (Andriacchi & Alexander, 2000; Umberger & Caldwell, 2014). What is more, most movement analyses involve the use of inverse dynamics to obtain joint moments and powers by using the motion of body segments (from a kinematic system), and ground reaction force (from a force plate) as input data (Whittlesey & Robertson, 2014; Whittle, 1996). Individuals are modeled as a linked-segment model based on anthropometric measures and captured data.

Through human movement analysis, temporal events and phases can be ad-

equately identified, kinematic and dynamic quantities as well as myoelectric changes associated with movement can be determined (Medved, 2001; Nigg & Herzog, 2007). As a result, such analyses have contributed to the advancement of fundamental knowledge, and have been conducted in various applied fields ranging from military applications to health care (Andriacchi & Alexander, 2000). Human movement analysis has been employed in sports, as well as in rehabilitation and treatment of injuries and diseases of the musculoskeletal system (Tao et al., 2012). For example, in sports, the biomechanical data gained, yield important insights into human movements and techniques, and consequently deliver useful information to improve training and to achieve performance enhancement (Bartlett, 2007; Buckeridge et al., 2015). In rehabilitation and treatment of injuries and diseases, human movement analysis is used to reveal deficits in patients, to monitor the healing progress (Krafft et al., 2017), or to evaluate the functionality of orthopedic devices (e.g., knee brace) (Maleki et al., 2016; Shaw et al., 2018), respectively. Additionally, human movement analysis can particularly improve medical diagnostics and provide treatment support. Studies highlighted that the management of patients and orthopedic decision making can benefit from movement analysis; i.e. in neuromuscular disorders such as cerebral palsy (Molenaers et al., 2006; Lofterod et al., 2007), or chronic disease such as knee osteoarthritis (Bennell et al., 2011; Reeves & Bowling, 2011; Ferreira et al., 2015).

However, standard human movement analysis based on a multi-camera motion capture system and force plates requires a specialized locomotion laboratory and has limitations in field settings (Ancillao et al., 2018; Tao et al., 2012). As a consequence, the estimation of biomechanical measures using alternative technologies such as wearable sensors have been enjoying great popularity (Godfrey et al., 2008).

1.4 Wearable sensor technology and applications

Advances in sensor technology as well as the low-cost production of Micro-Electro-Mechanical Systems (MEMS) technology have made the manufacture of highly miniaturized accelerometers, gyroscopes and magnetometers possible (Aroganam et al., 2019; Camomilla et al., 2018). Accelerometers, gyroscopes and magnetometers quantify the sum of gravitational and inertial linear accelerations, angular velocities, and magnetic forces in relation to the Earth's magnetic

field – along and about their sensing axes, respectively (Aroganam et al., 2019; Camomilla et al., 2018). Depending on the configuration of the sensor, it records one of the aforementioned physical quantities in one, two or three directions.
Accelerometers and gyroscopes are often combined in an Inertial Measurement Unit (IMU), where the term inertial is used because both sensors exploit the principle of inertia to provide either angular velocities or accelerations (Camomilla et al., 2018). Especially when 3D information is required, accelerometers and gyroscopes are combined with magnetometers to form the measuring unit, which is known by the acronym MIMU (Magnetic and Inertial Measurement Unit) (Camomilla et al., 2018). Applications of IMUs are found in diverse areas such as vehicles, robotics, shock and vibration testing, as well as position and velocity sensing. In human movement analyses using wearable sensors, IMUs are worn or attached to various parts of the body (e.g., waist). This approach was first suggested in the 1970s, but it has increasingly established itself during the last ten to twenty years (Godfrey et al., 2008). One of the benefits of wearable inertial sensors is their small dimension. They do not limit data collection to a laboratory environment, and they are relatively cheap compared to other more commonly used movement analysis equipment such as motion capture systems (Iosa et al., 2016; Kavanagh & Menz, 2008).
The output of a body mounted IMU is composed of a component of interest (e.g., acceleration caused by movement), a static component (e.g., gravity), and a certain amount of noise caused by biological and environmental influences (Kavanagh & Menz, 2008). Using an accelerometer, Godfrey et al. (2008) highlighted four factors that influence its output: first, position at which it is placed; second, its orientation; third, the posture of the subject; and fourth, the activity being performed by the subject. Following Kavanagh & Menz (2008) the measuring procedure from a body attached IMU can be described as follows. Physical quantities are measured in a local coordinate system of the IMU. This coordinate system will continually move during movement of the subject. As a consequence, for example, an accelerometer will indiscriminately detect rotational and translational accelerations to the extent that tangential or linear acceleration vectors of a moving body segment align with the device's sensing axes (Kavanagh & Menz, 2008).
The location at which an IMU is placed on the body is an important consideration. The IMU is normally attached to the part of the body whose movement

is being studied (Godfrey et al., 2008). Examples are the activity trackers that can be worn as bracelets, which have been proven to track and identify the most common daily activities as well as exercise levels (Ancillao et al., 2018; Rowlands et al., 2017). Different biomechanical parameters (temporal, kinematic and dynamic) can be estimated based on the detection of features in the measured signals, or on more sophisticated processing techniques (e.g., Kalman filter), which, for example, enable the combination of information from two or more sensors (Camomilla et al., 2018). In many cases, it is necessary to use multiple IMUs to assess biomechanical variables like joint kinematics (Faisal et al., 2019). The number of body segments to be analyzed usually dictates the number of sensors required (Sivakumar et al., 2016). Orientation of human body segments can be measured by placing IMUs on different segments (Luinge & Veltink, 2005). Consequently, IMU-based joint angle measurements for gait analysis have been proposed and delivered good accuracy (Karatsidis et al., 2017). For example, root mean square errors of the knee flexion/extension angles less than 1° when validating against an optical motion capture system (Seel et al., 2014). The algorithms employed to obtain joint angles typically scale a biomechanical model to the body dimensions of a subject.

As IMUs only enable the direct determination of kinematic data, the estimation of ground reaction forces (Karatsidis et al., 2017; Wouda et al., 2018) and joint dynamics (Konrath et al., 2019; Dorschky et al., 2019) from these data have recently gained importance. Several models and methods have been developed in the last few years as estimating dynamic quantities from kinematic data is not an easy task (Gurchiek et al., 2019; Ancillao et al., 2018). The majority of applied methods require, to a certain degree, the modeling of the musculoskeletal system, with mandatory embedded subject-specific anthropometric data (e.g., mass, dimensions and center of mass of the body segments) (Konrath et al., 2019; Dorschky et al., 2019). An alternative approach is the use of machine learning algorithms (see section 1.5).

Meanwhile, wearable sensors have been widely accepted as useful and practical sensors in the field of human movement analysis for sport performance diagnosis (Adesida et al., 2019; Camomilla et al., 2018), as well as in the field of clinical human movement analysis (Díaz et al., 2020; Faisal et al., 2019; Iosa et al., 2016; Kavanagh & Menz, 2008). These sensors have allowed the assessment of temporal, kinematic, and dynamic parameters of various everyday and

sport movements. Measuring movement outdoors created opportunities in team sports (e.g., rugby and soccer), individual sports (e.g., tennis and boxing), cyclical sports (e.g., running and swimming) as well as winter and other outdoor sports (e.g., cross-country skiing and skateboarding) (Camomilla et al., 2018). The primary focus in the fields of sport has been technique analysis (55.5%), followed by match analysis (20.7%), and capacity assessment (17.3%), with few investigations dealing with activity classification (6.5%) (Camomilla et al., 2018). Additionally, different wearable sensor-based methods have been developed to support and standardize researchers' and clinicians' decisions with respect to movement abnormalities or identifying changes due to orthopedic or physiotherapeutic interventions (Gurchiek et al., 2019; Horst et al., 2019). Gait analysis using wearable sensors has become increasingly established (Tao et al., 2012). In orthopedics and rehabilitation, wearable sensor systems have been developed to monitor the patient healing progress (Horak et al., 2015; Calliess et al., 2014; Patel et al., 2012). Additionally, systems to mobile assess knee joint biomechanics (Konrath et al., 2019), wearable visual feedback system for gait retraining (Karatsidis et al., 2018), as well as physical activity monitors (Verlaan et al., 2015) have been suggested for the assessment, treatment and monitoring of patients with Knee Osteoarthritis (KOA). In health diagnostics, ambulatory monitoring methods for applications to neurological disorders that cause gait and balance problems like Stroke, Alzheimer's disease and Parkinson's disease, have also been developed (Díaz et al., 2020; Buchman et al., 2014).

1.5 Machine learning in human movement analysis

Machine learning describes the study of how computer algorithms (i.e., machines) can learn complex relationships or patterns from empirical data by creating models linking a large number of input data to some target variable of interest (Cabitza et al., 2018; Obermeyer & Emanuel, 2016; Wang & Summers, 2012). Research in machine learning is one of the fastest growing fields in computer science (Alpaydin, 2020). At the same time, a remarkable expansion of learning algorithms into various fields of science, from astronomy to medicine and everyday life, has occurred (Alpaydin, 2020). For instance, machine-learning systems are used to identify objects in images, transcribe speech into text, or identify the uniqueness of individual gait patterns (Alpaydin, 2020; Horst et al., 2019). Especially the fast growing amounts of data in physical, chemical, biological and so-

cial systems as well as a largely increased computational power have accelerated the development of machine learning applications (Ferber et al., 2016; Alpaydin, 2020). In human movement analysis, laboratory-based experiments and wearable sensors offer biomechanists a wealth of data on healthy and pathological movement (Phinyomark et al., 2018; Halilaj et al., 2018). Consequently, machine learning techniques have started to complement traditional statistical tools to exploit the power of these data and make research more efficient (Halilaj et al., 2018; Phinyomark et al., 2018; Ferber et al., 2016; Schöllhorn, 2004).

Machine learning algorithms generally build a mathematical model based on a set of randomly chosen examples (training data) (Gupta & Sedamkar, 2020; Alpaydin, 2020). In this context, there are mainly two machine learning categories, namely supervised and unsupervised learning (Guleria & Sood, 2020; Phinyomark et al., 2018). An illustration of machine learning categories and corresponding algorithms is presented in Figure 1.1. On the one hand, in supervised learning, the training data is labeled and the response variable reflects discrete/qualitative data for classification tasks or continuous/quantitative data for regression tasks (Gupta & Sedamkar, 2020). Supervised learning has been the most popular machine learning approach in the medical sciences (Cabitza et al., 2018). On the other hand, when target classes/variables are not available, the machine learning models are built based on regularities in the input data using so-called unsupervised learning methods (Alpaydin, 2020). Within this approach, the algorithms themselves have to find underlying structures (e.g., groups) in the data (Gupta & Sedamkar, 2020). Clustering is one of the most widely used unsupervised learning method (Alpaydin, 2020; Halilaj et al., 2018). Machine learning has shown great promise in providing solutions for classifica-

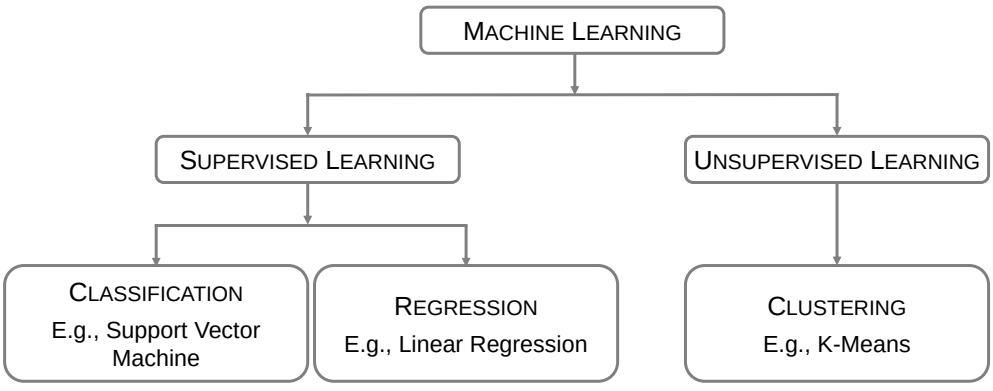

Figure 1.1: Main machine learning categories and exemplary algorithms (Guleria & Sood, 2020; Alpaydin, 2020; Rebala et al., 2019).

tion, regression and clustering tasks in biomechanical and health care applications (Halilaj et al., 2018; Cabitza et al., 2018; Ferber et al., 2016). One the one hand, classification and regression are typically used for predictive analyses in order to assign data into discrete categories (classification) or to predict numeric or continuous outcome values (regression) (Guleria & Sood, 2020; Halilaj et al., 2018). For instance, Christian et al. (2016) used a support vector machine for a computer aided analysis of gait patterns in patients with acute anterior cruciate ligament injury. Similarly, Matić et al. (2016) used a regression approach to obtain a model of useful indicators of anterior cruciate ligament deficiencies. On the other hand, the goal of clustering is to group elements that are close to each other (Rebala et al., 2019). This type of analysis is closely related to data mining, which aims to discover patterns in large databases (Alpaydin, 2020). The identification of sub-populations that exhibit different types of gait characteristics (Hörzer et al., 2015) or pathological gait pattern (Böhm et al., 2019; Rozumalski & Schwartz, 2009) is an example for clustering tasks. The systematic review by Halilaj et al. (2018) revealed that the majority of machine learning methods in human movement biomechanics are used for predictive tasks – mainly classification (80.6%) and regression (11.6%) – while a few focused on clustering (7.8%). Support vector machines, regression models and ANNs are the most used algorithms for predictive modeling, whereas the k-means method is most used for clustering (Halilaj et al., 2018).

One frequently applied machine learning-based method in human movement analysis are ANNs. ANNs can be described as analytical structures, which mimic the biological nervous system, particularly the human brain (Sivakumar et al., 2016; Nayak et al., 2001). The connection between an input and output layer by means of one or more processing layers –known as hidden layers– is characteristic for ANNs. Each layer is composed of simple processing units, which are named as 'nodes' or 'artificial neurons', by analogy with the biological neurons (Schöllhorn, 2004). The nodes are linked to each other and the weight level of a connection represent the strength of the specific connection (Sivakumar et al., 2016). During a learning phase, using a set of data that contains both inputs (e.g., IMU signals) and ground truth outputs (e.g., Knee Joint Forces (KJFs)), the weights of nodes are iteratively adjusted to learn the relationship from the provided examples (Sivakumar et al., 2016; LeCun et al., 2015; Schöllhorn, 2004; Nayak et al., 2001). Predictions for new data can be made by way of the learned

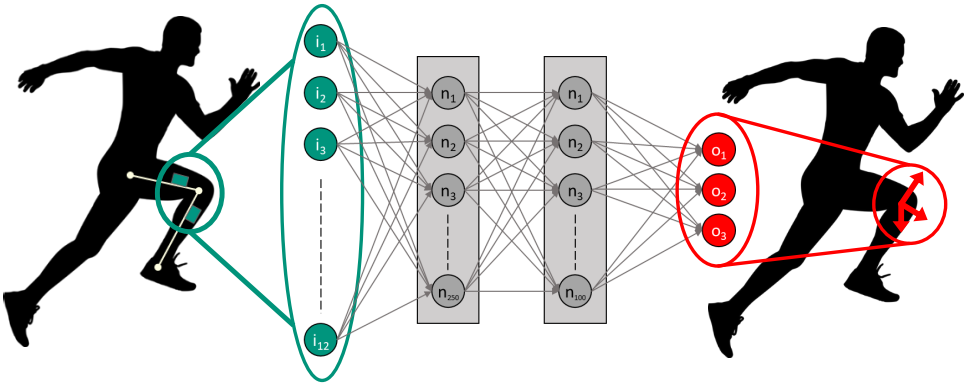

Figure 1.2: Abstract model of an Artificial Neural Network (ANN) using wearable sensor data as input (i_1 to i_{12}, illustrated in green) in order to estimate three-dimensional knee joint forces as the biomechanical output (o_1 to o_3, illustrated in red). The ANN shows two hidden layers (lightgrey boxes), one with 250 (n_1 to n_{250}) and one with 100 neurons (n_1 to n_{100}), which are connected to the input and output nodes. The circles represent the nodes of the ANN. Weights of the nodes (bows) are calculated during the learning phase of the ANN.

functions of a trained model. Consequently, ANNs offer a general framework and a very powerful tool for representing non-linear mappings form several input variables to several output variables (Bishop, 1995). An exemplary ANN architecture is shown in Figure 1.2.

Since the turn of the century, an increasing number of ANN approaches have been explored to extract insights from large, complex, heterogeneous, and noisy biomechanical datasets (Schöllhorn, 2004; Halilaj et al., 2018). For example, Kaczmarczyk et al. (2009) used an ANN on lower limb joint kinematics for classifying the gait patterns of post-stroke patients into groups in order to allow for a more effective treatment with appropriately targeted interventions. As another example, Favre et al. (2012) designed an ANN using inputs from ground reaction forces and anthropometric measurements to successfully predict knee adduction moments during walking. Moreover, there are many studies highlighting the usability of ANNs to estimate biomechanical load and performance metrics trough kinematic data from optical motion analysis systems (Ancillao et al., 2018; Kipp et al., 2018; Oh et al., 2013; Favre et al., 2012; Hahn & O'Keefe, 2008).

Parallel to the development of estimation models using established biomechanical measurements, an increasing number of wearable sensor-based approaches have been explored (Díaz et al., 2020; Gurchiek et al., 2019; Ancillao et al., 2018; Wouda et al., 2018). These approaches aiming to simplify data acquisition and modeling strategies for estimating target variables such as Ground Reaction

Forces (GRFs) (Díaz et al., 2020; Gurchiek et al., 2019; Ancillao et al., 2018; Wouda et al., 2018). Leporace et al. (2015) did one of the first studies combining wearable sensors and ANNs. They compared different ANNs to estimate 3D GRFs while walking based on data obtained from a 3D accelerometer attached to the distal and anterior part of the shank. In a later study, Wouda et al. (2018) used an ANN approach to estimate vertical GRFs and sagittal knee kinematics during running, based on three inertial sensors placed at the lower legs and the pelvis. The estimated force-time profiles and flexion/extension profiles showed high agreement with the optical and GRF reference measure. Gurchiek et al. (2019) identified in their recent review on estimating biomechanical time-series with wearable sensors, 23 studies estimating joint kinematics, 16 joint dynamics, seven segment dynamics, and five segment kinematics, respectively. ANNs were the most popular method. While joint contact forces, individual muscle forces, or muscle kinematics have not been estimated so far according to Gurchiek et al. (2019). Most studies focused on joint/segment biomechanics in the sagittal plane (87%), followed by the frontal plane (46%), and transverse plane (33%). Among the studies investigated by Gurchiek et al. (2019) the wrist joint received most attention, followed by the knee, the elbow, the ankle, the shoulder, and the hip. Overall, research at the intersection of wearable sensors, machine learning and biomechanics is still in a very early stage. Notwithstanding, there is enormous potential for positively influencing human movement research. In this process, machine learning techniques may support the development of wearable technology for quantifying sports performance and assessing loads on body structures, which play an important role in rehabilitation and health diagnostics of sports injuries as well as musculoskeletal diseases (Díaz et al., 2020; Verheul et al., 2020; Gurchiek et al., 2019; Halilaj et al., 2018).

1.6 Aims and scope of this thesis

This thesis aims to investigate the feasibility of using wearable sensors and machine learning techniques to obtain meaningful biomechanical measures with respect to sports performance and the load on body structures. Special consideration is given to unique movements such as ice hockey skating, as well as to the assessment of the load on body structures during the execution of everyday and sport movements using machine learning techniques.

Accordingly, this thesis is subdivided into four studies:

I. Automated gait event detection during ice hockey skating.

II. Mobile ice hockey skating performance analysis.

III. Estimation of knee joint forces in sport movements.

IV. Estimation of joint loading in knee osteoarthritis.

with the following specific aims:

I. to determine the agreement between a novel accelerometer-based approach for an automated identification of strides, contact phase, and swing phase during forward skating in ice hockey and an accepted method.

II. to investigate the feasibility of using body worn accelerometers to identify previous highlighted performance related biomechanical changes in forward ice hockey skating.

III. to develop an ANN that estimates net knee joint forces during sport movements, based on data obtained by wearable sensors integrated in a knee sleeve.

IV. to develop an ANN that estimates knee flexion moment and knee adduction moment during various locomotion tasks, based on data obtained by two wearable sensors integrated in a knee sleeve.

The subsequent chapter 2 to chapter 5 comprise four research articles that each reflects one of those studies. Chapters 2 and 3 encompass studies that examined ice hockey skating, while chapters 4 and 5 focused on assessing load on knee joint structures in various everyday and sport movements. All studies have been published in international peer-reviewed scientific journals between 2016 and 2020.

2 Study I – Automated gait event detection during ice hockey skating

Published as

Stetter, B. J., Buckeridge, E., von Tscharner, V., Nigg, S. R. & Nigg, B. M. (2016). A novel approach to determine strides, ice contact, and swing phases during ice hockey skating using a single accelerometer. *Journal of Applied Biomechanics*, 32(1), 101–106.

Acknowledgments

The authors would like to thank Marc LeVangie for his practical and technical support, the Reebok-CCM Hockey Inc. for providing the required equipment, as well as *Natural Sciences and Engineering Research Council* of Canada *(NSERC)*, Canada's federal funding agency for university-based research and student support.

2.1 Abstract

This study presents a new approach for automated identification of ice hockey skating strides and a method to detect ice contact and swing phases of individual strides by quantifying vibrations in 3D acceleration data during the blade-ice interaction. The strides of a 30-m forward sprinting task, performed by 6 ice hockey players, were evaluated using a 3D accelerometer fixed to a hockey skate. Synchronized plantar pressure data were recorded as reference data. To determine the accuracy of the new method on a range of forward stride patterns for temporal skating events, estimated contact times and stride times for a sequence of 5 consecutive strides was validated. Bland-Altman limits of agreement (95%) between accelerometer and plantar pressure derived data were less than 0.019 s. Mean differences between the 2 capture methods were shown to be less than 1 ms for contact and stride time. These results demonstrate the validity of the novel approach to determine strides, ice contact, and swing phases during ice hockey skating. This technology is accurate, simple, effective, and allows for in-field ice hockey testing.

2.2 Introduction

Small sensors that can be attached to the body or to sport equipment have become increasingly popular and important for biomechanical assessments and activity monitoring in the field of sport science (Boyd et al., 2013; Dadashi et al., 2012; Mihalik et al., 2012). The advantage of measuring data in a realistic environment is that the athlete is less inhibited or disturbed to perform their natural movement pattern. Furthermore, due to the small size of these sensors they can be used in unique environments like an ice rink, where commonly used gait analysis instruments cannot be used (Bergamini et al., 2012; Mariani et al., 2010). As a result, accelerometers may help to achieve a better understanding of biomechanics during ice hockey skating on an ice rink, and may extend the analysis capability of skating-specific movements. So far, only limited information about the biomechanics of ice hockey skating is available, which is most likely due to the difficulty of collecting biomechanical data on ice (Upjohn et al., 2008). Thereby, an accurate and efficient detection of temporal events, such as initial contact and blade-off, is essential to study temporal skating parameters, or to quantify other biomechanical variables.

An important consideration when using accelerometers for analyzing human

movement is the location at which an accelerometer is placed. In this context, the part of the body whose movement is being studied and the wearability for the user dictates the accelerometer placement (Yang & Hsu, 2010; Godfrey et al., 2008). Accelerations are measured in the coordinate system of the accelerometer. This coordinate system will continually move during movement. Therefore, translational and rotational accelerations of a moving body segment will be detected to the extent of the alignment of these vectors with the sensing axis of the accelerometer (Kavanagh & Menz, 2008; Elble, 2005). During this process, signal patterns are generated which can be used to extract pertinent features to derive the targeted measures. Previous research in walking has shown that accelerometers, and their expansion to inertial sensors (i.e., accelerometers combined with gyroscope and magnetometer) attached to the lower extremities can significantly reflect gait-related features during locomotion (Mariani et al., 2010; Rampp et al., 2015; Aminian et al., 1999). There is evidence that accelerometers can be used instead of foot switches, which are often attached beneath the heel and beneath the big toe to monitor heel strike and toe off, for quantifying spatiotemporal gait characteristics (Kavanagh & Menz, 2008). Furthermore, research in running has shown that inertial sensors can effectively be used to identify timing events during sporting activities (Bergamini et al., 2012; Lee et al., 2010; Auvinet et al., 2002). The level of agreement between mobile sensors and high speed cameras (Bergamini et al., 2012; Lee et al., 2010; Auvinet et al., 2002) or force plates (Bergamini et al., 2012) is high (95% limits of agreement less than 0.025 s) across a range of running velocities.

In ice hockey research, video analysis (Auvinet et al., 2002), pressure measurement (Lafontaine, 2007), and force transducer systems (Stidwill et al., 2010) have been used to estimate temporal characteristics. However, these instruments are either limited in terms of the capture volume or require a special instrumentation and a long postprocessing time. Therefore, as an alternative technology, accelerometers have the potential to simplify the analysis of ice hockey skating in a field setting.

The purpose of this study was to determine the agreement between a novel accelerometer-based approach for an automated identification of strides, contact phase, and swing phase during forward skating in ice hockey and an accepted method. Data provided by the accelerometer were simultaneously recorded with plantar pressure data within the skate and compared with the total plantar force.

2.3 Materials and methods

2.3.1 Participants and data acquisition

A group of six ice hockey players (age 29.8 ± 7.3 years, mass 84.2 ± 13.5 kg, height 174.3 ± 6.8 cm) participated in the study, after they signed an informed consent form in accordance with the University of Calgary's Conjoint Health Research Ethics Board. All players were free from recent injuries or other limiting conditions, which would affect their performance. Tests were carried out at an indoor ice rink at the Olympic Oval Calgary. Participants were instructed to perform five maximum effort 30 m forward skating sprints. The total sprint time was measured with light gates (Brower Timing Systems, Draper, UT, USA) and ranged from 4.11 s for the fastest trial to 5.18 s for the slowest trial, across all participants. Participants started in a standing position with their knees slightly flexed and both their feet parallel to the starting line. All skates were sharpened to a .5-in (1.3-cm) radius of hollow before data collection.

Each participant's right skate was equipped with a 3D accelerometer (Analog Devices Inc., Norwood, USA) at the center of the chassis (Figure 2.1). Care was paid to the fixation of the accelerometer in order to limit its oscillations relative to the skate chassis as well as to a consistent alignment of the sensitive axes of the accelerometer with the local coordinates of the skate (anterior-posterior, medio-lateral, and vertical). A solid contact between the flat surface of the accelerometer housing and the nearly flat surface of the chassis was ensured by securely placing cloth-based self-adhesive tape over the accelerometer and chassis. This procedure was performed always by the same investigator in order to keep potential movement artifacts of the sensor low and avoid variability in the fixation. The measuring range of the accelerometers was ±35 g with a sampling rate of 2400 Hz. We chose such a large measuring range and high sampling rate in order to cover a wide range of signal characteristics, and did not wanted to limit ourselves by missing useful information. In addition, synchronized skate pressure data were recorded with an insole pressure measurement system (Pedar-X, novel GmbH, Munich, Germany) with a sampling rate of 90 Hz. Pressure values were zeroed with the foot inside the skate, laces tied, and foot lifted off the ground. Synchronization was achieved by using a low/high-level analogous signal. A rising edge was initiated at the start of the plantar pressure system data acquisition, and sent to the data logger of the accelerometer. Participants wore a backpack, which contained two data logger boxes, an analog-to-digital

Figure 2.1: The 3D accelerometer firmly fixed with tape on the center of the skate chassis (black oval).

converter, and a tablet (Acer Iconia W 510, Acer Inc., Taipei, Republic of China). This system was remotely controlled for data acquisition from the side of the ice rink.

2.3.2 Data processing and method development

Signal processing and software routines were developed in-house using MATLAB™ (R2012b, MathWorks, Inc., Natick, MA). Data obtained from the 3D accelerometer were converted into units of gravity (g) by calibrating the voltage outputs for each of the sensitive axis through a 2-point linear calibration with and against the direction of gravity. Baseline correction was done by subtracting the mean value of a neutral standing trial (10 s) in each axis. There were 2 main features of the signal processing algorithm: (1) development of a tool to identify individual forward skating strides and (2) development of a tool to determine contact and swing phase of a single stride. The stride time was defined as initial contact to initial contact of the same foot, the contact phase as initial contact to blade-off, and swing phase as blade-off to initial contact of one foot.

Stride detection

Skating strides are characterized by a generic signal pattern (Figure 2.2). A 2 Hz wavelet low-pass filter (von Tscharner, 2000) was applied to the vertical acceleration signal to obtain the low frequency acceleration that represents the stride movement without the vibrations caused by the ice contact. The peaks of the low frequency acceleration were used for an automated extraction of strides from the entire recorded sequence. However, the low frequency acceleration

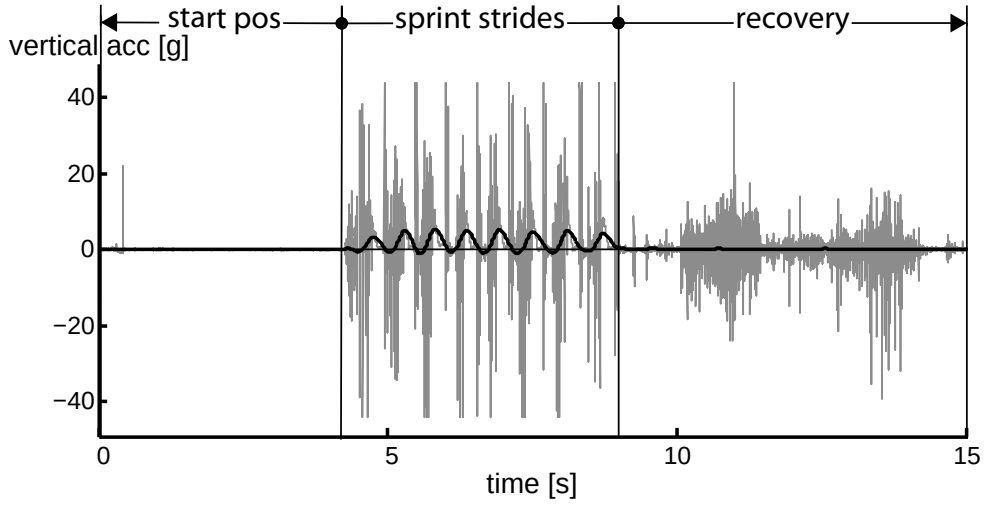

Figure 2.2: Raw vertical acceleration signal (gray) taken from 1 representative trial over the entire skating sequence. A 2 Hz wavelet low-pass filter (black) was applied to represent individual strides. This low frequency component of the signal exhibits high amplitudes when the skater lifts and lowers his foot to perform a stride. As a result, individual strides during the sprint are characterized by local maxima in the low frequency acceleration signal. Start pos = start position.

had an insufficient time resolution to detect the on ice period.

Determination of initial contact and blade-off

To extract temporal stride parameters from accelerometer signals, a novel method was developed. The fundamental approach behind this method was based on the observation that the acceleration signal during ice contact showed high-frequency vibrations. A wavelet-based approach was used to filter the raw signal (150 Hz low-pass) (Figure 2.3a). Subsequently, the squared difference, $d(s,a) = (r(s,a) - f(s,a))^2$, between the low-pass filtered signal $f(s,a)$ and raw signal $r(s,a)$ was calculated for each sample (s) in each axis (a). If the squared difference exceeded a predetermined threshold (0.03 voltage^2) in 1 of the 3 directions, the value in a new binary signal was set to high level (1) (Figure 2.3b). The point in time of the previously identified peak of the stride detection, which was consistently located within the first third of the swing phase, was used as the initial start point for searching initial contact and blade-off. To detect the beginning (IC_{acc}) of a high-frequency section in the binary signal, a threshold of 10 high-level samples within a forward moving window (of length 30 samples) had to be reached (Figure 2.3b–c). The first high-level signal within this window was selected as IC_{acc}. The detection of the end (BO_{acc}) of a high-frequency section in

the binary signal was performed in two steps. First, a potential blade-off frame was identified, and assigned to the first high-level signal within a 10 samples backward moving window when more than 5 high-level samples were detected. Second, if 100 of the 200 subsequent samples in positive direction were low-level samples, potential blade-off was considered as the real blade-off (BO_{acc}) (Figure 2.3b–c). This means that the method detects BO_{acc} from stride N and the initial contact from stride $N+1$. The most appropriate thresholds and window lengths were experimentally determined during the development phase of the method. Subsequently, these values were kept constant across all participants so that the stride detection algorithm could be an automated process that can identify Initial Contact (IC) and Blade-Off (BO) of all potential new participants.

2.3.3 Data extraction and analysis

Each recorded trial consisted of a minimum of 7 full strides. The stride detection tool was used to extract a 5-stride analysis sequence from the second to the sixth stride. To determine the validity of the new algorithms, estimated Contact Times ($\widetilde{CT} = BO_{acc} - IC_{acc}$) and Stride Times ($\widetilde{ST} = IC_{n+1} - IC_n$) were compared with those times obtained from the insole pressure measurement system (CT, ST). Therefore, plantar pressure data were up sampled to 2400 Hz using a linear interpolation function to match the sampling rate of the accelerometer. The total plantar force (Figure 2.3d) for the whole insole was calculated by summing up the converted pressure values at each cell (Pa) to force (N) based on the area of the cell, and was used to define the reference timing events (IC_{ref} and BO_{ref}). In addition, the first derivative of the total plantar force was extracted (Figure 2.3e). IC_{ref} was manually defined for each stride by selecting the peak in the first derivative, which occurs at an increasing slope of the total plantar force (Figure 2.3e). Similarly, the peak in the first derivative of the decreasing slope during blade-off was selected as BO_{ref} (Figure 2.3e).

Validation of the estimated contact times and stride times was performed by evaluating the absolute differences ($\Delta CT(acc, ref), \Delta ST(acc, ref)$) between the 2 methods by means of Bland-Altman plots (Bland & Altman, 2007) as well as by calculating the normalized Pairwise Variability Index for contact time ($nPVI_{CT}$) and stride time ($nPVI_{ST}$) as described by Dadashi et al. (2012). Limits of Agreement (95% LoA) for contact times and stride times were specified. Repeated-

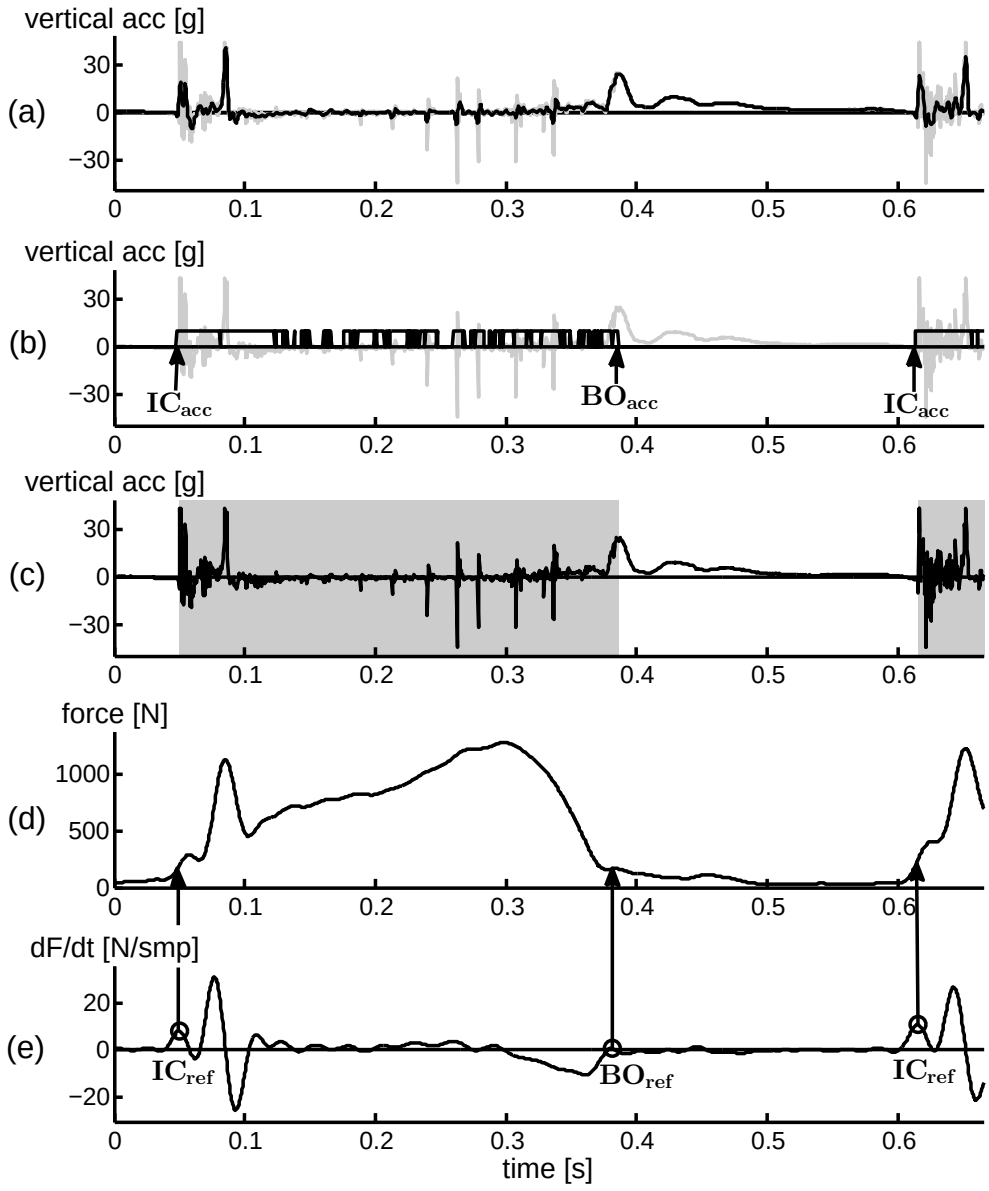

Figure 2.3: Main data processing steps to separate between contact and swing phase by using the 3D accelerometer signals (a-c) as well as the initial contact and blade-off definition for the reference system (d, e). Data are shown for 1 stride $\pm$ 50 milliseconds of a randomly selected participant, with reference to a randomly chosen stride between the second and sixth sprinting stride. (a) Filtered vertical acceleration signal (black) with a 150 Hz lowpass filter. (b) Calculated binary signal (black) by quantifying the amplitude differences between the raw and filtered signal. (c) Determination of contact (gray areas) and swing phase by using the beginning (IC_{acc}) and end (BO_{acc}) of high-frequency vibration sections in the acceleration signals. (d) Identified timing events of the total plantar force data by using the peaks in the first derivative of the total plantar force. (e) Symbol (o) indicates reference initial contact (IC_{ref}) and blade-off (BO_{ref}). The vertical arrows point to the corresponding events in the total plantar force.

measures ANOVA on $\Delta CT(acc, ref)$ and $\Delta ST(acc, ref)$ were performed to determine whether the accuracy of the method varies across strides ($P < .05$).

2.4 Results

Accelerometer-derived contact and stride times for 5 consecutive strides (a), as well as the reference contact and stride times derived from the total plantar force measures (b), are shown for a representative trial in Figure 2.4. The mean of the estimated contact times for all analyzed strides was 0.324 seconds ($SD = 0.032$ s), and the mean of the estimated stride times was 0.554 seconds ($SD = 0.042$ s). Bland-Altman plots indicated agreement between the reference and accelerometer-derived contact times and stride times (Figure 2.5). The 2 systems differed by 2.0% ($nPVI_{CT}$) for the contact time determination and by 1.0% ($nPVI_{ST}$) for the stride time determination. $\Delta CT(acc, ref)$ and $\Delta ST(acc, ref)$ were not statistically different across the 5 consecutive strides ($P = .587$ and $P = .647$, respectively). Difference between the duration measures ranged between –0.0187 seconds and 0.0185 seconds (95% LoA) and between –0.0168 seconds and 0.0152 seconds for contact time and stride time, respectively. The 95% LoA were close to the temporal resolution of the reference system (0.011 s). The low biases (contact time: –0.000093 s, stride time: –0.000827 s) indicated that the accelerometer system does not tend to determine constantly longer contact or stride times compared with the reference system.

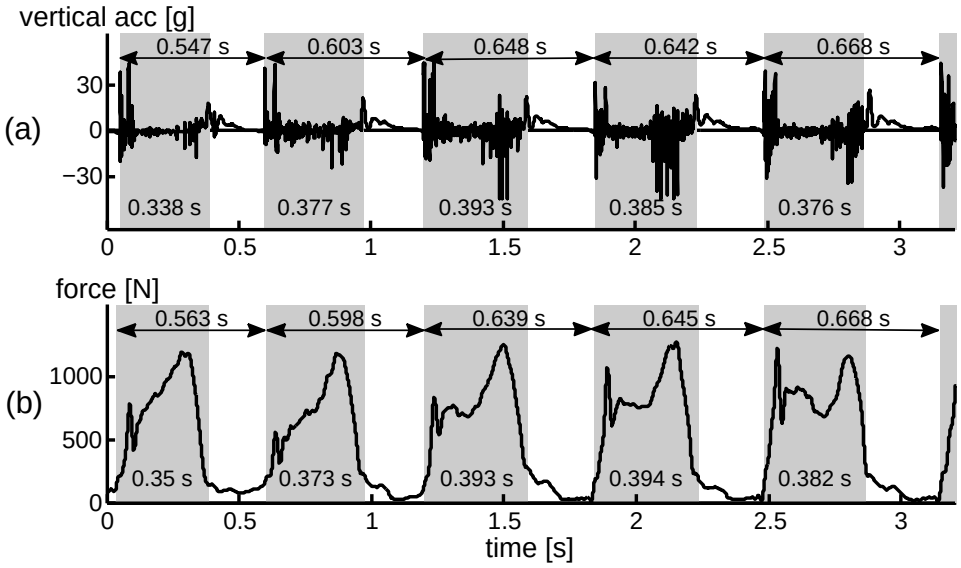

Figure 2.4: Accelerometer-derived contact (gray areas) and stride times (arrows) for 5 consecutive strides ± 50 milliseconds (a), as well as the reference contact and stride times derived from the total plantar force measures (b).

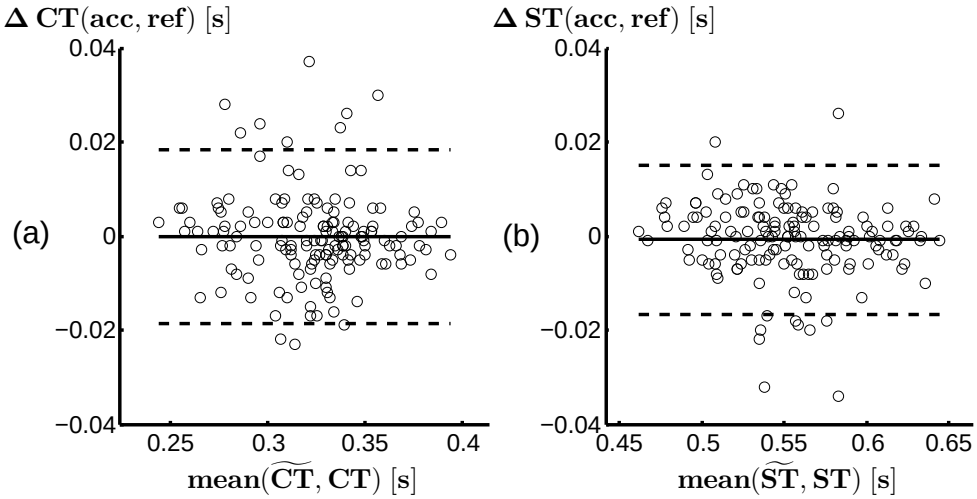

Figure 2.5: Bland-Altman plots indicating agreement between (a) contact times (CT) and (b) stride times (ST) of the reference system (CT, ST) and those estimated with an accelerometer ($\widetilde{CT}$, $\widetilde{ST}$). Mean difference (solid lines) and Limits of Agreement (95% LoA) (dashed lines) are presented.

2.5 Discussion

The precise identification of timing events during ice hockey skating is invaluable for the analysis of ice hockey skating biomechanics. This paper investigated the use of a single skate mounted 3D accelerometer for an automated detection of temporal events during forward ice hockey skating. The use of a low-pass filter enabled individual strides within a sequence to be consistently identified. Furthermore, we have proposed a new algorithm based on the quantification of vibrations to detect initial contact time and blade-off time from 3D acceleration signals. The phenomenon of extremely distinct high- and low-frequency sequences of the raw accelerometer signal correlates strongly with the ice contact and the swing phase of a skating stride, respectively. Vibrations occur during ice contact as a result of the interaction between the skate and the ice surface. In contrast to the contact phase, there are no additional external forces acting on the skate during the swing phase. Thus, the accelerometer detects only accelerations caused by movement, which contain lower frequencies.

To ensure that the vibration sequences adequately reflect the ice contact phase, a validation against a force measuring system was implemented. That is, 95% LoA for the data were less than $\pm$ 0.022 seconds (2 frames at 90 Hz for the reference system), coupled with small biases (< 1 ms), demonstrating a high conformity between the 2 methods. This result, as well as low nPVI values, shows that the difference in variability assessment of contact and stride time between the

2 systems is less than 2.0% and confirms the validity of the new method. A few outliers above and below the 95% LoA boarders were observed. Factors such as atypical skating stride patterns with an additional short ice contact after the actual blade-off or an uncertainty in the shape of the total plantar force curve could lead to such outliers. It is clear that the values of the thresholds for determining initial contact and blade-off can modify the results. The level of agreement in this study is comparable with other methods used to identify gait events during running (Bergamini et al., 2012; Lee et al., 2010). They showed similar 95% LoA (< 0.025 s) validated against a force plate and video camera as the gold standard. The difference (biases < 1 ms) between the accelerometer and plantar pressure system is comparable to other studies, which validated an inertial sensor approach with a standard method for walking (Salarian et al., 2004) or running (Lee et al., 2010).

The accelerometer placement in the center of the chassis was deliberately chosen to detect the majority of vibrations during the contact between the ice and the metal blade of the skate. This is effective in hockey skating as the movement pattern of the foot during a skating stride does not consist of a distinct heel or toe contact. Such foot strike patterns may require another location for an accurate detection of initial contact and blade-off.

The methodology developed in this paper appears to be valid for a wide range of forward stride patterns. The analyzed sequence, which ranged from the second to the sixth stride, included the transition for the accelerative phase to skating at a constant velocity. Lafontaine (2007) stated that as a skater raises speed, the skating motion changes. In addition, Stidwill et al. (2010) found differences in step mechanics. The force-time curves for the first 3 strides showed single force peaks, and were different from subsequent strides that showed double force peaks. Figure 4b depicts strides 2 to 6, and shows the same pattern where you see a single to double peak transition. This is reflective of the running to a gliding transition that has been previously described (Lafontaine, 2007; Stidwill et al., 2010). Therefore, despite notable differences in the stride pattern across progressive strides, no significant difference in the accuracy of the new method was found between strides.

Since the reference times were measured with a much lower sampling frequency, the data were interpolated to match the sampling frequency of the accelerometer. This is a potential limitation of the study. The pressure measurement system was

chosen as a mobile reference, in spite of its maximum sampling rate of 90 Hz, in order to avoid the drawback of video systems that the accuracy reduces by using a wide field of view to cover the distance of multiple strides (Lafontaine, 2007). However, the measured contact and stride times for consecutive strides in this study is supported by those times found by Stidwill et al. (2010). Due to the limitation of the mismatched sampling frequency, a validation of single strides against a high-speed video could provide greater confidence that the accelerometer-derived characteristics are accurate.

Overall, the novel method is able to define a skating stride as well as the contact and swing phase of a skating stride with a much higher sampling rate (2400 Hz) compared with previously used measurement systems (video cameras: 60–200 Hz (Upjohn et al., 2008; Lafontaine, 2007), strain gauges: 100 Hz (Stidwill et al., 2010)). However, sufficient high-frequency vibrations during the blade to ice contact could potentially be gathered with a lower sampling rate, and still provide accurate stride timing characteristics. The degree to which this sampling rate can be reduced, if necessary for practical reasons, without losing pertinent information to make the method operable must be determined in the future. The use of these novel algorithms to calculate timing events during ice hockey skating based on acceleration signals is beneficial to researchers in terms of ease of use and on-ice equipment limitations. From the perspective of a player and/or coach, this tool allows for measurements of important timing characteristics during skating on ice, thus lending itself as a future digital coaching tool. Accelerometers can potentially substitute for more cumbersome systems, such as instrumented insoles or a motion capture system, in terms of quantifying accurate stride characteristics. To extend the application of the proposed methods, other movements fundamental to ice hockey skating, such as turning and backward skating, must be addressed. In addition, the application in other skating disciplines like figure skating or speed skating could be taken into account.

2.6 Conclusion

The novel approach presented in this study provides the potential for an accurate and capable means for in-field ice hockey testing estimation of contact and stride times for forward skating based on acceleration signals. Changes in the forward stride pattern throughout the phase from acceleration to skating at a constant velocity did not influence the level of agreement between the pro-

posed accelerometer approach and times determined by plantar force data. This mobile analysis system provides accurate timing characteristics during forward skating and has potential to be used as a digital coaching tool.

3 Study II – Mobile ice hockey skating performance analysis

Published as

Stetter, B. J., Buckeridge, E., Nigg, S. R., Sell, S. & Stein, T. (2019a). Towards a wearable monitoring tool for in field ice hockey skating performance analysis. *European Journal of Sport Science*, 19(7), 893–901.

Acknowledgments

The authors would like to thank Marc LeVangie for his help with data collection.

3.1 Abstract

The capturing of movements by means of wearable sensors has become increasingly popular in order to obtain sport performance measures during training or competition. The purpose of the current study was to investigate the feasibility of using body worn accelerometers to identify previous highlighted performance related biomechanical changes in terms of substantial differences across skill levels and skating phases. Twenty-two ice hockey players of different caliber were equipped with two 3D accelerometers, located on the skate and the waist, as they performed 30 m forward skating sprints on an ice rink. Two measures of the temporal stride characteristics (contact time and stride time) and one measure of the propulsive power (stride propulsion) of a skating stride were calculated and checked for discriminating effects across (i) skill levels and (ii) sprint phases as well as for their (iii) strength of association with the sprint performance (total sprint time). High caliber players showed an increased stride propulsion ($+22\%$, $P < 0.05$) and shorter contact time (-5%, $P < 0.05$). All three analysed variables highlighted substantial biomechanical differences between the accelerative and constant velocity phases ($P < 0.05$). Stride propulsion of acceleration strides primarily correlated to total sprint time ($r = -0.57$, $P < 0.05$). The results demonstrate the potential of accelerometers to assess skating technique elements such as contact time or elements characterizing the propulsive power such as center of mass acceleration, to gauge skating performance. Thus, the findings of this study might contribute to establishing wearable sensors for in-field ice hockey skating performance analysis.

3.2 Introduction

Ice hockey is a fast-paced sport which requires excellent physical conditioning as well as accuracy and control of technical skills such as skating (Upjohn et al., 2008). Highly developed skating skills are crucial to a player's overall success (Renaud et al., 2017). Players with the ability to start quickly and skate at a high speed, are more likely to win puck possession or outmaneuver their opponents. Instantaneous leg power is required to apply an appropriately large impulse to the body's center of mass, to achieve maximum speed in a short time (Farlinger et al., 2007; Pearsall et al., 2000).

Traditionally, biomechanical performance analysis of ice hockey skating is either done in a laboratory environment using skating treadmills (Upjohn et al.,

2008) and synthetic ice surfaces (Stidwill et al., 2010) or with extensive measurement equipment on an ice rink (Buckeridge et al., 2015; Renaud et al., 2017). These approaches are typically highly standardized and allow a precise and unobtrusive measurement of multiple performance variables, which yield insight to human movements and techniques (Schmidt et al., 2017). The biomechanical data gained, deliver useful information to improve training and to achieve performance enhancement (Buckeridge et al., 2015; Renaud et al., 2017).

Within the last two decades, advances in the microelectromechanical sensor (MEMS) have opened the capability to evaluate sport-specific movements under field-based conditions. The integration of such sensors (e.g. accelerometers or gyroscopes) in sports equipment (e.g. shoes) or fixed to the athlete, allows the integration of biomechanical measurement methods during training or competition (Camomilla et al., 2018). These devices are commonly referred to as wearable sensors (Chambers et al., 2015). The field-based analysis opens opportunities to capture data in realistic settings (in training or competition) and to get a (nearly) real-time monitoring to better measure the effects of training or game performance (Neville et al., 2010; Schmidt et al., 2017). In the meantime, the capturing of sport-specific movements under field-based conditions has become a high priority and has become more and more common, which is reflected in the development of wearable systems for a wide range of sports (Camomilla et al., 2018; Chambers et al., 2015). This expansion is reflected in the fast growing number of related studies. In 2015 Chambers et al. identified 28 studies addressing the use of microsensors within individual (e.g. tennis and golf) and team sports (e.g. baseball and rugby). Whereas in a recent review, Camomilla et al. (2018) identified over 300 related studies in the field of wearable sensors for sports performance evaluation. Specifically, for locomotion tasks such as running, wearable sensors show valid and reliable results for the analysis of biomechanical parameters (Lee et al., 2010; Purcell et al., 2005; Strohrmann et al., 2012). Moreover, research in ice hockey skating related areas, such as speed skating and cross-country skiing, has proven that wearable sensors are a feasible tool for the measurement of biomechanical skating variables (e.g. center of mass displacement and lean angle of the skate) as well as for the distinction between different skating techniques (Myklebust et al., 2014, 2015; van der Kruk et al., 2016). Wearable sensors could be used to provide feedback on performance related variables without influencing the natural skating pattern, in order to im-

prove training and to achieve performance enhancement (Cox et al., 1995).

Previous research in forward skating biomechanics has highlighted substantial differences at various levels (e.g. temporal, kinematic and kinetic) with respect to the skating phase (Buckeridge et al., 2015; De Koning et al., 1995; Stidwill et al., 2009) and in relation to a skater's skill level (Buckeridge et al., 2015; Renaud et al., 2017; Upjohn et al., 2008).

Differences between fundamental phases (accelerative and steady- state) of ice hockey skating show how skating technique changes in accordance with increased skating speed (Buckeridge et al., 2015; Stidwill et al., 2009). As previously shown for speed skating (De Koning et al., 1995) athletes change from a running-like technique at the initial push offs to a gliding technique during steady-state skating (Buckeridge et al., 2015). An increased propulsive demand for the running-like motion compared to a gliding motion is underlined by a larger plantar push-off force and greater muscle activity of the gastrocnemius during the initial sprint phase (Buckeridge et al., 2015). In addition, Stidwill et al. (2009) descriptively reported difference in temporal characteristics. Contact times for running-like strides (0.31 s) were notably shorter than for steady-state strides (0.38 s).

The identification of biomechanical differences between elite and recreational hockey players has been used to improve the understanding for the relationship between skating biomechanics and performance (Buckeridge et al., 2015; Renaud et al., 2017; Upjohn et al., 2008). A few previous studies have compared lower limb joint kinematics (Buckeridge et al., 2015; Renaud et al., 2017; Upjohn et al., 2008), body Center of Mass (CoM) movement (Renaud et al., 2017), plantar force application (Buckeridge et al., 2015) and muscle activation pattern (Buckeridge et al., 2015) between high and low caliber ice hockey players. Renaud et al. (2017) have shown differences in CoM accelerations between caliber, and the authors emphasized the use of CoM variables to assess skating performance. In order to yield important insight into skating performance, accelerometer-derived variables should be able to reveal substantial biomechanical differences with respect to the skating phases and skill level of the players. In the long term, the assessment and monitoring of specific stride variables (e.g. CoM acceleration) could allow coaches to gauge the impact of training (Camomilla et al., 2018) or even neuromuscular fatigue (Buchheit et al., 2015).

The purpose of the current study was to investigate the feasibility of using

body worn accelerometers to identify previous highlighted performance related biomechanical changes in forward skating. It was hypothesized that accelerometer-derived variables show discriminating effects across (i) skill levels and (ii) sprint phases; and that (iii) the strength of association between the derived variables and skating performance is high. The findings of this study could help to overcome current restrictions in the performance assessment of ice hockey skating and open new possibilities for in-field diagnosis.

3.3 Materials and methods

3.3.1 Participants

Twenty-two male hockey players (age 32.1 years $\pm$ 7.7, height 178.7 $\pm$ 5.7 cm, body mass 86.7 $\pm$ 10.5 kg) participated in this study. To represent a range of different calibers, members of the University of Calgary men's ice hockey team and recreational players from local hockey teams were recruited as participants. All participants were free from injury at the time of participation. The study was approved by the University of Calgary's Conjoint Health Research Ethics Board. All participants were informed of the experimental procedures and gave informed written consent prior to the test. All participants' skates were sharpened to the same hollow prior to data collection. Tests were subsequently carried out at an indoor ice rink.

3.3.2 Protocol

After fitting the participants with the data collection gear, participants were provided with a 5 min warm-up and familiarization period. Participants were then instructed to perform fifteen maximum effort 30 m forward skating sprints. The Total Sprint Time (TST) was measured with timing light gates (Brower Timing Systems, Draper, UT, USA). Participants started in a standing position with their knees slightly flexed and both their feet parallel to the starting line. They were told not to perform a crossover start and they were instructed to accelerate as fast as possible, and skate the 30 m distance with maximal effort.

3.3.3 Instrumentation

Two three-dimensional (3D) accelerometers (combination of ADXL78 and ADXL278, Analog Devices, Inc., Norwood, MA, USA) were used in this study. The measuring range of the accelerometers was $\pm$35 g with a sampling rate

Figure 3.1: Placement of accelerometers used in the study. Cloth-based self-adhesive tape was used to attach the accelerometers.

of 2400 Hz. Accelerometer positions were the center of the right skate chassis and the lower back at the level of the fifth lumbar vertebrae (Figure 3.1). The accelerometers were firmly fixed with cloth-based self-adhesive tape in order to restrict the accelerometers from movement with respect to the skate or back. Care was paid to the fixation of the accelerometers in order to limit its oscillations, as well as to consistently align axes of the accelerometers with the local coordinates of the skate and back. The mounting was performed always by the same investigator, in order to keep potential movement artifacts of the sensors low and avoid variability in the fixation. A data acquisition box (Biovision, Wehrheim, Germany), and a tablet (Acer Iconia W510, Acer Inc., Taipeh, Republic of China) were placed in a backpack for data recording. Participants gave subjective feedback that they felt no constraints due to the instrumentation. An external laptop, wirelessly connected to the tablet was used to control data acquisition. In addition to the measurement devices, participants wore a helmet, and gloves for safety, and carried a stick to mimic a hockey setting.

3.3.4 Performance groups

K-means clustering was applied to the performance outcome of the skating task (i.e. TST) in order to isolate the high caliber players from the low caliber players. This technique is a powerful tool to organize subjects into characteristic groups without predefining the number of members of each group or setting an artificial threshold for the separation (Figueiredo et al., 2016; Hörzer et al., 2015). The three fastest sprint trials were identified for each player. Subsequently, the three shortest TSTs of each player were input to a k-means clustering algorithm, with k pre-defined as two. Table 3.1 shows the group characteristics for the identified

Table 3.1: Group characteristics.

	Overall	High Caliber	Low Caliber	*P*
Participants [n]	22	9	13	
Age [yrs]	31.6 ± 7.4	26.3 ± 5.8	35.2 ± 6.3	0.003*
Body height [m]	1.79 ± 0.06	1.80 ± 0.05	1.78 ± 0.06	0.424
Body mass [kg]	87.1 ± 10.5	87.7 ± 7.5	86.8 ± 12.5	0.849
Total sprint time [s]	4.57 ± 0.21	4.35 ± 0.09	4.73 ± 0.10	<0.001*

Values are mean ± SD. P values as revealed by independent t-tests ($P < 0.05$): *statistically significant.

performance groups. The identified groups corresponded well with the players' performance level.

3.3.5 Data analysis

Signal processing and data analysis were performed in MATLAB™ R2017b, (The MathWorks Inc. Natick, MA, USA). The accelerometers were manually calibrated with a two-point calibration for all three orthogonal axes (Kavanagh & Menz, 2008). This was done to convert the raw accelerometer signal from millivolts (mV) to gravity units (g).

Contact time and stride time

The approach presented by Stetter et al. (2016) for stride identification, ice contact and swing phase determination based on a 3D accelerometer on the skate was applied to extract valid timing characteristics. The Contact Time (CT) was calculated over the period of contact with the skate and the ice. The Stride Time (ST) was calculated from initial contact to subsequent ice contact of the same skate.

Stride propulsion

The 3D acceleration signal of the lower back accelerometer was low pass filtered (6 Hz, wavelet filter) (Camomilla et al., 2018) and used to quantify the propulsive power of skating strides. For each of the three axes of the accelerometer, a 0.5 Hz low pass filtered signal (wavelet filter) were subtracted (Wixted et al., 2007) from the original signal, to remove the static acceleration component from the signals. The remaining signals were used to estimate the propulsion power during a stride. A stride specific value was obtained by calculating summed acceleration magnitudes of the three axes, normalized to the stride duration, and defined as

Stride Propulsion (SP) (equation 3.1).

$$SP = \frac{1}{ST}\left(\int_0^{ST} |x(t)|\mathrm{d}t + \int_0^{ST} |y(t)|\mathrm{d}t + \int_0^{ST} |z(t)|\mathrm{d}t \right) \tag{3.1}$$

$x(t)$, $y(t)$, and $z(t)$ refer to the components of the x-, y-, and z- axis samples and ST represents the stride time.

All biomechanical variables were calculated for the second and sixth strides of the same three trials as used for the identification of the performance groups. These strides were selected, as they represent the accelerative and steady-state phases of forward skating (Pearsall et al., 2001), and were derived from the skate mounted accelerometer.

3.3.6 Statistics

Group means and standard deviations of all variables were computed. Two-way mixed model analyses of variance (ANOVAs) with between-subject factor of player caliber (high/low) and within-subject factor of stride type (acceleration/ steady-state) were used to perform statistical comparisons of the biomechanical variables (CT, ST, SP). Additionally, Pearson's correlations were calculated to examine associations between the biomechanical variables (CT, ST, SP) and the performance variable (TST). The size of the correlation coefficient r was indicated as follows: small correlations by $0.10 < r < 0.30$, medium correlations by $0.30 < r < 0.50$ and large correlations by $r > 0.50$ (Cohen, 1988). The level of statistical significance was set at $P < 0.05$. Statistical tests were carried out with IBM SPSS Statistics (Version 25.0, SPSS Inc., IBM, Armonk, NY, USA).

3.4 Results

3.4.1 Differences across skill levels and sprint phases

Mean and standard deviation for the biomechanical variables (CT, ST, SP) as well as P values and effect sizes of the ANOVAs are shown in Table 3.2. During both stride types, high caliber exhibited a shorter CT and an increased SP than low caliber ($P < 0.05$). ST did not differ across player caliber. When comparing acceleration and steady-state strides, CT and ST was seen to be significantly shorter during the accelerative phase compared to the steady-state phase ($P < 0.05$). In addition to changes in timing characteristics, SP was seen to be significantly higher for acceleration strides compared to steady-state

Table 3.2: Differences in skating biomechanics (CT = contact time, ST = stride time, SP = stride propulsion) across skill level (high caliber and low caliber) and sprint phase (acceleration = 2nd stride, steady-state = 6th stride).

	Stride	High Caliber	Low Caliber	Difference	P_{group}	$\eta^2_{\text{p group}}$	P_{stride}	$\eta^2_{\text{p stride}}$
CT [%]	2nd	55.14 ± 5.18	58.60 ± 3.17	3.46	0.046*	0.184	0.010*	0.288
	6th	58.02 ± 2.83	60.36 ± 3.35	2.34				
ST [s]	2nd	0.51 ± 0.04	0.54 ± 0.05	0.02	0.252	0.065	<0.001*	0.840
	6th	0.60 ± 0.04	0.62 ± 0.05	0.02				
SP [g]	2nd	1.93 ± 0.33	1.58 ± 0.24	0.35	0.005*	0.335	<0.001*	0.515
	6th	0.60 ± 0.04	0.62 ± 0.05	0.02				

Notes: Values are mean ± SD. P values and effect sizes (Partial Eta Squared η^2_{p}) as revealed by two-way mixed model analyses of variance ($P < 0.05$): * statistically significant; small effect: $\eta^2_{\text{p}} \geq 0.01$; medium effect: $\eta^2_{\text{p}} \geq 0.06$; large effect: $\eta^2_{\text{p}} \geq 0.14$ (Cohen, 1988).

strides ($P < 0.05$). The two-way ANOVAs did not show any significant interactions with respect to player caliber or stride type.

3.4.2 Relationship to sprint performance

Correlations between each biomechanical variable (CT, ST, SP) and the sprint performance (TST) are presented in Figure 3.2. SP was found to be largely correlated with the TST for an acceleration stride ($r = -0.57$, $P < 0.05$) and moderately correlated with the TST for a steady-state stride ($r = -0.44$, $P < 0.05$), respectively. For both stride types (acceleration and steady-state), no significant correlation with TST were seen for CT and ST. R values of 0.34–0.42 and 0.16–0.25 indicate a moderate and small relationship with performance (TST) for CT and ST, respectively.

3.5 Discussion

The current study investigated the feasibility of using body worn accelerometers to identify performance related biomechanical changes in forward skating. In-field diagnosis opens new possibilities to gauge the impact of training or monitor individual skating performance (Camomilla et al., 2018; Myklebust et al., 2015; van der Kruk et al., 2016). For this purpose, two 3D accelerometers were placed on the participants while they performed 30 m skating sprints. Two measures of the temporal stride characteristics (CT and ST) and one measure of the propulsive power of a skating stride (SP) were evaluated as meaningful biomechanical variables. Previous research in forward skating biomechanics (Buckeridge et al., 2015; Renaud et al., 2017; Stidwill et al., 2009; Upjohn et al., 2008)

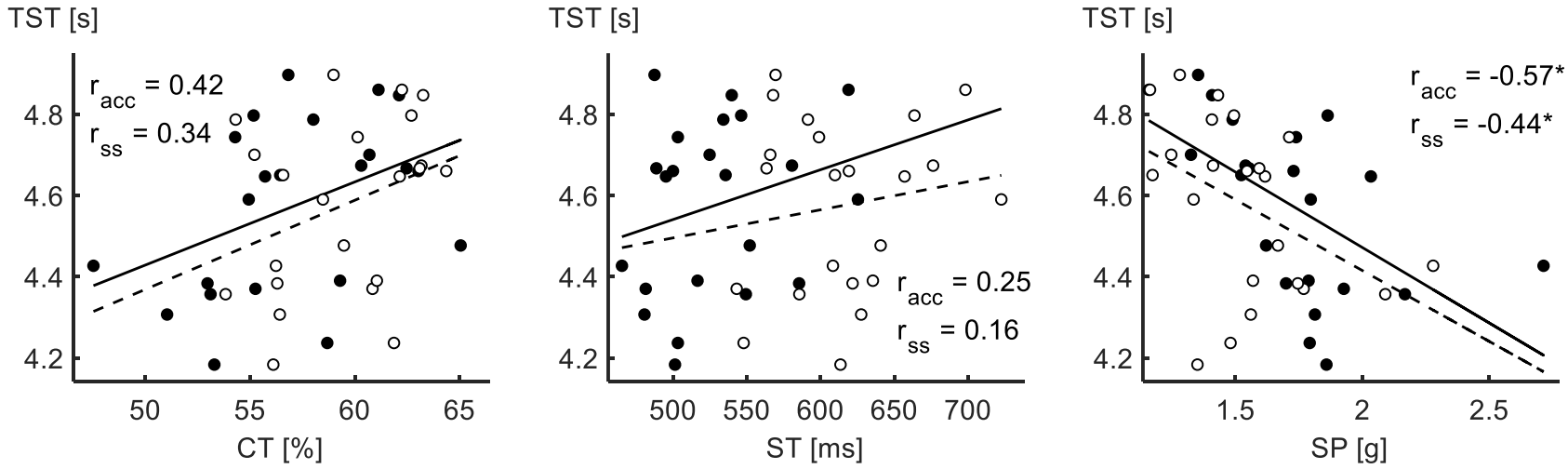

Figure 3.2: Scatterplots of Total Sprint Time (TST) versus Contact Time (CT), Stride Time (ST) and Stride Propulsion (SP), respectively. Filled circles indicate the acceleration (2nd) strides and empty circles the steady-state (6th) strides. Solid lines refer to correlations for acceleration strides (r_{acc}) and dashed lines refer to correlations for steady-state strides (r_{ss}). Correlation coefficients r are given as revealed by Pearson's correlations (*statistically significant; $P < 0.05$).

has highlighted that skating technique elements such as CT or elements characterizing the propulsive power such as CoM acceleration are closely related to skating performance. Based on the current literature, we expected that our measures show discriminating effects across skill levels and sprint phases and we speculated that the measures indicate a strong relationship to the overall skating performance (TST).
The study revealed that: (i) the variables CT and SP discriminated between high and low caliber ice hockey players; (ii) the variables CT, ST and SP discriminated between fundamental skating phases (accelerative and steady-state); (iii) SP of acceleration strides primarily correlated to skating performance (TST). In consequence, the results indicate that accelerometer-derived biomechanical variables are effective at predicting skating performance.

3.5.1 Differences across skill level

High caliber players performed the 30 m sprint 9% (average decrease of the TST) faster than the low caliber players, which corresponds to a 0.56 m/s increased average skating velocity (high caliber: 6.90 m/s, low caliber: 6.34 m/s). This highlights a clear distinction in terms of the skating performance. The first hypothesis was confirmed by the main effects of player caliber for SP and CT. The increased SP and shorter CT of high caliber players is in line with previous findings on the level of lower limb joint kinematics (Buckeridge et al., 2015; Renaud et al., 2017; Upjohn et al., 2008), CoM movement (Renaud et al., 2017), plantar force application (Buckeridge et al., 2015) and muscle activation pattern (Buckeridge et al., 2015). In particular, the 22% increased SP (average increase) of high caliber players highlights their skills to apply a relatively large impulse to the body's center of mass when compared to the recreational player. Leg strength is of importance in this context, as previous studies have either linked differences between high and low caliber players (Buckeridge et al., 2015; Upjohn et al., 2008) or identified leg power measures (e.g. long jumps) as predictors of skating sprint performance (Farlinger et al., 2007). As reported for the sprint start in running (Mero et al., 1992), high caliber players have the ability to generate maximal forward acceleration to attain high forward velocity of the CoM.
High caliber players also showed a decreased CT, which goes along with an increased swing phase duration (Pearsall et al., 2000). The finding of a decreased CT for high caliber players is in agreement with the findings for other temporal

variables (e.g. double-support time). Renaud et al. (2017) found a decreased double-support time for high caliber players in comparison with low caliber players. The coupling between the biomechanical changes with respect to the skating performance (TST) can be described as follows: A high propulsive power (i.e. increased SP) is necessary to skate fast. Therefore, the consequence of skating with a higher power leads to a change in the timing characteristic of the stride. The contact phase decreases (i.e. shorter CT), while the swing phase increases in order to not compromise stride rate/time. This results in having a higher stride propulsion, which leads to a change in timing characteristics, and ultimately, a higher skating performance as shown for high caliber players (i.e. shorter TST). The described coupling is supported by studies in cross-country skiing (Nilsson et al., 2004) and roller skating (Lindinger et al., 2009), which highlighted similar relationships between biomechanical variables and skating performance.

3.5.2 Differences across sprint phases

In terms of the comparison between the two stride types, significant differences were seen for CT and ST as well as for the SP. These findings confirm hypothesis two. Substantial biomechanical differences between the accelerative and steady-state sprint phase were revealed and provide evidence that the accelerometer-derived variables are sensitive to modifications in skating technique. Our results confirm earlier studies in ice hockey skating related areas, such as speed skating and cross-country skiing, which showed the sensitivity of accelerometers to capture biomechanical skating variables and distinguish skating technique (Myklebust et al., 2014, 2015; van der Kruk et al., 2016). Differences in the movement strategies between the two sprint phases of forward skating have been shown in ice hockey (Buckeridge et al., 2015; Stidwill et al., 2009) and speed skating (De Koning et al., 1995) studies. The observed increase in the SP correspond well with the larger plantar push-off force during the initial sprint phase shown by Buckeridge et al. (2015) and underline the increased propulsive demands for a running-like motion compared to a gliding motion. During the accelerative phase, the player pushes against a fixed point on the ice, in order to increase the skating velocity (De Koning et al., 1995). During the constant velocity phase, the skater can typically take advantage of a gliding push-off technique (De Koning et al., 1995), which corresponds to a longer CT and ST.

3.5.3 Biomechanics and sprint performance

The three analyzed biomechanical variables showed varying levels of association with the skating performance. Our third hypothesis was not supported, as the correlation results indicated only for SP a strong relationship to the total sprint time. The negative correlations ($r_{acc} = -0.57$, $r_{ss} = -0.44$) between the SP and the TST has shown that a higher stride intensity is associated with a higher performance (i.e. shorter sprint time). In light of the importance attributed to SP by our analysis, the results of the present study are consistent with the results of Farlinger et al. (2007), who identified primary leg power variables in off-ice tests (e.g. off-ice sprint and 3 hop jumps) as the best predictors of on-ice skating performance. The derived SP from the acceleration of a single sensor positioned on the lower back, nearby the position of the CoM, can provide useful information as an intensity measure for an in-field skating performance evaluation. As stated by Myklebust et al. (2014) for skiing, such measures are suitable for direct feedback systems, comparison of different level of athletes in the field, documenting development of technique over time, and also detecting changes in technique due to fatigue.

CT showed positive correlations at moderate strength with TST ($r_{acc} = 0.42$, $r_{ss} = 0.34$), which indicates that a shorter total sprint time was reached with a shorter CT. Due to low correlations between the ST and TST ($r_{acc} = 0.25$, $r_{ss} = 0.16$), ST was not a clear indicator for high skating performance. This is in accordance with the absence of a significant group effect for ST between low and high caliber player. However, similar as shown for running (Buchheit et al., 2015), temporal variables could be beneficial for monitoring acute neuromuscular fatigue and serve as fatigue-sensitive measures.

Overall, our results showed higher correlations with the total sprint time for acceleration strides than for maximum velocity strides. These results demonstrate the accelerative phase as a key portion of forward skating, which has been highlighted in previous studies (Buckeridge et al., 2015; Marino, 1995; Renaud et al., 2017). The accelerative phase requires high mechanical power so as to overcome inertia. Greater propulsive capabilities can lead to larger initial propulsion. In addition, the accelerative phase of skating is considered to be crucial to a player's success in a game situation (Renaud et al., 2017) and emphasized in skill development (Marino, 1995), thus supporting the higher association of accelerative strides with skating performance.

3.5.4 Limitations

The players needed to carry a backpack with data acquisition equipment (total mass approximately 4 kg), which could have limited them in their usual skating style. However, the natural hockey setting was mimicked by wearing essential security gear and skating with a stick, as per their natural skating environment. Participants gave subjective feedback that they felt no constraints in their skating style caused by the test setting or equipment.

Although care was paid to the fixation of the accelerometers to limit their oscillations and any misalignment, we cannot fully ensure that the fixation technique excluded this source of error due to the explosive task and an eventual loosening of tape across the lumbar accelerometer. However, in order to control for this issue, the attachment of the accelerometer was checked periodically and replaced when necessary.

The SP was calculated on acceleration data in all three axes of the accelerometer on the lower back. Therefore, a differentiated consideration of acceleration caused by a high propulsive effort in forward direction and acceleration due to an inefficient skating technique (e.g. vertical motion of the CoM) is not possible. This combined consideration of the 3D acceleration for the estimation of the propulsion power of a skating stride is a potential limitation of the study. Future studies could focus on the quantification of energy fluctuations during skating. In this context, the coupling of accelerometers with gyroscopes could help to estimate the displacement of the CoM in vertical, sideward and forward direction (Myklebust et al., 2015). Advantages of the combined consideration of the 3D acceleration are the prevention of inaccuracies due to the discrepancy between the movement in a global coordinate system and the sensing of acceleration with an accelerometer attached to a part of the body (Kavanagh & Menz, 2008) as well as the prevention of inaccuracies when estimating and analysing linear velocity and displacement by numerical integration of acceleration signals (Camomilla et al., 2018). It must be noted that it remains unknown to what extent the lower back located accelerometer can capture the actual acceleration of the CoM. As stated by Myklebust et al. (2015), CoM variables estimated from a lower back located accelerometer does not take into account the movement of the upper limbs. Nevertheless, SP provided a clear distinction between high and low caliber players and showed a high relationship to skating performance, which can be valuable in in-field diagnosis without requiring cumbersome setup.

3.6 Conclusions

This study demonstrated the use of two body worn 3D accelerometers to perform biomechanical performance analysis of ice hockey skating. The results highlight the feasibility of obtaining skating performance data from body worn accelerometers. Based on the findings of this study further investigations are warranted, which aim to monitor biomechanical performance variables, such as SP, over a longer period of time (e.g. training session) and at various levels of intensity, and the analysis of different ice hockey-related movement tasks. In a first step, the combination of a biomechanical performance variable extraction, as presented in this paper, combined with an automated stride detection would be advantageous. It could be interesting to measure temporal events bilaterally, whereby the time play between both legs can be analyzed, and variables such as the double support time could be extracted. As a consequence, the quality of training and player development can benefit from wearable performance sensors.

4 Study III – Estimation of knee joint forces in sport movements

Published as

Stetter, B. J., Ringhof, S., Krafft, F. C., Sell, S. & Stein, T. (2019b). Estimation of knee joint forces in sport movements using wearable sensors and machine learning. *Sensors*, 10(8), 7772–7788.

Acknowledgments

We would like to thank Marian Hofmann for recommendations on machine learning and helpful discussion. We also thank Cagla Fadillioglu for her support on data processing. We acknowledge support by the KIT-Publication Fund of the Karlsruhe Institute of Technology.

4.1 Abstract

Knee Joint Forces (KJFs) are biomechanical measures used to infer the load on knee joint structures. The purpose of this study is to develop an Artificial Neural Network (ANN) that estimates KJF during sport movements, based on data obtained by wearable sensors. Thirteen participants were equipped with two Inertial Measurement Units (IMUs) located on the right leg. Participants performed a variety of movements, including linear motions, changes of direction, and jumps. Biomechanical modelling was carried out to determine KJF. An ANN was trained to model the association between the IMU signals and the KJF time series. The ANN-predicted KJF yielded correlation coefficients that ranged from 0.60 to 0.94 (vertical KJF), 0.64 to 0.90 (anterior-posterior KJF) and 0.25 to 0.60 (medial-lateral KJF). The vertical KJF for moderate running showed the highest correlation (0.94 ± 0.33). The summed vertical KJF and peak vertical KJF differed between calculated and predicted KJF across all movements by an average of $5.7\% \pm 5.9\%$ and $17.0\% \pm 13.6\%$, respectively. The vertical and anterior-posterior KJF values showed good agreement between ANN-predicted outcomes and reference KJF across most movements. This study supports the use of wearable sensors in combination with ANN for estimating joint reactions in sports applications.

4.2 Introduction

Knee pain and injury are common problems in both elite and recreational athletes in team and individual sports, and represent a large part of the costs of medical care (de Loes et al., 2000). Studies have highlighted that team sports that involve start-stop movements, rapid changes in direction, intense jumps and landings are prone to knee injuries (Weiss & Whatman, 2015; Hootman et al., 2007). Furthermore, epidemiological studies in team sports (Ingram et al., 2008) and individual sports, such as running (Taunton et al., 2002), found the knee to be one of the most frequently injured parts of the human body. The knee, as an important load-bearing joint in the body, undergoes huge stress during activities, due to the multidirectional forces exerted on the joint (Besier et al., 2001; D'Lima et al., 2012, 2008; Mündermann et al., 2008). Therefore, forces transmitted by the knee are of great significance, as they provide a resource to estimate the internal loading of the anatomical structures (e.g., bones) (Umberger & Caldwell, 2014; Vanrenterghem et al., 2017).

A common way of assessing the load on internal anatomical structures is through the use of biomechanical modelling. Inverse dynamics can be calculated by means of three-dimensional (3D) motion capture and force plate data (Whittlesey & Robertson, 2014). Inverse dynamics studies have been carried out to determine knee kinetics during various movements, such as walking (Morgenroth et al., 2014; Stief et al., 2008), running (Stief et al., 2008; Cole et al., 1996), cutting (McLean et al., 2004; Kaila, 2007), and jumping (Milner et al., 2011; Sell et al., 2006). It must be noted that two different types of knee forces can be calculated by means of biomechanical modelling. First are net joint forces (also termed as joint intersegmental forces or joint reaction forces), calculated using the traditional Newton-Euler inverse dynamics method (Whittlesey & Robertson, 2014; Zajac et al., 2002); second are joint contact forces, representing the sum of the net joint forces and the compressive joint forces (Umberger & Caldwell, 2014; Zajac et al., 2002; Shelburne et al., 2006). The compressive joint forces are mainly caused by muscle forces, and can be obtained via musculoskeletal modelling (Umberger & Caldwell, 2014; Zajac et al., 2002; Shelburne et al., 2006). Knee joint contact forces have additionally been measured in vitro by means of an instrumented implant (D'Lima et al., 2008; Mündermann et al., 2008). Therein, it was shown that knee joint contact forces are closely related to the activity (D'Lima et al., 2008; Mündermann et al., 2008). High-impact activities, such as tennis, generate peak tibial forces of up to four times the body weight (D'Lima et al., 2008). Net joint forces underestimate the actual internal load, but their determination require less complex modelling (Umberger & Caldwell, 2014; Zajac et al., 2002). However, neither the biomechanical modelling nor direct force measurement can be readily added to an athletes' natural sports environment.

As a consequence, alternative technologies, such as wearable Inertial Measurement Units (IMUs), have experienced tremendous advances within the last two decades (Chambers et al., 2015; Camomilla et al., 2018). The integration of such sensors into sports equipment (e.g., shoes) or attachment to an athlete has allowed the assessment of temporal, kinematic, and dynamic parameters (Camomilla et al., 2018). The recent review by Camomilla et al. (2018) highlighted the potential of wearable inertial sensors for sports performance evaluation. However, performance indicators are not necessarily appropriate to characterize the loads on specific body structures, especially joints. The estimation of

biomechanical variables has not yet been fully established, primarily due to the difficulty in assessing external forces (Camomilla et al., 2018).

Recently, estimating the Ground Reaction Force (GRF) by means of wearable sensors has gained more attention (Ancillao et al., 2018; Shahabpoor & Pavic, 2018). The majority of applied methods require modelling of the musculoskeletal system to a certain extent, which requires subject-specific data (e.g., mass, dimensions, and center of mass of the body segments), which inevitably introduce inaccuracies and uncertainty (Ancillao et al., 2018; Karatsidis et al., 2017; Guo et al., 2017). As a consequence, several studies have explored modern machine learning techniques to simplify modelling and data acquisition strategies (Guo et al., 2017; Wouda et al., 2018; Leporace et al., 2015). The recent study by Wouda et al. (2018) presented an Artificial Neural Network (ANN) approach to estimate vertical GRF during running, based on vertical accelerations and lower limb joint angles. The estimated GRF profiles of the non-personalized ANN showed a high correlation (> 0.90) with the actual force time series. Guo et al. (2017) used directly-measured acceleration signals without providing joint kinematics, as well as a slightly different model (nonlinear, autoregressive moving average model with exogenous inputs) to estimate vertical GRF during walking. In this study, a minimum model prediction error of 3.8% was shown when comparing the predicted vertical GRF time series to data measured directly from pressure insoles. Although the studies described above have estimated forces during locomotion, no study has yet performed a direct estimation of knee joint forces; these are of paramount importance, as the GRF is not necessarily an accurate predictor of knee joint loading, due to modulations within the kinetic chain of the lower extremity (Morgenroth et al., 2014; Cole et al., 1996; Matijevich et al., 2019).

In summary, having a field-based method to quantify and monitor knee joint forces in the field is of substantial importance from two viewpoints: (i) studying the relationship between force measures and injury helps to establish effective injury prevention strategies; and (ii) to monitor an athlete's workload is important in setting up effective training programs, which provide an adequate training stimulus while minimizing the risk of non-functional overreaching (e.g., pain). Providing this feedback to athletes, coaches, and physicians is highly relevant, especially during rehabilitation after an injury.

Therefore, the purpose of this study was to develop an ANN that estimates net

knee joint forces during sport movements, based on data obtained by wearable sensors. The findings of this study could help to overcome current restrictions in the mobile assessment of knee joint forces and open new possibilities for in-field diagnosis, which could help to provide better injury prevention strategies in the future.

4.3 Materials and methods

4.3.1 Participants

A total of 13 healthy male sport students (age: 26.1 $\pm$ 2.9 years; height: 178.7 $\pm$ 5.5 cm; body mass: 78.4 $\pm$ 5.9 kg) voluntarily participated in this study. None reported recent injuries. The study was approved by the ethics committees of the Karlsruhe Institute of Technology. All participants were informed of the experimental procedures and gave informed written consent prior to the test.

4.3.2 Measurement protocol

All participants came once to the institutional motion analysis laboratory. After signing the study documents, anthropometric measurements were taken, and the data collection equipment was attached. After warming up by running on a treadmill for 5 min at a self-selected speed, participants were instructed to perform a variety of sport-specific movements, including moderate running; fast running; running 90° clockwise turns; running 90° counterclockwise turns; sprint start; full-stop after sprinting; left-sided cutting maneuver; right-sided cutting maneuver; side shuffle cut; straight ahead walking; walking 90° clockwise turns; walking 90° counterclockwise turns; one-leg horizontal jumps (submaximal; distance = 50% body height); and maximal, two-leg, vertical counter movement jumps. For a detailed description of the cutting maneuver (called a "v-cut") and side shuffle cut, see Neptune et al. (1999). The 90° turns were carried out following Krafft et al. (2015).

4.3.3 Measurement setup

Full-body kinematics were recorded with a marker-based motion capture system (11 MX-13 cameras, 200 Hz, Vicon, Oxford, UK). A total of 42 spherical reflective markers were placed on the participants' skin using the ALASKA Dynamicus protocol (ALASKA, INSYS GmbH, Germany). 3D GRF data were collected simultaneously from two plates (1000 Hz; AMTI Inc., Watertown, MA,

USA) embedded in the floor and centered in the capture volume. Two identical, custom-built, six-degrees-of-freedom IMUs (1500 Hz, ± 8 g accelerometer, $\pm 2000\ ^\circ/s$ gyroscope) were attached to each participant's right leg via a knee sleeve, in order to capture IMU signals related to knee kinematics and dynamics. The IMUs were positioned at the upper and lower frontal end of the sleeve (Figure 4.1), and connected to a data acquisition unit. The data collecting systems were synchronized during post-processing by an analog signal, induced by the 3D motion capture system each time data acquisition was initiated.

Figure 4.1: Placement of Inertial Measurement Units (IMUs) used in the study. The IMUs were positioned in the two black patch pockets at the upper and lower frontal end of the sleeve.

4.3.4 Data processing and biomechanical modelling

The 3D trajectories of the markers were reconstructed using Vicon Nexus V1.8.5. After 15 Hz low-pass filtering (Butterworth fourth-order filter) of the 3D marker coordinates and GRF data (Härtel & Hermsdorf, 2006), net Knee Joint Force (KJF) (F_v = vertical, F_{ap} = anterior–posterior, and F_{ml} = medial–lateral component) were determined via inverse dynamic modelling, using the full-body Dynamicus 9 model (Härtel & Hermsdorf, 2006; Willwacher et al., 2017). Each participant was individually modeled as a linked-segment model based on standardized anthropometric measures (Robertson, 2014). By means of the recorded

full-body kinematics and external forces, inertial net forces were calculated (Whittlesey & Robertson, 2014). A 20 N threshold of the vertical GRF was used to extract the stance phase for each locomotion movement (Milner & Paquette, 2015). Two separate stance phases were extracted for the jumps. The first represented take-off, starting at the time point when vertical GRF undercut the body weight, and ending when vertical GRF was zero (beginning of the flight phase). The second stance phase represented the landing, starting when vertical GRF was greater than zero (end of the flight phase), and ending when vertical GRF equaled body weight. As a consequence, each of the two jump forms consisted of two conditions, whereas the other twelve movements consisted of one condition. Ten trials were excluded from the inverse dynamic calculation, due to measurement errors of the 3D motion capture system, resulting in a total of 198 trials (13 participants' x 16 conditions $-$ 10 invalid trials).
The IMU signals were also filtered (Butterworth fourth-order filter; cut-off frequency of 15 Hz) and each trial was cropped to contain data for the same phase as the KJF. Subsequently, the KJF time series and IMU signals were organized to represent 0%–100% of the stance phase. Finally, an IMU signal matrix and a KJF matrix were created by vertically concatenating the IMU signals and KJF time series, respectively, of all the trials. Both matrices contained 19,800 rows (198 trials x 100 time points), with 12 columns for the IMU signal matrix (six acceleration signals $+$ six angular velocity signals) and three columns for the KJF matrix (three spatial dimensions).

4.3.5 Neural network modelling

The ANN developed for this study maps the IMU signals of all movements to the KJF time series of all movements, and was set up with the Neural Network Toolbox in MATLAB R2018b (The MathWorks, United States). The IMU signal matrix served as the input and the KJF matrix served as the target (output). Thus, the ANN had 12 variables (i.e., nodes) in its input layer and three variables in its output layer. The ANN had two hidden layers, one with 250 and one with 100 neurons, which were connected to the input and output nodes (Wouda et al., 2018). The ANN was trained with a Levenberg-Marquardt, back-propagated error correction, and a random division of 70/15/15 was used for the respective training/validation/testing. Hyperbolic tangent sigmoid activation functions were defined between the hidden layers. The network was trained for 1000

iterations, and training was stopped if the gradient did not decrease for six consecutive iterations, or if the gradient was smaller than $1\ x\ 10^{-6}$. Evaluation of the ANN was done using a leave-one-subject-out cross-validation, in order to assess the performance of a non-personalized model. The cross-validation involved training the ANN with all trials from 12 participants (i.e., the training set), and then testing with the trials from the remaining participant (i.e., the test set).

4.3.6 Statistical analysis

For each movement, the similarity between the ANN-predicted KJF time series (F_v^*, F_{ap}^* and F_{ml}^*) and the calculated inverse dynamics (F_v, F_{ap} and F_{ml}) was assessed using Pearson's correlation coefficient (r) and relative Root-Mean-Squared Error (rRMSE) (Ren et al., 2008). The averages and standard deviations from the 13 cross-validation subsets were calculated for r and the rRMSE. A Fishers z-transformation of r was performed to calculate the mean correlation coefficient. Mean values were expressed as r by reversing the transformation. Additionally, classical discrete biomechanical metrics of knee loading were evaluated by means of peak F_v and summed F_v over the stance phase. *%Diff* between ANN-predicted peak F_v, inverse-dynamic calculated peak F_v, and summed F_v were used to provide a pragmatic interpretation.

4.4 Results

Table 4.1 shows an overview of the estimated accuracy for all movements. The ANN-predicted KJF yielded r values that ranged from 0.60 to 0.94 (F_v^* vs. F_v), 0.64 to 0.90 (F_{ap}^* vs. F_{ap}) and 0.25 to 0.60 (F_{ml}^* vs. F_{ml}) for the different movements. F_v^* for moderate running showed the highest correlation with F_v (0.94 ± 0.33). The rRMSE between F_v^* and F_v, F_{ap}^* and F_{ap}, and F_{ml}^* and F_{ml} ranged between 14.2% and 25.9%, 17.4% and 27.1%, and 27.7% and 45.9%, respectively. The estimation of F_v for moderate running and walking yielded the lowest rRMSE (14.2% each). The time series of estimated KJF are shown in Figure 4.2 for three representative movements (moderate running, walking a 90° counterclockwise turn, and a one-leg horizontal jump take-off). The KJF time series of all movements are provided as Supplementary Material (S1).

Results of the discrete outcomes (peak F_v and summed F_v) are presented in Table 4.2. The mean peak F_v difference between ANN-predicted and the ref-

Table 4.1: Accuracy (r: Pearson's correlation coefficient; rRMSE: relative root-mean-squared error) of the predicted continuous knee joint force outcomes (vertical (F_v^*), anterior–posterior (F_{ap}^*), and medial–lateral (F_{ml}^*)). Values are presented as mean (and standard deviation).

Movement task	Component					
	F_v^*		F_{ap}^*		F_{ml}^*	
	r	rRMSE [%]	r	rRMSE [%]	r	rRMSE [%]
Moderate running	0.94 (0.33)	14.2 (4.0)	0.90 (0.30)	18.9 (5.5)	0.43 (0.26)	41.7 (11.5)
Fast running	0.89 (0.43)	20.3 (5.8)	0.88 (0.44)	22.9 (9.5)	0.42 (0.41)	43.4 (12.0)
Running 90° clockwise turn	0.89 (0.40)	17.2 (4.0)	0.82 (0.36)	21.0 (6.5)	0.38 (0.35)	36.7 (18.4)
Running 90° counter-clockwise turn	0.87 (0.35)	17.5 (5.3)	0.88 (0.43)	19.5 (8.1)	0.37 (0.42)	37.2 (11.5)
Sprint start	0.73 (0.45)	25.9 (8.8)	0.76 (0.40)	25.8 (9.3)	0.31 (0.29)	43.3 (10.0)
Full-stop	0.78 (0.45)	24.7 (7.2)	0.80 (0.34)	21.8 (7.5)	0.45 (0.29)	37.7 (9.0)
Left-sided cutting maneuver	0.86 (0.44)	19.4 (6.6)	0.86 (0.41)	22.0 (7.3)	0.30 (0.42)	44.8 (13.0)
Right-sided cutting maneuver	0.86 (0.39)	19.0 (5.4)	0.84 (0.35)	21.5 (5.2)	0.25 (0.39)	45.7 (9.0)
Side shuffle cut	0.79 (0.47)	20.4 (6.6)	0.81 (0.43)	19.8 (6.0)	0.35 (0.45)	36.5 (9.3)
Walking	0.87 (0.32)	14.2 (4.3)	0.71 (0.39)	20.8 (5.6)	0.60 (0.31)	27.7 (5.7)
Walking 90° clockwise turn	0.81 (0.27)	16.9 (4.5)	0.65 (0.31)	23.0 (6.2)	0.31 (0.20)	34.1 (8.1)
Walking 90° counter-clockwise turn	0.83 (0.29)	15.3 (4.0)	0.64 (0.30)	22.7 (5.8)	0.48 (0.34)	29.1 (6.0)
One-leg jump take-off	0.92 (0.39)	15.4 (6.6)	0.89 (0.25)	17.4 (5.5)	0.31 (0.46)	45.9 (19.7)
One-leg jump landing	0.84 (0.43)	16.7 (7.2)	0.77 (0.53)	25.1 (9.4)	0.42 (0.38)	38.9 (14.4)
Two-leg jump take-off	0.60 (0.36)	23.0 (8.6)	0.82 (0.40)	20.5 (7.4)	0.51 (0.23)	27.8 (2.9)
Two-leg jump landing	0.61 (0.34)	25.9 (6.2)	0.65 (0.36)	27.1 (5.5)	0.54 (0.32)	37.6 (6.8)
Mean	0.82 (0.10)	19.1 (4.0)	0.79 (0.09)	21.8 (2.6)	0.40 (0.10)	38.0 (6.1)

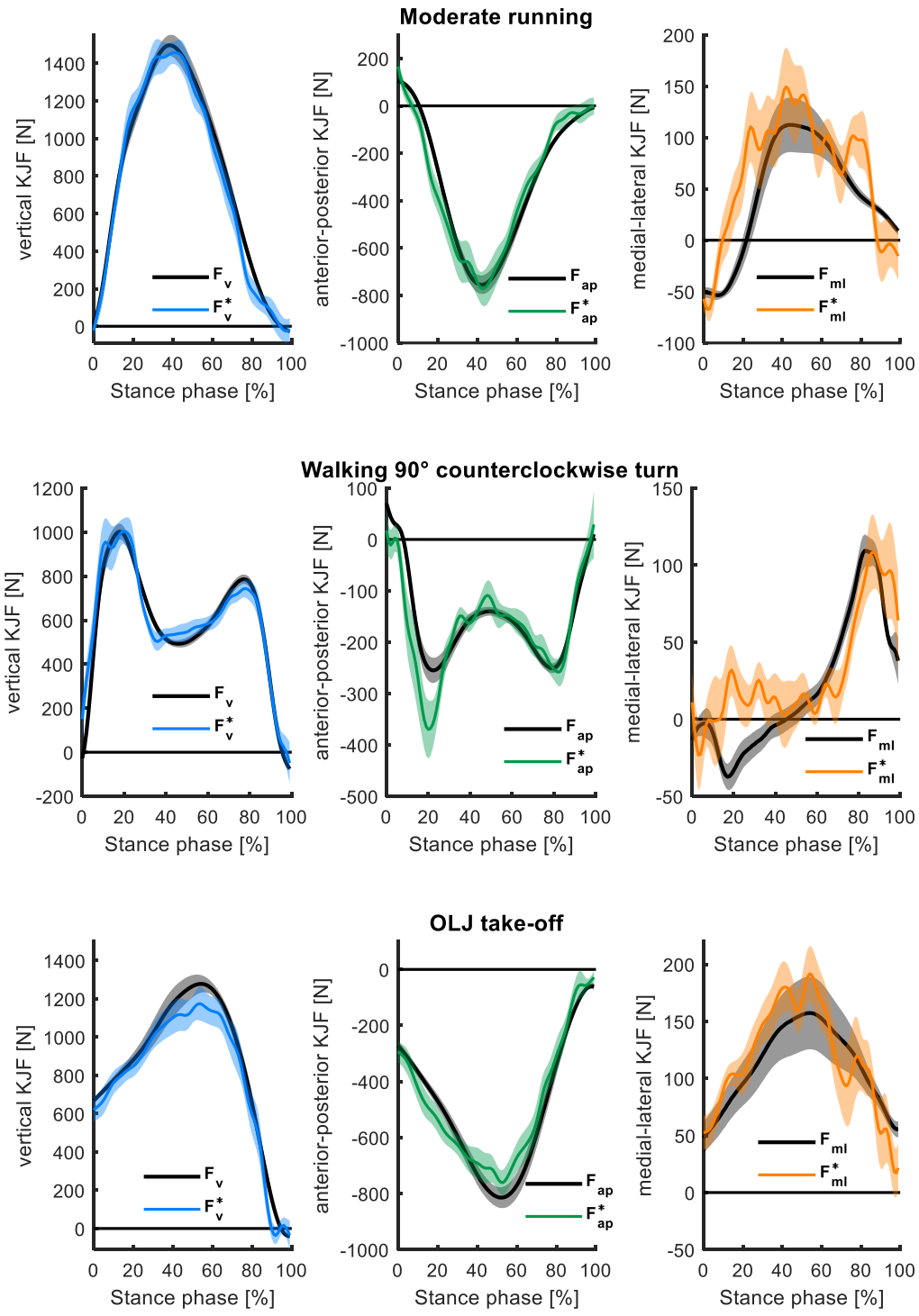

Figure 4.2: Mean (and standard error) of the estimated three-dimensional (3D) Knee Joint Force (KJF) (F_v^*, F_{ap}^*, and F_{ml}^*) for moderate running (top), walking a 90° counterclockwise turn (middle), and One-Leg horizontal Jump (OLJ) take-off are presented (normalized to the stance phase), compared to their respective reference values (inverse dynamics-calculated knee joint forces F_v, F_{ap}, and F_{ml}).

erence values across all movements was 17.0% ± 13.6%. The smallest *%Diff* values were seen for side shuffle cut (2.6% ± 19.3%). Differences between the ANN-predicted and the reference values were smaller for the summed F_v (mean differences across all movements = 5.7% ± 5.9%) compared to the peak F_v (mean differences across all movements = 17.0% ± 13.6%). Of the 16 movements, 13 had a *%Diff* for summed F_v smaller than 6.8%. Two-leg jump take-off and landing yielded substantial differences for both metrics (*%Diff* peak $F_v \geq$ 22.9%; *%Diff* summed $F_v \geq$ 16.1%).

Table 4.2: Absolute Percent Differences (*%Diff*) between ANN-predicted peak, inverse dynamic-calculated peak, and summed vertical knee joint force (F_v). The superscript minus indicates an underestimation of the ANN.

Movement task	Discrete biomechanical metrics	
	Peak F_v	Summed F_v
	%Diff	*%Diff*
Moderate running	10.0 (12.8)	3.0 (11.0)$^-$
Fast running	16.1 (34.2)	2.8 (15.5)$^-$
Running 90° clockwise turn	17.4 (36.3)	6.8 (15.2)$^-$
Running 90° counter-clockwise turn	19.3 (28.0)	2.3 (9.6)$^-$
Sprint start	24.9 (26.7)	1.5 (31.0)$^-$
Full-stop	3.3 (23.3)	2.6 (32.0)$^-$
Left-sided cutting maneuver	21.0 (25.6)	0.8 (15.8)
Right-sided cutting maneuver	17.2 (20.2)	1.9 (16.4)
Side shuffle cut	2.6 (19.3)$^-$	15.0 (7.3)$^-$
Walking	13.8 (16.2)	0.9 (9.3)
Walking 90° clockwise turn	8.7 (12.6)	2.1 (12.7)
Walking 90° counter-clockwise turn	19.5 (24.5)	2.6 (7.5)
One-leg jump take-off	8.0 (18.7)	6.5 (17.0)$^-$
One-leg jump landing	6.4 (12.6)$^-$	6.1 (10.5)$^-$
Two-leg jump take-off	60.8 (59.8)	16.1 (31.2)
Two-leg jump landing	22.9 (34.7)	19.5 (30.0)
Mean	17.0 (13.6)	5.7 (5.9)

4.5 Discussion

This study investigated the feasibility of an ANN approach to estimate KJF during sport-specific movements based on data from two IMUs. Mobile assessment of KJF allows measurement of biomechanics outside the laboratory. The accuracy of ANN estimation of various common sport-specific movements was

compared to standard inverse dynamic-calculated KJFs.

The results indicated that the estimation accuracy of the ANN varied between movements, but that accuracy was good for most movements. With respect to the three different force components, vertical KJF showed the highest agreement between the ANN-predicted outcomes and the inverse dynamics-calculated data, followed by the anterior–posterior KJF, and finally the medial–lateral. For 13 of the 16 movements, discrete biomechanical measures showed a *%Diff* for summed F_v of less than 6.8%; and 12 of the 16 movements showed a *%Diff* for peak F_v of less than 19.3%.

4.5.1 Comparison of different movements

In general, good agreement ($r \geq 0.81$ and rRMSE $\leq 20.3\%$) was found for F_v of the majority (11 out of 16) of the analyzed movements. Ten of the 16 movements showed comparable estimation accuracies ($r \geq 0.80$ and rRMSE $\leq 22.9\%$) for F_{ap}. However, there was a pronounced drop ($r \leq 0.60$ and rRMSE $\geq 27.7\%$) in estimation accuracy for F_{ml}.

When comparing the estimation accuracy for F_v across the different movements, moderate running had the highest predictive power. Alterations of the running movement, such as running turns and cutting maneuvers, as well as walking forms, showed slight reductions in the estimation accuracy. A potential reason for the higher predictive power of moderate running is the repeatable characteristic of the movement, while other movements are performed with a higher rate of variation (Morgan et al., 1991). Similar changes in estimation accuracy were shown by Fluit et al. (2014) when they evaluated a prediction model for GRFs and moments during various activities of daily living, by means of 3D full-body motion. The limited estimation accuracy for sprint starts, full-stops, and side shuffle cuts may be explained by higher variations in the execution of such movements. Reduced estimation accuracy in continuous outcomes does not necessarily mean an inaccurate estimation of discrete variables, as seen for full stops. However, it must be noted that both variables show a high standard deviation, which indicates a wide dispersion across participants.

Across all movements, differences for summed F_v were lower than for peak F_v. Therefore, estimated peak F_v should be treated with caution. The ANN often overestimated the peak F_v, but slightly underestimated the summed F_v for the majority of the movements. A study by Charry et al. (2013), which investigated

the predictive ability of tibial accelerations to estimate peak vertical GRF in running, showed lower deviations (rRMSE $\approx$ 6%) for comparable discrete variables. However, their method was only applied to training and testing on individuals. Distinct differences (r for take-off: 0.92 vs. 0.60; r for landing: 0.84 vs. 0.61) in estimation accuracy were seen between one-leg jumps and two-leg jumps, respectively. Additionally, a high *%Diff* was seen between ANN-predicted and inverse dynamics-calculated peak F_v and summed F_v for two-leg jumps. One reason for the reduced estimation accuracy for two-leg jumps may be the bipedal characteristic of the movement. Potential inaccuracies in KJF estimations are caused by the distribution of the total external load on both legs. Combining KJF estimations with an activity recognition approach could help to overcome such limitations by selecting individual prediction models for movement categories.

4.5.2 Comparison with related methods

Overall, machine learning-based approaches do not need an a priori knowledge of the model or require modelling of the musculoskeletal system, since they build up their model as they go using training data (Ancillao et al., 2018). It should be noted that ground truth reference data, such as the calculated KJFs by means of biomechanical modelling, are necessary for the model development process. Such methods run on the hypothesis that a relationship exists between the sensor signals measured somewhere on the body and the biomechanical target variable (e.g., KJF) (Ancillao et al., 2018). This is supported by the relationship between acceleration and force, according to Newton's second law of motion, as well as by the relationship between the measured quantities and the segment's motion (Karatsidis et al., 2017; Wouda et al., 2018). There are many studies highlighting the usability of ANN to estimate GRF or joint moments by means of kinematic data obtained from an optical motion analysis system (Ancillao et al., 2018; Hahn & O'Keefe, 2008; Kipp et al., 2018; Oh et al., 2013). In contrast to a machine learning-based approach, kinematics and kinetics of the lower limb joints can be estimated by means of posture information obtained from wearable sensors and an analytical model (Yang & Mao, 2015). Such approaches typically require the modelling of the biomechanical system (e.g., trunk, thigh, shank, and foot) to a certain extent. For the most part, complex modelling is necessary to obtain reasonable results, as discrepancies in subject-specific parameters, such as masses, dimensions, etc., inevitably intro-

duce inaccuracies (Ancillao et al., 2018).

One of the first studies combining wearable sensors and ANN was done by Leporace et al. (2015). Their findings revealed the lowest r in the medial–lateral component when they estimated 3D GRF with an ANN during walking. In the present study, the medial–lateral KJF were also found to have the lowest r value compared to the other two components across all investigated movements. Previous studies estimating the GRF highlighted similar findings and suggested that this was due to the small magnitude of the lateral measurements, which causes a larger impact of small errors on final estimates (Karatsidis et al., 2017; Fluit et al., 2014; Oh et al., 2013). Karatsidis et al. (2017) compared the GRF estimation accuracy of a full-body inertial motion capture and optical motion capture system. Their results showed slightly higher r values (ranging from to 0.82 to 0.99 and 0.76 to 0.99 for the inertial and optical motion capture systems, respectively) and lower rRMSE values (ranging from around 5% to 15% for both systems) for walking than the present study.

Wouda et al. (2018) used a similar machine-learning approach to the one we used for estimating vertical GRF and sagittal knee kinematics during running. The estimated vertical GRF profiles of their non-personalized ANN showed a slightly higher agreement ($r > 0.94$) with the actual force time series for five of their eight participants. One reason for the slightly lower accuracy in our study may be the less specific model with respect to single movements. Overall, a more generic model for multiple movements decreases the performance for some movements (as described above), but provides the advantage that not every movement must be modeled. From a practical point of view, this ultimately enlarges the use. However, it remains unclear if the level of accuracy would be high enough for applications of interest, such as tracking fatigue-related changes, which may be related to increased chance of injury (Halson, 2014). This is especially due to the fact that research in this area is limited, and much of what we know about monitoring comes from personal experience (Halson, 2014). Future research in applied settings would be indispensable to observe and analyze biomechanical risk factors over a defined exposure time, with the ability to influence injury prevention models (Adesida et al., 2019).

4.5.3 Limitations

Attention was paid to the fixation of the IMUs to limit their oscillations and any misalignment; however, we cannot fully ensure that the fixation technique excluded this source of error, due to the explosive characteristic of some tasks. To control for this issue, the exact fit of the sleeve was checked periodically and replaced when necessary. Additionally, the IMUs measure acceleration and angular velocity on the body surface, and relative movements may occur with respect to the bone (Roetenberg et al., 2009). Such movements may negatively affect the estimation of the KJFs, especially for movements that are highly dynamic.

As the estimation accuracy of the proposed approach depends on the neural network architecture, this is a potential limitation of the study. Our ANN was built in accordance with previous work (Wouda et al., 2018), and is capable of mapping non-linearity between input and output; however, we cannot exclude that other model specifications would result in an improved outcome. In addition, a relatively small sample size was used to build the ANN. This represents a limitation of the study, as the robustness of the relationship between the input and output variables of the ANN depends on the amount of training data (Ancillao et al., 2018). The ANN was trained with data from all tested movements. As a consequence, it remains unclear to which extent an ANN built with a subset of movements could estimate KJFs of movements that were not included in the training of the model. It is worth noting that the net KJF used to build the ANN represent only a part of the internal loading of the anatomical structures. Muscles forces, which contribute to the total force transmitted by the joint, were not incorporated in the biomechanical modelling (Umberger & Caldwell, 2014; Shelburne et al., 2006).

In the current approach, direct acceleration and angular velocity measures were input to the ANN. The amplitudes of such signals are sensitive to the placement and fixation technique, as well as participant anthropometrics and soft tissue characteristics (Godfrey et al., 2008). In order to keep potential artefacts low, this study involved only young and healthy male sport students. Further research is necessary to better assess the effects of inter-participant variabilities on input signals for the model building, as well as to translate the results of this study to other age and sex groups or athletes in rehabilitation. Body weight normalization of the KJF time series could help to compensate for variations across

individuals.

4.6 Conclusion

The results of this study show that a machine-learning approach can be very useful to estimate KJF for various movements based on data obtained by two wearable sensors. Specifically, the vertical and anterior–posterior KJF showed good agreement between the ANN-predicted outcomes and inverse dynamic-calculated forces for a variety of movements. However, caution is required for tasks with lower estimation accuracy (e.g., two-leg jumps). It could be helpful to develop individual prediction models for movement categories, such as bilateral tasks, in order to strengthen the overall estimation accuracy. Additionally, a comparison of ANN with different configurations and inputs could help to improve the estimation accuracy, as well as perform a sensor-to-segment calibration for aligning wearable sensors with human body segments. The scaling of input signals (e.g., acceleration signals to body mass) or the normalization of the KJF time series to body weight could help to compensate for inter-individual differences. Future research could focus on the combination of the presented approach with musculoskeletal modelling or with direct force measurements, using an instrumented knee prosthesis. Providing the best means of reference data for the ANN modelling could help to assess the internal loadings on the knee joint structures more precisely. Looking ahead, this study supports the use of wearable sensors in combination with machine-learning techniques for estimating joint reactions in sports applications. Ultimately, this has high practical implications, as new possibilities for in-field diagnosis can help to provide better injury prevention strategies in the future.

5 Study IV – Estimation of joint loading in knee osteoarthritis

Published as

Stetter, B. J., Krafft, F. C., Ringhof, S., Stein, T. & Sell, S. (2020). A machine learning and wearable sensor based approach to estimate external knee flexion and adduction moments during various locomotion tasks *Frontiers in Bioengineering and Biotechnology*, 8, 9.

Acknowledgments

The authors would like to thank Cagla Fadillioglu for her support on data processing. We acknowledge support by the KIT-Publication Fund of the Karlsruhe Institute of Technology.

5.1 Abstract

Joint moment measurements represent an objective biomechanical parameter of knee joint load in Knee Osteoarthritis (KOA). Wearable sensors in combination with machine learning techniques may provide solutions to develop assistive devices in KOA patients to improve disease treatment and to minimize risk of non-functional overreaching (e.g., pain). The purpose of this study was to develop an Artificial Neural Network (ANN) that estimates external Knee Flexion Moments (KFMs) and external Knee Adduction Moments (KAMs) during various locomotion tasks, based on data obtained by two wearable sensors. Thirteen participants were instrumented with two Inertial Measurement Units (IMUs) located on the right thigh and shank. Participants performed six different locomotion tasks consisting of linear motions and motions with a change of direction, while IMU signals as well as full body kinematics and ground reaction forces were synchronously recorded. KFM and KAM were determined using a full body biomechanical model. An ANN was trained to estimate the KFM and KAM time series using the IMU signals as input. Evaluation of the ANN was done using a leave-one-subject-out cross-validation. Concordance of the ANN-estimated KFM and reference data was categorized for five tasks (walking straight, 90° walking turn, moderate running, 90° running turn and 45° cutting maneuver) as strong ($r \geq 0.69$, rRMSE ≤ 23.1) and as moderate for fast running ($r = 0.65 \pm 0.43$, rRMSE = 25.5% $\pm$ 7.0%). For all locomotion tasks, KAM yielded a lower concordance in comparison to the KFM, ranging from weak ($r \leq 0.21$, rRMSE $\geq 33.8\%$) in cutting and fast running to strong ($r = 0.71 \pm 0.26$, rRMSE = 22.3% $\pm$ 8.3%) for walking straight. Smallest mean difference of classical discrete load metrics was seen for KFM impulse, $10.6\% \pm 47.0\%$. The results demonstrate the feasibility of using only two IMUs to estimate KFM and KAM to a limited extent. This methodological step facilitates further work that should aim to improve the estimation accuracy to provide valuable biofeedback systems for KOA patients. Greater accuracy of effective implementation could be achieved by a participant- or task-specific ANN modeling.

5.2 Introduction

Medio-tibiofemoral Knee Osteoarthritis (KOA) is a major cause of disability in elderly people (Hurley et al., 1997) and accounts for high socio-economic burden in industrial countries (Neogi et al., 2009; Reeves & Bowling, 2011; Ferreira

et al., 2015). Symptoms known as knee pain, functional impairment and a loss of mobility, can lead to physical and psychological disability and reduced quality of life (Bennell et al., 2011; Richards et al., 2017).

Mechanical factors, particularly the knee joint load have shown to profoundly influence the severity and progression of KOA (Sharma et al., 1998; Andriacchi & Mundermann, 2006; Foroughi et al., 2009; Bennell et al., 2011; Reeves & Bowling, 2011). A widely used surrogate measure of the compressive load of the medial compartment is the external Knee Adduction Moment (KAM) (Sharma et al., 1998; Bennell et al., 2011; Reeves & Bowling, 2011; Ferreira et al., 2015). Moreover, the Knee Flexion Moment (KFM) has been highlighted as a critical measure to assess the loading of the medial compartment (Walter et al., 2010; Ferreira et al., 2015; Cheung et al., 2018) as well as to quantify the progression of patellofemoral cartilage damage (Teng et al., 2015; Crossley et al., 2016).

Beside other non-pharmacological conservative treatments (e.g., bracing or footwear interventions) (Sarzi-Puttini et al., 2005; Reeves & Bowling, 2011), gait modification approaches by gait retraining therapies (e.g., modifying the foot progression angle) have shown to be effective to reduce the KAM during walking and to improve the symptoms of patients (Barrios et al., 2010; Cheung et al., 2018; Karatsidis et al., 2018). Richards et al. (2017) stated in their systematic review that a strong potential exists for the development of biofeedback systems for reducing KAM and pain and for improving knee joint function in KOA patients. The development of assistive devices (e.g., a smart knee sleeve to monitor the knee load in combination with a smartphone-based user feedback system) could help to provide effective disease-enhancing interventions to slow down the loss of cartilage volume (Shull et al., 2014). Additionally, as exercise is a key component of the KOA management (Bennell et al., 2011; Ferreira et al., 2015; Richards et al., 2017), assistive devices could be beneficial in supporting therapeutical exercise. However, most of the current studies with respect to the assessment of knee joint loading were conducted in a laboratory setting using motion capture and force plate measurements (Barrios et al., 2010; Richards et al., 2017; Cheung et al., 2018). The major shortcoming of such laboratory-based methods is that they cannot be completely included into a patients' habitual environment (Muro-de-la Herran et al., 2014; Shull et al., 2014).

As a consequence, alternative measurement technologies have been provided progressive advances over the past years (Muro-de-la Herran et al., 2014; Wong

et al., 2015). One of the first studies towards a wearable measurement tool was done by van den Noort et al. (2011). The authors tested the effect of an instrumented force shoe in combination with an optoelectronic marker system on target variables (e.g., KAM) in 20 KOA patients. Therein, the authors stated the necessity of additional measurement equipment (e.g., inertial sensors) to obtain joint positions and orientations as a complement to Ground Reaction Force (GRF) measurements in order to calculate the KAM. Karatsidis et al. (2017) compared GRF estimation accuracies of a full-body inertial motion capture and optical motion capture system due to the importance of the GRF measures as input in biomechanical analysis to estimate joint kinetics. Their results showed comparable results between the two systems. Therefore, the authors concluded that the inertial sensor-based system has a high potential in monitoring critical biomechanical parameters in habitual conditions. Yang & Mao (2015) postulated a method for evaluating the intersegmental forces and moments acting on the lower limbs during walking solely based on posture data obtained from seven inertial sensors placed on the lower limbs and trunk in combination with a 3D analytical model. In 2018 Karatsidis et al. proposed and evaluated a wearable visual feedback system for gait retraining using inertial sensing with seven Inertial Measurement Units (IMUs) and augmented reality technologies. The foot progression angle was used for visual feedback and was tracked by the wearable system with a root mean square error of 2.4°, compared to an optical motion capture system. Knee joint kinetics were not analyzed in this study. A further approach of a mobile assessment of knee joint biomechanics in natural environment was recently provided by Konrath et al. (2019). The authors estimated the KAM and the tibio-femoral joint contact force during activities of daily living by means of combining musculoskeletal modeling with inertial motion capture (17 IMUs). The results showed comparable estimation accuracies for the IMU-based approach compared to the same musculoskeletal model using optical motion capture and force plate measurements.

The majority of applied methods require modeling of the musculoskeletal system to a certain degree, with mandatory embedded subject-specific anthropometric data (e.g., mass, dimensions and center of mass of the body segments). However, such modeling processes inevitably introduce inaccuracies (van den Noort et al., 2013; Faber et al., 2016; Ancillao et al., 2018). In contrast, machine learning-based approaches do not need an a priori knowledge of the model as

they build up their model by using training data (Sivakumar et al., 2016; Ancillao et al., 2018; Halilaj et al., 2018). Accurate predictions for new data can be made by learning the relationship between a set of independent variables (e.g., IMU signals) and one or more dependent variables (e.g., KAM) (Lin et al., 2016; Halilaj et al., 2018). Several studies have shown that machine learning techniques, such as Artificial Neural Network (ANN), are powerful tools to deduce biomechanical variables based on measured accelerations or angular velocities of body segments (Leporace et al., 2015; Guo et al., 2017; Ancillao et al., 2018; Wouda et al., 2018; Stetter et al., 2019b). The study by Wouda et al. (2018) used an ANN approach to estimate vertical GRFs and sagittal knee kinematics during running, based on three inertial sensors placed at the lower legs and the pelvis. The estimated force-time profiles and flexion/extension profiles showed high agreement with the optical and GRF reference measure. In a recent study we presented an ANN approach to estimate knee joint forces in sport movements (Stetter et al., 2019b). Good agreement between ANN-estimated outcomes and inverse dynamics-calculated vertical and anterior-posterior knee joint forces were shown, which highlights the feasibility of an ANN approach to estimate internal loadings on the knee joint structures.

Although the above described studies have estimated joint kinematics and kinetics during locomotion, no study has directly estimated biomechanical surrogate measures for knee joint load in KOA using an ambulatory minimal body-worn sensor setup so far. Therefore, the purpose of this study was to develop an ANN that estimates KFM and KAM during various locomotion tasks based on data obtained by two wearable sensors integrated in a knee sleeve. The findings of this study could help to (i) overcome current restrictions in the mobile assessment of knee joint loading in KOA patients and (ii) open new possibilities in diagnosing the patients' habitual life, which could help to improve disease treatment strategies and minimizing the risk of non-functional overreaching (e.g., pain).

5.3 Materials and methods

5.3.1 Participants

The current study used data from the sample presented in Stetter et al. (2019b) and forms a secondary dataset analysis. The sample consisted of thirteen healthy males (age: 26.1 $\pm$ 2.9 years; height: 178.7 $\pm$ 5.5 cm; body mass: 78.4 $\pm$ 5.9 kg). All participants exhibited bowlegs (minimum inter-knee distance of 0.05 m),

which mimics the common varus malalignment of medial KOA patients (Bennell et al., 2011). All participants gave written informed consent in accordance with the Declaration of Helsinki. The study was approved by the ethics committee of the Karlsruhe Institute of Technology.

5.3.2 Experimental protocol

Measurements were performed at the BioMotion Center, Institute of Sports and Sports Science, Karlsruhe Institute of Technology, Karlsruhe, Germany. Two identical custom-built 6DOF IMUs (1500 Hz, $\pm$8 g accelerometer, $\pm$2000 $^\circ/s$ gyroscope) were attached to each participant's right leg while they performed six different locomotion tasks at self-selected speed: walking straight, 90° walking turn, moderate running, fast running, 90° running turn and 45° cutting maneuver. Participants were instructed to perform the 90° turns in clockwise direction. A detailed description of the right orientated cutting maneuver (named as v-cut) is described by Neptune et al. (1999). Participants were instructed to perform at least three successful trials of each task. A trial was considered successful when the right foot landed cleanly within the boundaries of a force plate. The IMUs were positioned in two patch pockets at the upper and lower frontal end of a customized knee sleeve (Figure 5.1). This positioning was chosen in order to capture IMU signals closely related to knee kinematics and dynamics, as the recent study by Matijevich et al. (2019) has highlighted that a targeted approach is necessary to obtain structure-specific loading.

Full body kinematics and GRFs (1000 Hz, AMTI Inc., Watertown, MA) were collected synchronously using a marker-based motion capture system (11 MX-13 cameras, 200 Hz, Vicon, Oxford, UK) in order to perform biomechanical modeling. A total of 42 spherical reflective markers were placed on the participants' body segments in accordance to the ALASKA Dynamicus protocol (ALASKA, INSYS GmbH, Germany) (Härtel & Hermsdorf, 2006; Willwacher et al., 2017). Prior to the attachment of the data collection equipment, standardized anthropometric measurements were exhibited. The measurements consisted of a total of 22 length, width and circumference measures of the body segments. Prior to performing trials, a static calibration trial was recorded for each participant in a natural upright posture.

Figure 5.1: A participant wearing the knee sleeve on the right leg. The two inertial measurement units were placed in the patch pockets at the upper and lower frontal end of the knee sleeve.

5.3.3 Biomechanical model

The 3D marker coordinates and GRF data were reconstructed and filtered with a 15 Hz low-pass filter (zero-phase Butterworth 4th order) (Kristianslund et al., 2012). Inverse dynamics modeling was performed using the full-body Dynamicus 9 model (Härtel & Hermsdorf, 2006; Willwacher et al., 2017). Each participant was individually scaled to the generic linked-segment model using the measured anthropometrics and the static calibration trial (Whittlesey & Robertson, 2014). In a next step, the marker trajectories and GRFs acquired from the dynamic trials were used to determine the Knee Flexion Moment (KFM) and the Knee Adduction Moment (KAM). A 20 N threshold of the vertical GRF was used to extract the stance phase for each locomotion movement (Milner & Paquette, 2015). KFM and KAM time series were time-normalized to 100 time steps representing 0 to 100% of the stance phase. Joint moment amplitudes were normalized to body weight and expressed as external moments.

5.3.4 Machine learning model

ANN modeling was set up with the Neural Network Toolbox in MATLAB R2019a (The MathWorks, USA). The IMU signals were low-pass filtered (zero-

phase Butterworth 4th order filter; cut-off frequency of 15 Hz) and each trial was cropped to contain data for the same phase as the biomechanical data. An IMU signal matrix (rows: 13 participants x three trials x six tasks x 100 time steps; columns: two locations x six spatial dimensions) and a biomechanical data matrix (rows: 13 participants x three trials x six tasks x 100 time steps; columns: two variables) were created by vertically concatenating the IMU signals and KFM and KAM time series of all trials, respectively. An ANN was trained to model the association between the IMU signals and the KFM and KAM time series. The IMU signal matrix served as input and the biomechanical data matrix served as output (target). As a consequence, the ANN had 12 and 2 variables (i.e., nodes) in its input and output layer, respectively. The ANN architecture was inspired by previous work (Favre et al., 2012; Wouda et al., 2018) and had two hidden layers with 100 and 20 neurons, which were connected to the input and output nodes. The hidden layers and the output layer consisted of hyperbolic tangent sigmoid transfer functions and a linear transfer function, respectively. Initialization of the ANN was done using the Nguyen-Widrow initialization function. The ANN was trained for 1000 iterations with Levenberg-Marquardt back-propagated error correction (Moré, 1978) and training was stopped if the gradient did not decrease for 6 consecutive epochs or if the gradient was smaller than $1\ x\ 10^{-6}$. Evaluation of the ANN was done using a leave-one-subject-out cross-validation (Halilaj et al., 2018). The cross-validation involved training the ANN with all trials from 12 participants (i.e., the training set) and then testing with the trials from the remaining participant (i.e., the test set). As cross-dependencies between the input and output in a combined estimation model for KFM and KAM may affect the estimation accuracy (Wouda et al., 2018), independent models for KFM and KAM were also build. Independent models were trained and evaluated in the same manner as the combined model, beside the fact that only one variable was chosen in its output layer.

5.3.5 Statistical analysis

According to previous studies, for each movement, the agreement between the ANN-estimated outcomes (KFM* and KAM*) and the inverse dynamics-calculated data (KFM and KAM) was derived from Pearson's correlation coefficients, which were categorized as weak ($r \leq 0.35$), moderate ($0.35 < r \leq 0.67$), strong ($0.67\ r \leq 0.90$) and excellent ($r > 0.90$) (Taylor, 1990; Fluit et al., 2014;

Karatsidis et al., 2017). Additionally, the Root-Mean-Squared Error (RMSE) and relative Root-Mean-Squared Error (rRMSE) were determined to assess the accuracy of the ANN-estimations (Ren et al., 2008). The rRMSE facilitates the comparison between the different locomotion tasks with different moment amplitudes. The averages and standard deviations were calculated for r, RMSE and rRMSE from the 13 cross-validation subsets. Average r values across participants were computed using Fisher's z transformation (Corey et al., 1998). Mean r values were expressed in the original range from -1 to 1 by reversing the transformation. Furthermore, peak KFM* and KFM* impulse as well as peak KAM and KAM impulse were evaluated as classical discrete load metrics (Bennell et al., 2011; Teng et al., 2015). Impulse represents the area under the corresponding moment-time curve. Percent Differences (*%Diff*) between ANN-estimated and inverse-dynamic calculated peak and impulse metrics were used to provide a pragmatic interpretation.

5.4 Results

5.4.1 Estimated continuous outcomes

The ANN-estimated KFM* and KAM* time series of the whole stance phase are illustrated in Figure 5.2 and Figure 5.3, respectively, with the measured references used for comparison. An overview of the estimated accuracy for all movements is presented in Table 5.1.

For the different locomotion tasks, the ANN-estimated time series revealed moderate to strong correlations for the KFM* and weak to strong correlations for the KAM*. The highest correlation for KFM* and KAM* was observed for moderate running ($r = 0.85 \pm 0.43$; mean $\pm$ standard deviation) and for walking straight (0.71 ± 0.26), respectively. For all locomotion tasks, the RMSE for KFM* was between 0.26 ± 0.09 Nm/kg and 1.13 ± 0.46 Nm/kg, whereas for KAM*, that was between 0.18 ± 0.06 Nm/kg and 0.92 ± 0.54 Nm/kg. The rRMSE for the different locomotion tasks ranged between $17.2\% \pm 3.1\%$ (walking 90° turn) and $25.5\% \pm 7.0\%$ (fast running) for KFM* and between $22.3\% \pm 8.3\%$ (walking straight) and $37.2\% \pm 7.8\%$ (cutting maneuver) for KAM*.

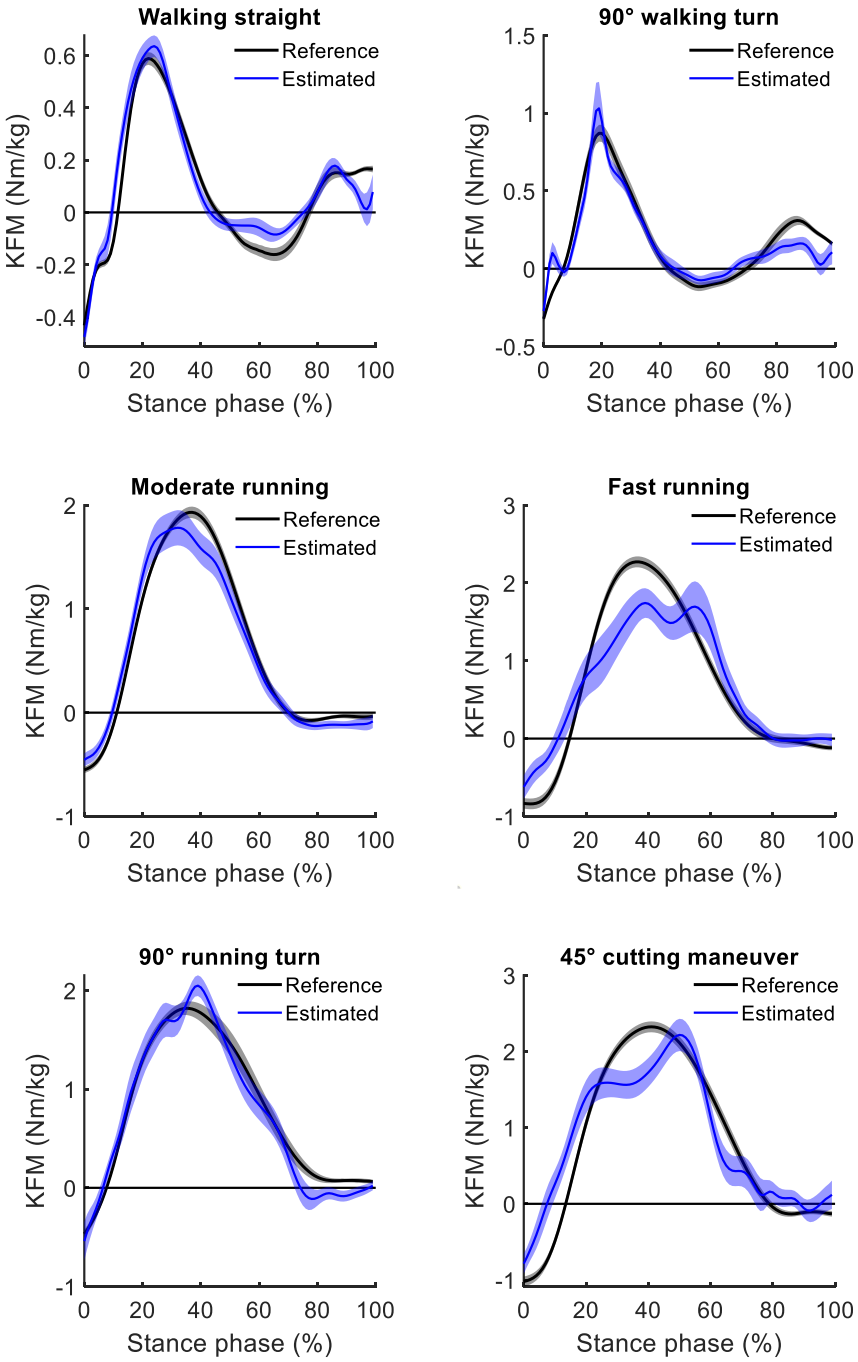

Figure 5.2: Mean (and standard error) of the estimated Knee Flexion Moments (KFMs) (blue) for the six analyzed locomotion tasks compared to their respective inverse dynamics-calculated values (black). Positive values indicate external flexion moments and negative values indicate external extension moments.

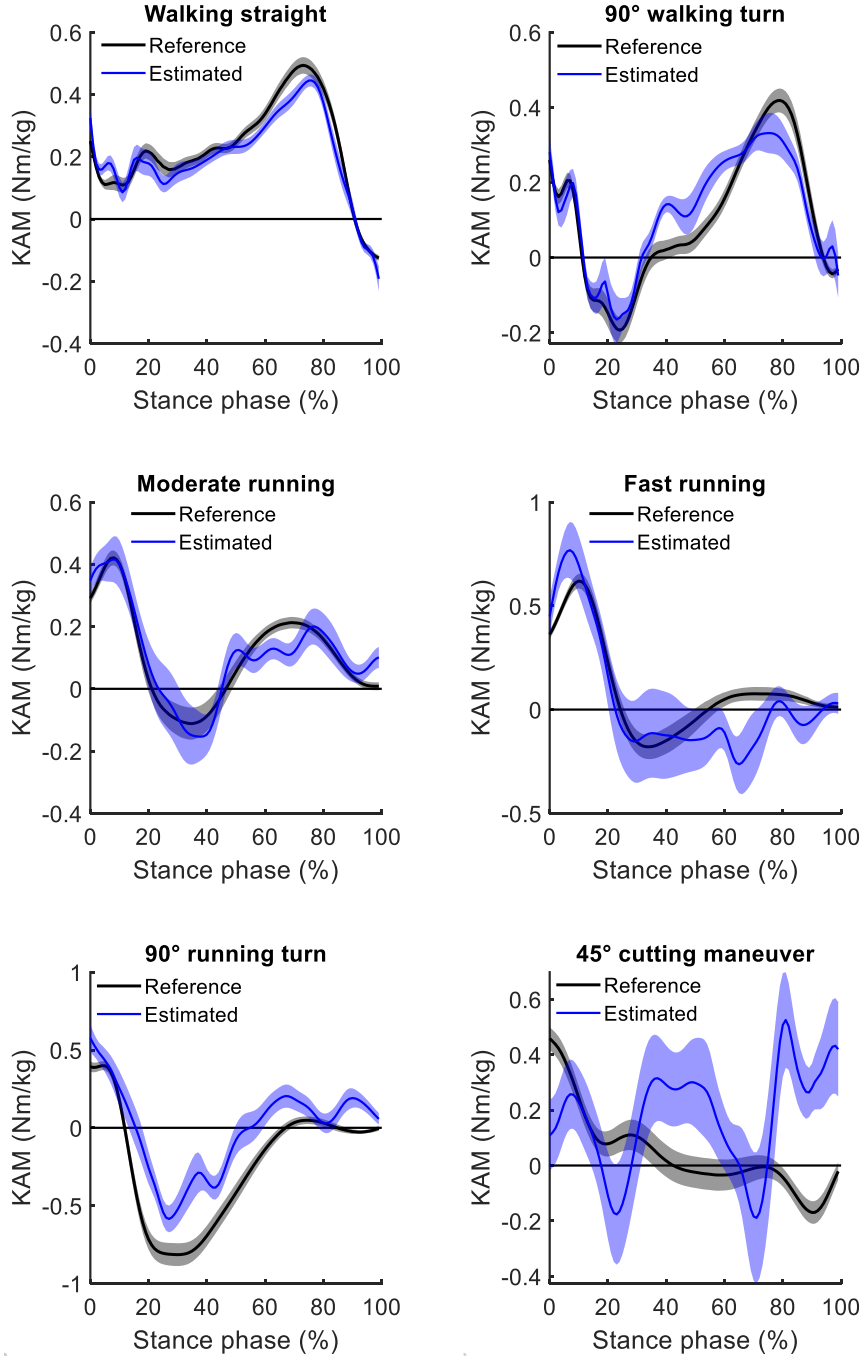

Figure 5.3: Mean (and standard error) of the estimated Knee Adduction Moments (KAMs) (blue) for the six analyzed locomotion tasks compared to their respective inverse dynamics-calculated values (black). Positive values indicate external adduction moments and negative values indicate external abduction moments.

Table 5.1: Accuracy (*r*: Pearson's correlation coefficient; RMSE: root-mean-squared error; rRMSE: relative root-mean-squared error) of the estimated continuous outcomes (knee flexion moment (KFM*), and knee adduction moment (KAM*)). Data are presented as mean ± standard deviations. Mean *r* and *r* standard deviation were computed using Fisher's z transformation.

Locomotion task	KFM*			KAM*		
	r	RMSE [Nm/kg]	rRMSE [%]	*r*	RMSE [Nm/kg]	rRMSE [%]
Walking straight	0.72 ± 0.32	0.26 ± 0.09	18.4 ± 5.3	0.71 ± 0.26	0.18 ± 0.06	22.3 ± 8.3
90° walking turn	0.69 ± 0.31	0.32 ± 0.10	17.2 ± 3.1	0.56 ± 0.33	0.29 ± 0.10	23.9 ± 6.4
Moderate running	0.85 ± 0.43	0.58 ± 0.20	19.7 ± 7.9	0.40 ± 0.35	0.37 ± 0.14	34.4 ± 13.5
Fast running	0.65 ± 0.43	1.13 ± 0.46	25.5 ± 7.0	0.21 ± 0.47	0.80 ± 0.46	33.8 ± 8.5
90° running turn	0.79 ± 0.28	0.77 ± 0.20	20.8 ± 4.5	0.51 ± 0.22	0.62 ± 0.19	27.9 ± 3.9
45° cutting maneuver	0.73 ± 0.41	1.05 ± 0.41	23.1 ± 6.5	-0.05 ± 0.30	0.92 ± 0.54	37.2 ± 7.8
Mean	0.74 ± 0.36	0.67 ± 0.24	20.8 ± 5.7	0.39 ± 0.32	0.53 ± 0.25	29.9 ± 8.1

5.4.2 Discrete load metrics

The inverse dynamics-calculated and ANN-estimated discrete load metrics (peak moments and moment integrals) are shown in Table 5.2. Table 5.3 presents the *%Diff* results for each of the performed locomotion tasks. The 90° walking turn showed the smallest *%Diff* (6.7% ± 31.3%) for the ANN-estimated KFM impulse in comparison to the reference values. In contrast, *%Diff* of KAM impulse were higher with a minimum value of 42.7 ± 108.9% for moderate running. The smallest *%Diff* for the estimation of peak KFM and KAM was 24.7% ± 33.0% (moderate running) and 39.1% ± 101.0% (walking straight), respectively. Across all locomotion tasks, mean differences of peak moments and moment integrals were lower for the KFM* in comparison to the KAM* (40.4% ± 56.5% vs 130.3% ± 157.3% and 10.6% ± 47.0% vs. 161.4% ± 252.8%, respectively).

5.4.3 Model comparison

The changes in estimation accuracy due to independent model building for KFM and KAM for each of the analyzed locomotion tasks is presented in Table 5.4. Independent model building resulted in a lower *r* value for both KFM and KAM in the majority (5 out of 6) of the analyzed locomotion tasks in comparison to the combined estimation model. Across all locomotion tasks, mean RMSE and mean rRMSE increased for KFM* (RMSE = 0.15, rRMSE = 1.18) and KAM*

Table 5.2: Inverse dynamics-calculated (KFM and KAM) and ANN-estimated (KFM* and KAM*) discrete load metrics (peak and impulse). Data are presented as mean ± standard deviations; KFM, knee flexion moment; KAM, knee adduction moment.

Locomotion task	KFM		KAM		KFM*		KAM*	
	Peak [Nm/kg]	Impulse [Nm/kg]	Peak [Nm/kg]	Impulse [Nm/kg]	Peak [Nm/kg]	Impulse [Nm/kg]	Peak [Nm/kg]	Impulse [Nm/kg]
Walking straight	0.67 ± 0.13	45.72 ± 14.52	0.54 ± 0.15	69.16 ± 26.03	0.91 ± 0.30	52.31 ± 24.83	0.65 ± 0.18	64.23 ± 13.76
90° walking turn	1.02 ± 0.38	71.79 ± 36.05	0.57 ± 0.18	44.65 ± 21.96	1.55 ± 1.19	70.12 ± 31.23	0.90 ± 0.44	52.06 ± 17.00
Moderate running	2.03 ± 0.34	193.05 ± 58.08	0.52 ± 0.16	43.48 ± 21.81	2.57 ± 0.92	197.00 ± 90.16	0.84 ± 0.39	56.35 ± 50.26
Fast running	2.49 ± 0.35	246.20 ± 71.51	0.77 ± 0.20	51.35 ± 27.01	3.44 ± 1.92	259.80 ± 118.59	1.72 ± 0.99	91.98 ± 62.78
90° running turn	2.20 ± 0.40	240.28 ± 83.01	0.60 ± 0.17	20.80 ± 6.56	3.12 ± 0.88	253.13 ± 91.06	1.45 ± 0.73	61.94 ± 31.19
45° cutting maneuver	2.52 ± 0.50	284.58 ± 85.73	0.61 ± 0.23	43.97 ± 35.24	3.50 ± 1.29	310.16 ± 144.96	2.11 ± 1.38	120.90 ± 110.35
Mean	1.82 ± 0.79	180.27 ± 98.86	0.60 ± 0.09	45.57 ± 15.56	2.52 ± 1.07	190.42 ± 106.46	1.28 ± 0.57	74.58 ± 26.66

Table 5.3: Percent Differences (*%Diff*) of discrete load metrics (peak and impulse). Data are presented as mean ± standard deviations; KFM, knee flexion moment; KAM, knee adduction moment.

Locomotion task	KFM*		KAM*	
	Peak *%Diff*	Impulse *%Diff*	Peak *%Diff*	Impulse *%Diff*
Walking straight	44.3 ± 70.8	27.4 ± 83.9	39.1 ± 101.0	62.0 ± 253.1
90° walking turn	47.1 ± 60.6	6.7 ± 31.3	82.4 ± 110.5	69.3 ± 127.5
Moderate running	24.7 ± 33.0	0.65 ± 37.2	68.7 ± 94.5	42.7 ± 108.9
Fast running	37.2 ± 68.7	6.8 ± 40.7	123.5 ± 124.1	94.2 ± 145.3
90° running turn	44.9 ± 45.2	12.1 ± 46.5	159.8 ± 157.1	230.0 ± 179.9
45° cutting maneuver	44.1 ± 60.7	10.0 ± 42.6	308.2 ± 356.5	470.0 ± 702.0
Mean	40.4 ± 56.5	10.6 ± 47.0	130.3 ± 157.3	161.4 ± 252.8

Table 5.4: Increase (+) or decrease (–) in estimation accuracy (*r*: Pearson's correlation coefficient; RMSE: root-mean-squared error; rRMSE: relative root-mean-squared error) due to independent model building in comparison to the combined model. KFM*, knee flexion moment; KAM*, knee adduction moment.

Locomotion task	KFM*			KAM*		
	r	RMSE [Nm/kg]	rRMSE [%]	*r*	RMSE [Nm/kg]	rRMSE [%]
Walking straight	0.03	0.00	0.5	–0.2	0.05	2.64
90° walking turn	–0.02	0.03	1.56	–0.08	0.07	0.09
Moderate running	–0.02	0.18	1.31	–0.1	0.09	–1.58
Fast running	-0.03	0.15	0.9	–0.04	0.2	1.87
90° running turn	–0.08	0.11	0.85	–0.14	0.16	–0.87
45° cutting maneuver	–0.07	0.44	1.94	0.26	0.22	–0.57
Mean	–0.03	0.15	1.18	–0.05	0.13	0.26

(mean RMSE = 0.13, rRMSE = 0.26) due to independent model building.

5.5 Discussion

This study was aimed to develop and train an ANN model to estimate KFM and KAM during various locomotion tasks based on data obtained by two wearable sensors. The mobile assessment of knee joint loading enlarges the scope of diagnostic methods and disease management of KOA, which could help to improve disease treatement strategies and minimizing the risk of non-functional overreaching (e.g., pain).

The results of the study show a higher estimation accuracy of the KFM compared to the KAM over most locomotion task. However, estimation accuracy highly varied between tasks for both the KFM and the KAM, especially with increasing intensity and movement velocity. Apart from walking straight, for all

locomotion tasks, a distinct reduced level of agreement was found between the ANN-estimated outcomes and reference data for the KAM (mean $r = 0.39 \pm 0.32$, mean rRMSE = 29.9% $\pm$ 8.1%) in comparison to the KFM (mean $r = 0.74 \pm 0.36$, mean rRMSE = 20.8% $\pm$ 5.7%). Discrete load metrics highlighted lower *%Diff* of KFM impulses in comparison to KFM peaks in all locomotion tasks, whereas *%Diff* of KAM impulses were lower compared to KAM peaks only in three out of the six locomotion tasks.

5.5.1 Estimation accuracy across different locomotion tasks

In general, when comparing the estimation accuracy across the different locomotion tasks, predictive power was always better and *%Diff* was always less for KFM than for KAM. On average, strong correlations ($r = 0.74$) and rRMSE of 20.8% for KFM and moderate correlations ($r = 0.39$) with rRMSE of 29.9% for KAM were found. Nonetheless, distinct differences between KFM and KAM estimation values were evident across the locomotion tasks.

For KFM, highest correlations with the inverse dynamics calculations were found for moderate running ($r = 0.85$), which is reinforced by lowest *%Diff* for both the peak and impulse of the KFM. The lowest correlations and largest rRMSE were found for fast running ($r = 0.65$; rRMSE = 25.5%). Nevertheless, *%Diff* for KFM peaks and impulses during fast running were lower than for most of the other locomotion tasks, except for moderate running. Interestingly, the largest *%Diff* was found for walking straight, while *%Diff* of moment integrals were in general lower compared to *%Diff* of peak moments. These findings indicate that our ANN-configuration is more appropriate for estimating knee joint loading over the stance phase than for estimating the peak moment of the stance phase. In particular, during walking straight, the low knee flexion moment peaks and impulses might account for the strong correlations but large *%Diff*. Albeit, for KFM generally high agreement was found for ANN-estimated outcomes, with a reduced performance for the high intensity movements running and cutting maneuvers. In contrast, in these movements lower *%Diff* occurred to the lower-intensity movements.

For the estimation of KAM, overall weak to strong correlations were found for the analyzed movements. Estimation accuracy was highest in walking straight ($r = 0.71$, rRMSE = 22.3%). Mediocre correlations were found in moderate running as well as 90° walking/running turns ($0.40 \leq r \leq 0.56$), and low or nega-

tive correlations in fast running and 45° cutting maneuvers ($-0.05 \leq r \leq 0.21$). With regard to rRMSE, alterations of locomotion speed (walking to running) and direction (turning and cutting) led to slight reductions in accuracy of the ANN-estimations. Concomitant, large increases in *%Diff* along with high variability were detected in fast running, 90° running turns and 45° cutting maneuvers (KAM impulse: 94.2, 230.0 and 470.0%, respectively). A potential reason for the less estimation accuracy and larger differences for movements with increased velocity and changes of direction might be the higher variation in the execution of these movements, while locomotor tasks such as walking or moderate running are performed automatically with repeatable characteristics (Schmidt & Lee, 2011). Similarly, variability in estimation accuracy was also shown by Fluit et al. (2014), evaluating a prediction model for GRFs and moments during various activities of daily living by means of 3D full-body motion.

However, a generalization of the estimation accuracies cannot be deduced, as a reduced estimation accuracy in continuous outcomes does not necessarily result in an inaccurate estimation of discrete variables, as it was seen in the KFM during fast running. Similarly, good agreement in continuous outcomes does not implicate accurate estimation of discrete load metrics, as seen in 90° running turn. Furthermore, it must be noted that most the KFM and KAM show high standard deviations, which indicates a wide dispersion across participants. Nonetheless, *%Diff* of KFM were entirely lower in the impulses compared to the peak values. In contrast, *%Diff* of KAM impulse were lower compared to the peak values only in three out of the six locomotion tasks (90° walking turn, moderate and fast running). Summarized, KAM estimations were less accurate both for continuous and for discrete outcomes compared to KFM and should therefore be treated with caution. The more pronounced characteristic changes in the KAM time series between locomotion tasks in comparison to the KFM time series are a potential reason for the reduced estimation accuracy in KAM (see Figure 5.2 and Figure 5.3).

Furthermore, with respect to the comparison of a combined estimation model for KFM and KAM and independent models for KFM and KAM, the results show that an independent model building leads to slightly decreased estimation accuracy of the KFM and a more pronounced decrease of the KAM, concomitant with increased RMSE and rRMSE in the investigated locomotion tasks. Hence, if only one variable was chosen as an output, decreased performance for the

model was observed, indicating that cross-dependencies between input and output in the combined estimation model clearly affected the estimation accuracy. Overall, the combined estimation model for KFM and KAM presented a fair estimation accuracy, especially, in the low-intensity movements.

5.5.2 Comparison of different wearable measurement systems

A novel machine learning based method was developed and applied in this study to estimate KFM and KAM based on data obtained by two wearable sensors integrated in a knee sleeve. Various approaches have experienced progressive advances to assess the mechanical loading of KOA patients in their habitual environment over the past years. The majority of the approaches were based on analytical biomechanical models, which typically determine joint moments by means of the inverse dynamics calculations. As a consequence, GRF measurements and kinematic data are necessary to perform such analysis (Whittlesey & Robertson, 2014).

van den Noort et al. presented in 2011 an instrumented force shoe as an alternative to force plate measurements. Subsequently, an ambulatory measurement system, consisting of the instrumented force shoe and an inertial measurement system combined with a linked-segment model, was used to compare KAM measures with a laboratory based system in KOA patients (van den Noort et al., 2013). Limited accuracy was shown and the authors concluded that a more advanced calibrated linked-segment model should be investigated (van den Noort et al., 2013). As an alternative to a direct measurement of GRF, Karatsidis et al. (2017) estimated GRF by means of a full-body inertial motion capture system during walking. Their results showed for the comparison with an optical motion capture system higher r values (range 0.82 to 0.99 and 0.76 to 0.99 for the inertial and optical motion capture systems, respectively) and lower rRMSE values (range from 5% to 15% for both systems) compared to the KFM and KAM estimations present in this study. More recent studies from Dorschky et al. (2019) and Konrath et al. (2019) used inertial motion capturing and musculoskeletal modeling to estimate biomechanical variables, such as joint kinematics and kinetics without GRF data. Dorschky et al. (2019) presented high correlations for sagittal plain kinematics ($r > 0.93$) and kinetics ($r > 0.90$) in gait and running. In accordance, Konrath et al. (2019) estimated the KAM and the tibio-femoral joint contact force during daily living activities (e.g., stair walking) with moderate to

strong correlation coefficients. However, such approaches using inertial sensor data and musculoskeletal models require more IMUs (seven IMUs in Dorschky et al. (2019) and 17 IMUs in Konrath et al. (2019)) compared to this study's approach.

Parallel to the analytical model development, an increasing number of machine learning approaches have been explored to simplify data acquisition and modeling strategies to estimate target variables, such as the KAM (Liu et al., 2009; Favre et al., 2012; Wouda et al., 2018). ANN modeling does not require modeling of the musculoskeletal system, as the relationship between the input IMU signals and the target variables is build up during the training process of the model (Halilaj et al., 2018; Wouda et al., 2018). However, ground truth reference data, such as the inverse dynamics-calculated KFMs and KAMs, are required during the supervised learning process of the model. Providing a large amount of known output data is essential to establish a robust model (Sivakumar et al., 2016; Halilaj et al., 2018). Wouda et al. (2018) used similar ANN modeling to the one used in this study for estimating vertical GRF and sagittal knee kinematics during running. The estimated vertical GRF profiles of their non-personalized ANN developed by eight participants showed a higher correlation ($r > 0.90$) to the actual force time series. The slightly reduced estimation accuracy in the current study ($r < 0.85$) may depend on the variety of locomotion tasks included in the model building. A more locomotion task-specific modeling may lead to an increased estimation accuracy for individual tasks, but has the disadvantage that each task must be modeled by itself (Wouda et al., 2018). In consequence, the combination with an activity recognition approach could help to select individual estimation models in practical applications.

5.5.3 Limitations

Certain limitations of this study need to be considered when interpreting the results. One consideration worth noting is that the estimation accuracy depends on the neural network architecture. The ANN was built on previous work (Favre et al., 2012; Wouda et al., 2018), which highlighted that such configuration is capable of mapping non-linearity between input and output; however, other model specifications may result in an improved estimation accuracy. The ANN was trained with data from multiple participants as well as various locomotion tasks, which should rather lead to a less participant- and task-specific

but a more generic model. As a consequence, this approach rather yields a decreased performance due to a lack of individualization, but has the advantage that not every new user needs to perform a training phase (Favre et al., 2012; Wouda et al., 2018). Further research is necessary to assess if a single participant learning approach increases the estimation accuracy. Another limitation is that we included a homogeneous group of participants consisting of only males without any musculoskeletal disorders and the translation of the results to the target group of KOA patients remains speculative. Nonetheless, future clinical studies may benefit from the use of the method developed in this study, especially in low-intensity movements (Richards et al., 2017). Beyond, the sample size was rather small, including thirteen participants. Similar investigations included comparable numbers of participants (e.g., sample of eight participants in Wouda et al. (2018) or sample of seventeen participants in Leporace et al. (2015)). The small sample size potentially limits the outcome, as the robustness of the relationship between the input and output variables of the ANN depends on the amount of training data (Sivakumar et al., 2016; Ancillao et al., 2018; Halilaj et al., 2018). Finally, it cannot be fully ensured that the fixation technique excluded any oscillations or misalignment of the IMUs, even though the exact fit of the sleeve and the sensors was repetitively checked. However, the wearable sensors were integrated in a knee sleeve on purpose to mimic natural effects and to capture IMU signals closely related to the joint under investigation.

5.6 Conclusion

This study demonstrated the potential of estimating KFM and KAM for various locomotion tasks using a minimal body-worn sensor setup consisting of two IMUs integrated in a knee sleeve. The agreement between the ANN-estimated outcomes and inverse dynamics-calculated data was strong for the majority of analyzed locomotion tasks in the KFM and moderate in the KAM. Overall, higher estimation accuracies were seen for the KFM in comparison to the KAM across all locomotion tasks. The accuracy limitations especially of KAM estimation makes prediction of knee joint loading challenging. In order to reach an acceptable level of accuracy related to critical changes due to KOA, typically characterized by relatively small kinetic differences, a participant- or task-specific modeling could be helpful. This has important implications for the development of wearable devices as well as for scientific research on KOA. The highest

estimation accuracy for both KFM and KAM of walking straight matches the main characteristic of KOA therapy and treatment by low-intensity movements (e.g., walking). Looking ahead, wearable technology could serve as a rehabilitation aid for patients with KOA leading to an improved load management, which could result in a slower progression.

6 Discussion

6.1 Aims of the thesis and main findings

This thesis aims at investigating the use of wearable sensors and machine learning techniques to obtain meaningful biomechanical measures with respect to sports performance and the load on body structures. Special consideration is given to ice hockey skating performance diagnosis as well as to the assessment of the knee joint loading during various everyday and sport movements using machine learning techniques. Wearable sensors in the field of sports and clinical human movement analysis enlarge the scope of diagnostic methods. This is of great importance not only for sports performance diagnosis but also for health diagnostics and rehabilitation of injuries or musculoskeletal disease.

The presented approach in study I – the automated identification of temporal events during ice hockey skating based on a 3D accelerometer fixed on the skate chassis – shows a high level of agreement (95% Limits of Agreement (LoA) < 0.022 seconds) when comparing with simultaneously recorded plantar force data. This approach was then used in the subsequent study (study II), to gauge in-field ice hockey skating performance. The results demonstrate that it is feasible to identify previously highlighted performance related biomechanical changes in terms of substantial differences across skill levels and skating phases using two 3D accelerometers, which were located on the skate and the waist. Specifically, high caliber players show a 22% increased SP compared to recreational players, which highlights their skills to apply a relatively large impulse to the body's center of mass.

Study III and study IV devotes particular attention to the development of machine learning models to estimate loads on knee joint structures by means of wearable sensor data. The results of study III show that KJFs can be estimated using only two wearable sensors positioned at the upper and lower frontal end of a knee sleeve. In particular, the vertical and anterior-posterior KJF time series are estimated with good accuracy with respect to reference inverse dynamics calculations ($r \geq 0.81$ and rRMSE $\leq 20.3\%$ as well as $r \geq 0.80$ and rRMSE $\leq 22.9\%$

for 11 and 10 out of 16 movements, respectively). Furthermore, an ANN trained to estimate knee joint moments (study IV) using the same minimal sensor setup achieves moderate to strong concordance with reference data for KFM across different locomotion tasks, but shows accuracy limitations for KAM. Apart from walking straight a distinct reduced level of agreement is found between the ANN-estimated outcomes and reference data for the KAM (mean r = 0.39 $\pm$ 0.32, mean rRMSE = 29.9% $\pm$ 8.1%) in comparison to the KFM (mean r = 0.74 $\pm$ 0.36, mean rRMSE = 20.8% $\pm$ 5.7%) for all locomotion tasks.

6.2 Wearable sensor based ice hockey skating analysis

In modern times, the capturing of movements by means of wearable sensors has become increasingly popular and important for sport performance assessment. A primary benefit of wearable sensor based human movement analysis is the potential for measuring data in a realistic environment, which limits inhibition or disturbance of natural movement patterns. Furthermore, due to the small size of these sensors they can be easily attached to various parts of the body (e.g., waist) or integrated into sports equipment (e.g., shoes). Consequently, the application is even possible in unique environments like an ice rink, where commonly used movement analysis instruments are of limited use (Díaz et al., 2020; Adesida et al., 2019). Multiple applications have been created for team (e.g., rugby and soccer) and individual sports (e.g., running and tennis) (Camomilla et al., 2018). However, ice hockey has received limited attention so far despite the sport's worldwide appeal (Camomilla et al., 2018). The lack of knowledge may be due to the dynamic characteristics of the sport and its unique on-ice conditions (Buckeridge et al., 2015; Upjohn et al., 2008). Two studies were conducted to address this lack of knowledge by investigating the potential of wearable sensors for a biomechanical ice hockey skating performance analysis.

In study I, the use of a single skate mounted 3D accelerometer for an automated detection of temporal events during forward ice hockey skating was investigated. As an accurate and efficient detection of timing events is invaluable to study temporal movement characteristics or to quantify other biomechanical variables (Camomilla et al., 2018; Iosa et al., 2016), the findings of this study are of great significance. Research in running has shown that inertial sensors can effectively be used to identify timing events (Bergamini et al., 2012; Lee et al., 2010; Auvinet et al., 2002). The proposed algorithm for forward skating in ice

hockey showed an comparable level of agreement (95% LoA < 0.025 s) as other methods used to identify gait events during running (Bergamini et al., 2012; Lee et al., 2010). The difference (biases < 1 ms) between the accelerometer and plantar pressure system is comparable to other studies, which validated an inertial sensor approach with a standard method for walking (Salarian et al., 2004) or running (Lee et al., 2010). Additionally, the methodology developed appears to be valid for a wide range of forward stride patterns. Despite the fact that there are notable differences in the stride pattern across progressive strides (Stidwill et al., 2010; Lafontaine, 2007), no significant difference in the accuracy of the new method was found between strides.

In study II, a second accelerometer was placed at the lower back as a complementary tool for characterizing the propulsive power during skating. Two measures of the temporal stride characteristics (CT and ST) and one measure of the propulsive power of a skating stride (SP) were evaluated. Biomechanical literature shows that such skating technique elements are closely related to skating performance (Buckeridge et al., 2015; Renaud et al., 2017; Stidwill et al., 2009; Upjohn et al., 2008). The results highlight that (1) the variables CT and SP discriminated between high and low caliber ice hockey players; (2) the variables CT, ST and SP discriminated between fundamental skating phases (accelerative and steady-state); (3) SP of acceleration strides primarily correlated to skating performance (TST). In particular, a 22% increased SP (average increase) of high caliber players was observed, which highlights their skills to apply a relatively large impulse to the body's center of mass when compared to the recreational player. Previous studies have revealed that leg strength is of importance in this context (Buckeridge et al., 2015; Farlinger et al., 2007). This applies to situations, when observing differences between high and low caliber players (Buckeridge et al., 2015; Upjohn et al., 2008) or identifying predictors of skating sprint performance (e.g., leg power variables in off-ice sprints and jumps) (Farlinger et al., 2007). Although temporal variables (CT and ST) showed only limited correlation with the skating performance (i.e., TST), such variables could potentially serve as fatigue-sensitive measures, as mentioned by Buchheit et al. (2015).

In general, the location at which an IMU is placed on the body plays an important role in analyzing specific movements. In study I, the accelerometer was deliberately placed in the center of the chassis in order to detect the majority of vibrations during the contact between the ice and the metal blade of the skate.

This setup is effective in hockey skating since the movement pattern of the foot during a skating stride does not consist of a distinct heel or toe contact (Pearsall et al., 2000), such as for example in running (Lieberman et al., 2010). In study II, the propulsion power of skating strides were considered beside timing characteristics. As underlined by the findings in study II, the placement near the waist is a useful location because of its proximity to the center of mass, and represents the major acceleration of the body (Yang & Hsu, 2010).

The results of the two studies confirm earlier studies in ice hockey skating related areas, such as speed skating and cross-country skiing (Myklebust et al., 2014, 2015; van der Kruk et al., 2016). The sensitivity of wearable sensors to capture biomechanical skating variables as well as to distinguish skating technique was shown (Myklebust et al., 2014, 2015; van der Kruk et al., 2016). Overall, the current results underline the potential of wearable sensors to assess skating technique elements (e.g., contact time) or elements to gauge skating performance (e.g., center of mass acceleration). Nevertheless, further research is warranted, which aims to monitor biomechanical variables over a longer period of time (e.g., training session). Objective field-based biomechanical metrics can help to control for sufficient training loads that are required to achieve beneficial physical adaptations, whilst preventing overuse (Verheul et al., 2020; Camomilla et al., 2018). As a consequence, the quality of training and player development can increasingly benefit from wearable sensors in the future.

6.3 Estimating knee joint dynamics with machine learning

Understanding and quantifying the load on body structures is important for injury prevention in sports and for the management of chronic disease and is traditionally assessed by using a multi-camera motion capture system and force plates (Verheul et al., 2020; Adesida et al., 2019; Konrath et al., 2019). In this context, joint dynamics (especially forces and moments) are biomechanical measures used to infer the load on knee joint structures (Vanrenterghem et al., 2017; Bennell et al., 2011; Miyazaki et al., 2002; Zernicke & Whiting, 2000). For instance, the knee joint is continuously subjected to forces that vary in magnitude, location, direction, duration, frequency, variability and rate during athletic activities (Zernicke & Whiting, 2000). In many cases, obtaining biomechanical measures under non-laboratory conditions is indispensable, e.g. for monitoring an athlete's workload or for the ambulant assessment of patients. As stated pre-

viously, wearable sensors are an ideal alternative to laboratory based techniques for performing human movement analyses in habitual sport and everyday environments. However, as these sensors only provide kinematic data, modeling approaches are required to obtain joint dynamics (Gurchiek et al., 2019; Lim et al., 2019; Dorschky et al., 2019). An additional challenge is to measure all necessary data with a limited number of wearable sensors, as a large number of sensors can inhibit the natural movement (Gurchiek et al., 2019; Lim et al., 2019; Dorschky et al., 2019). To overcome these current limitations, two studies (study III and study IV) where conducted within this thesis to investigate the feasibility of machine-learning methods to estimate loads on knee joint structures by way of an ambulatory minimal body-worn sensor setup.

In study III, an ANN was developed for various common sport-specific movements and the accuracy of ANN KJF estimations was compared to standard inverse dynamics calculations. Apart from the medial–lateral force component (F^*_{ml}: $r \leq 0.60$ and rRMSE $\geq 27.7\%$), high agreement between the ANN-predicted outcomes and the inverse dynamics-calculated data was identified (F^*_v: $r \geq 0.81$ and rRMSE $\leq 20.3\%$; F^*_{ap}: $r = \geq 0.80$ and rRMSE $\leq 22.9\%$, respectively) for the majority of the analyzed movements (11 and 10 out of 16, respectively). Similarly, an early study from Leporace et al. (2015) which combined wearable sensors and ANN highlighted the lowest r in the medial–lateral component when they estimated 3D GRF with an ANN during walking. Additionally, further studies estimating the GRF based on 3D full-body motion revealed similar findings and suggested that this was due to the small magnitude of the lateral measurements, which caused a larger impact of small errors on final estimates (Karatsidis et al., 2017; Fluit et al., 2014; Oh et al., 2013). When comparing the results for KJF estimations with GRF estimations, slightly lower correlations are demonstrated for KJFs (e.g., mean r for $F^*_v \leq 0.82 \pm 0.10$). Karatsidis et al. (2017) showed $r \geq 0.82$ for GRF estimations using a biomechanical model and the Newton equations of motion. Furthermore, Wouda et al. (2018) presented $r > 0.94$ for GRF estimations using a machine-learning approach based on vertical accelerations and lower limb joint angles. One reason for the slightly lower accuracy when estimating KJFs in study III may be the less specific model with respect to single movements. Individual prediction models for single movements or movement categories based on an activity recognition approach could help to strengthen the overall estimation accuracy. In terms of applications of interest such as track-

ing fatigue-related changes, it remains unclear if the current level of accuracy is sufficient. This comes especially from the fact that research in this area is rather limited, and much of what we know about monitoring comes from personal experience (Halson, 2014). It is noteworthy that the detection of critical changes is generally challenging. The body has a high capacity to tolerate forces. Consequently, in most cases acting forces can be withstand. However, when loads exceed the physiological range, body structures can experience overload and sustain injury (Verheul et al., 2020; Zernicke & Whiting, 2000). Future research in applied settings is indispensable to observe and analyze biomechanical risk factors over a defined exposure time, with the ability to influence injury prevention models (Adesida et al., 2019; Verheul et al., 2020).

Study IV built up on study III and was aimed to explore the potential for an ambulatory assessment of joint loading in KOA using the same wearable sensor system as before. Consequently, a case-specific ANN was developed that estimates external KFMs and external KAMs during various locomotion tasks as objective biomechanical measures of knee joint load in KOA (Bennell et al., 2011; Miyazaki et al., 2002). The results of the study showed a higher estimation accuracy of the KFM (mean r = 0.74 $\pm$ 0.36, mean rRMSE = 20.8% $\pm$ 5.7%) compared to the KAM (mean r = 0.39 $\pm$ 0.32, mean rRMSE = 29.9% $\pm$ 8.1%) over most locomotion tasks. Concordance of the ANN-estimated KFM and reference data of five tasks (walking straight, 90° walking turn, moderate running, 90° running turn and 45° cutting maneuver) was strong ($r \geq 0.69$, rRMSE $\leq$ 23.1) and moderate for fast running ($r = 0.65 \pm 0.43$, rRMSE = 25.5% $\pm$ 7.0%). Due to the generally lower *%Diff* of KFM integrals compared to *%Diff* of peak KFMs, the findings indicate that the ANN-configuration is more appropriate for estimating knee joint loading over the stance phase than for estimating the peak moment of the stance phase. Nevertheless, caution is required when interpreting the results for KAMs as large *%Diff* were detected along with high variability (KAM impulse: 94.2, 230.0 and 470.0%, in fast running, 90° running turns and 45° cutting maneuvers, respectively). This is problematic, especially because the KAM is a widely used surrogate measure of the compressive load of the medial compartment (Ferreira et al., 2015; Bennell et al., 2011; Reeves & Bowling, 2011; Sharma et al., 1998).

The recent studies from Dorschky et al. (2019) and Konrath et al. (2019) used inertial motion capturing and musculoskeletal modeling to estimate joint dynamics.

Dorschky et al. (2019) presented high correlations for sagittal plain moments ($r > 0.90$) in gait and running. Accordingly, Konrath et al. (2019) showed moderate to strong correlations for estimating the KAM and the tibio-femoral joint contact force during daily living activities (e.g., stair walking). However, such approaches that use inertial sensor data and musculoskeletal models require noticeably more IMUs (seven IMUs in Dorschky et al. (2019), 17 IMUs in Konrath et al. (2019)) compared to the presented ANN approach. Especially, the results for the external KFM demonstrated the potential of estimating joint dynamics using a minimal body-worn sensor setup and ANN modeling. Earlier attempts toward a wearable measurement tool, e.g. consisting of an instrumented force shoe and an inertial measurement system (van den Noort et al., 2013, 2011), also yielded limited accuracy at an early stage. To reach an acceptable level of accuracy related to critical changes due to KOA a participant or task-specific ANN modeling could be helpful in the future.

In both studies (study III and study IV), movements characterized by a high repeatability showed an increased estimation accuracy (e.g., F_v^* for moderate running in study III), when comparing the estimation accuracy across the different movements. Higher variation in the execution of movements with changes in velocity (e.g., sprint starts and full-stops) or changes of direction (e.g., running turns and cutting maneuvers) might be a potential reason for the lower estimation accuracy and larger differences in such movements (Morgan et al., 1991; Schmidt & Lee, 2011). Similarly, Fluit et al. (2014) also showed changes in estimation accuracy by evaluating a prediction model for GRFs as well as moments during various activities of daily living using 3D full-body motion. A more movement-specific modeling approach could help to overcome such limitations. However, individual prediction models have the disadvantage that each movement must be modeled by itself (Wouda et al., 2018). In practical applications, the selection of individual estimation models could be realized by an activity recognition approach.

Novel machine learning models (ANNs) were applied to estimate joint dynamics (forces and moments) based on data obtained by two wearable sensors integrated in a knee sleeve. ANN modeling does not require modeling of the musculoskeletal system, as the relationship between the input IMU signals and the target variables is build up during the training process of the model (Halilaj et al., 2018; Wouda et al., 2018). Such methods are based on the hypothesis

that a relationship exists between the sensor signals measured somewhere on the body and the biomechanical target variable (e.g., KJF) (Ancillao et al., 2018). This assumption is supported by the relationship between acceleration and force, according to Newton's second law of motion, as well as by the relationship between the measured quantities and the segment's motion (Karatsidis et al., 2017; Wouda et al., 2018). Nevertheless, providing the best means of ground truth reference data, such as the inverse dynamics-calculated joint reactions, are indispensable for the learning process of the model. Furthermore, a large amount of known output data are essential to establish a robust model (Sivakumar et al., 2016; Halilaj et al., 2018). In contrast to machine learning-based approaches, joint dynamics can be estimated by means of posture information obtained from wearable sensors as well as by means of an analytical model (Yang & Mao, 2015). For the most part, complex modeling is necessary to obtain reasonable results, because discrepancies in subject-specific parameters, such as masses, dimensions, etc., inevitably introduce inaccuracies (Ancillao et al., 2018). Additionally, these approaches often require considerably more wearable sensors (typically between seven and 17 IMUs (Konrath et al., 2019; Dorschky et al., 2019; Yang & Mao, 2015)) in comparison to the presented machine learning-based approach. The findings of study III and study IV highlight the large benefit of machine learning models to solve the tradeoff between data quantity and wearable convenience (Lim et al., 2019). Consequently, such models provide an opportunity to simplify practical implementation while preventing inhibitions of the natural movement (Gurchiek et al., 2019).

6.4 Current limitations and future research directions

When interpreting the findings of this thesis, the reader should be aware of a number of limitations.

First, in study I, reference times were measured with a rather low sampling frequency (90 Hz), and the data were interpolated to match the sampling frequency of the accelerometer (2400 Hz). This might indicate a potential limitation of this study. However, the measured contact and stride times for consecutive strides are supported by those times found by Stidwill et al. (2010). Despite this agreement, validation of single strides against a high-speed video could provide greater confidence that the accelerometer-derived temporal characteristics are accurate.

Second, with respect to study II, the SP was calculated by means of acceleration data in all three axes of the accelerometer on the lower back. Therefore, a differentiated consideration of acceleration caused by a high propulsive effort in forward direction and acceleration due to an inefficient skating technique (e.g., vertical motion of the CoM) is not possible. Future studies could focus on the quantification of energy fluctuations during skating. In this context, the coupling of accelerometers with gyroscopes could help to determine the displacement of the CoM in vertical, sideward and forward direction (Myklebust et al., 2015).

Third, in study I and study II, methodologies were developed and tested in an isolated 30 m forward sprinting task on an ice rink. This is a major limitation, as other movements fundamental to ice hockey skating, such as turning and backward skating, are also important for detailed athlete monitoring purposes. Consequently, future investigations should extend the application of the proposed methods to other essential ice hockey movements. A future step would be to monitor biomechanical performance variables, such as stride propulsion, over a longer period of time (e.g., training session) and at various levels of intensity.

Fourth, in study III and study IV, ANNs were trained with data from multiple participants as well as various locomotion tasks, which should rather lead to a less participant- and task-specific but a more generic model. Therefore, this approach might lead to a decreased performance due to a lack of individualization, but has the advantage that not every new user needs to perform a training phase (Wouda et al., 2018; Favre et al., 2012). Further research is needed to assess if a single participant or single task learning approach could increase estimation accuracy. Recent literature suggests the development of hybrid estimation models, taking advantage of the strengths of both analytical/biomechanical models and machine learning (Gurchiek et al., 2019; Ancillao et al., 2018). Consequently, additional research is required to investigate whether such a combined approach leads to an increased overall estimation accuracy. Besides that, the translation of the results to target groups, such as athletes in rehabilitation or KOA patients, should be investigated in the future.

Finally, the small sample size in study III and study IV limits the external validity of these studies as the robustness of the relationship between the input and output variables of the ANN depends on the amount of training data (Sivaku-

mar et al., 2016; Ancillao et al., 2018; Halilaj et al., 2018). Similar investigations were based on a comparable number of participants (e.g., a sample of eight participants in Wouda et al. (2018) or a sample of seventeen participants in Leporace et al. (2015)). Nevertheless, whether or not a training data set containing a larger number of observations yield an increased estimation accuracy remains subject to speculation. With respect to the model building, it is worth noting that reference inverse dynamics calculations only allow for the determination of the resultant rather than individual forces and moments acting on the knee joint. Combining the presented approach with musculoskeletal modeling or with direct force measurements (e.g., using an instrumented knee prosthesis) could help to assess the internal loadings on the knee joint structures more precisely. Independent of present limitations, wearable sensors and machine learning provide the technology for the development of viable monitoring systems, which can turn related studies (clinical and not clinical) in a new direction (Faisal et al., 2019; Gurchiek et al., 2019). Overall, further research effort is needed to transfer developments in real-world applications. Despite promising results, novel health technology must be evaluated in real-world settings using structured research frameworks like randomized controlled trials (Cabitza et al., 2018).

6.5 Conclusion

The results of this thesis show that wearable sensors and machine learning techniques are valuable tools to obtain meaningful biomechanical measures with respect to sport and medical applications. The findings of study I and study II help to overcome restrictions in the performance assessment of sport-specific movements under field-based conditions, particularly with respect to ice hockey skating. Consequently, this opens new possibilities for in-field diagnosis. As a result, the quality of training and player development can increasingly benefit from wearable technology and associated applications for providing feedback. Furthermore, the methodological steps and findings of study III and study IV demonstrate the high potential of estimating joint dynamics, as a resource to assess the internal loading of anatomical structures (e.g., cartilage) for various everyday and sport movements. The developed ANNs for estimating knee joint forces in sport movements as well as to estimate joint loading in knee osteoarthritis showed a high level of agreement with gold-standard inverse dynamics-calculated data, for the majority of the investigated movements. Nevertheless,

accuracy limitations were observed for certain movements (e.g., tow-leg jumps) as well as specific spatial dimensions (e.g., medial-lateral KJF and KAM). Overall, high model quality is of paramount importance, as critical biomechanical changes due to overuse or musculoskeletal diseases are typically characterized by relatively small differences, to prevent incorrect diagnosis or treatment.

Overall, future research at the intersection of wearable sensors, machine learning and biomechanics offers great promise for advancing wearable monitoring and health technology. Ultimately, this has high practical implications, as wearable human movement analysis can facilitate sports performance diagnosis, improve health diagnostics and rehabilitation of injuries as well as musculoskeletal diseases.

References

Adesida, Y., Papi, E., & McGregor, A. H. (2019). Exploring the role of wearable technology in sport kinematics and kinetics: A systematic review. *Sensors*, 19(7), 1597.

Alpaydin, E. (2020). *Introduction to Machine Learning*. Adaptive Computation and Machine Learning series. MIT Press, fourth edition.

Aminian, K., Rezakhanlou, K., de Andres, E., Fritsch, C., Leyvraz, P. F., & Robert, P. (1999). Temporal feature estimation during walking using miniature accelerometers: an analysis of gait improvement after hip arthroplasty. *Medical & Biological Engineering & Computing*, 37(6), 686–691.

Ancillao, A., Tedesco, S., Barton, J., & O'Flynn, B. (2018). Indirect measurement of ground reaction forces and moments by means of wearable inertial sensors: A systematic review. *Sensors*, 18(8), 2564.

Andriacchi, T. P. & Alexander, E. J. (2000). Studies of human locomotion: past, present and future. *Journal of Biomechanics*, 33(10), 1217–1224.

Andriacchi, T. P. & Mundermann, A. (2006). The role of ambulatory mechanics in the initiation and progression of knee osteoarthritis. *Current Opinion in Rheumatology*, 18(5), 514–518.

Aroganam, G., Manivannan, N., & Harrison, D. (2019). Review on wearable technology sensors used in consumer sport applications. *Sensors*, 19(9), 1983.

Auvinet, B., Gloria, E., Renault, G., & Barrey, E. (2002). Runner's stride analysis: comparison of kinematic and kinetic analyses under field conditions. *Science & Sports*, 17(2), 92–94.

Barrios, J. A., Crossley, K. M., & Davis, I. S. (2010). Gait retraining to reduce the knee adduction moment through real-time visual feedback of dynamic knee alignment. *Journal of Biomechanics*, 43(11), 2208–2213.

Bartlett, R. (2007). *Introduction to sports biomechanics: Analysing human movement patterns*. London: Routledge, second edition.

Bennell, K. L., Bowles, K.-A., Wang, Y., Cicuttini, F., Davies-Tuck, M., & Hinman, R. S. (2011). Higher dynamic medial knee load predicts greater cartilage loss over 12 months in medial knee osteoarthritis. *Annals of the Rheumatic Diseases*, 70(10), 1770–1774.

Bergamini, E., Picerno, P., Pillet, H., Natta, F., Thoreux, P., & Camomilla, V. (2012). Estimation of temporal parameters during sprint running using a trunk-mounted inertial measurement unit. *Journal of Biomechanics*, 45(6), 1123–1126.

Besier, T. F., Lloyd, D. G., Cochrane, J. L., & Ackland, T. R. (2001). External loading of the knee joint during running and cutting maneuvers. *Medicine & Science in Sports & Exercise*, 33(7), 1168–1175.

Bishop, C. M. (1995). *Neural Networks for Pattern Recognition*. Oxford University Press.

Bland, J. M. & Altman, D. G. (2007). Agreement between methods of measurement with multiple observations per individual. *Journal of Biopharmaceutical Statistics*, 17(4), 571–582.

Böhm, H., Oestreich, C., Rethwilm, R., Federolf, P., Döderlein, L., Fujak, A., & Dussa, C. U. (2019). Cluster analysis to identify foot motion patterns in children with flexible flatfeet using gait analysis-a statistical approach to detect decompensated pathology? *Gait & Posture*, 71, 151–156.

Boyd, L. J., Ball, K., & Aughey, R. J. (2013). Quantifying external load in australian football matches and training using accelerometers. *International Journal of Sports Physiology and Performance*, 8(1), 44–51.

Buchheit, M., Gray, A., & Morin, J.-B. (2015). Assessing stride variables and vertical stiffness with gps-embedded accelerometers: Preliminary insights for the monitoring of neuromuscular fatigue on the field. *Journal of Sports Science & Medicine*, 14(4), 698–701.

Buchman, A. S., Leurgans, S. E., Weiss, A., VanderHorst, V., Mirelman, A., Dawe, R., Barnes, L. L., Wilson, R. S., Hausdorff, J. M., & Bennett, D. A. (2014). Associations between quantitative mobility measures derived from components of conventional mobility testing and parkinsonian gait in older adults. *PloS one*, 9(1), e86262.

Buckeridge, E., LeVangie, M. C., Stetter, B., Nigg, S. R., & Nigg, B. M. (2015). An on-ice measurement approach to analyse the biomechanics of ice hockey skating. *PloS one*, 10(5), e0127324.

Cabitza, F., Locoro, A., & Banfi, G. (2018). Machine learning in orthopedics: A literature review. *Frontiers in Bioengineering and Biotechnology*, 6.

Calliess, T., Bocklage, R., Karkosch, R., Marschollek, M., Windhagen, H., & Schulze, M. (2014). Clinical evaluation of a mobile sensor-based gait analysis method for outcome measurement after knee arthroplasty. *Sensors*, 14(9), 15953–15964.

Camomilla, V., Bergamini, E., Fantozzi, S., & Vannozzi, G. (2018). Trends supporting the in-field use of wearable inertial sensors for sport performance evaluation: A systematic review. *Sensors*, 18(3), 873.

Cappozzo, A., Della Croce, U., Leardini, A., & Chiari, L. (2005). Human movement analysis using stereophotogrammetry. part 1: theoretical background. *Gait & Posture*, 21(2), 186–196.

Chambers, R., Gabbett, T. J., Cole, M. H., & Beard, A. (2015). The use of wearable microsensors to quantify sport-specific movements. *Sports Medicine*, 45(7), 1065–1081.

Charry, E., Hu, W., Umer, M., Ronchi, A., & Taylor, S. (2013). Study on estimation of peak ground reaction forces using tibial accelerations in running. *IEEE Eighth International Conference on Intelligent Sensors, Sensor Networks and Information Processing (2013) Melbourne*, (pp. 288–293).

Cheung, R. T. H., Ho, K. K. W., Au, I. P. H., An, W. W., Zhang, J. H. W., Chan, Z. Y. S., Deluzio, K., & Rainbow, M. J. (2018). Immediate and short-term effects of gait retraining on the knee joint moments and symptoms in patients with early tibiofemoral joint osteoarthritis: a randomized controlled trial. *Osteoarthritis and Cartilage*, 26(11), 1479–1486.

Christian, J., Kröll, J., Strutzenberger, G., Alexander, N., Ofner, M., & Schwameder, H. (2016). Computer aided analysis of gait patterns in patients with acute anterior cruciate ligament injury. *Clinical Biomechanics*, 33, 55–60.

Cohen, J. (1988). *Statistical power analysis for the behavioral sciences*. Hillsdale, NJ: Erlbaum, second edition.

Cole, G. K., Nigg, B. M., van den Bogert, A. J., & Gerritsen, K. G. (1996). Lower extremity joint loading during impact in running. *Clinical Biomechanics*, 11(4), 181–193.

Corey, D. M., Dunlap, W. P., & Burke, M. J. (1998). Averaging correlations: Expected values and bias in combined pearson rs and fisher's z transformations. *The Journal of General Psychology*, 125(3), 245–261.

Cox, M. H., Miles, D. S., Verde, T. J., & Rhodes, E. C. (1995). Applied physiology of ice hockey. *Sports Medicine*, 19(3), 184–201.

Crossley, K. M., Stefanik, J. J., Selfe, J., Collins, N. J., Davis, I. S., Powers, C. M., McConnell, J., Vicenzino, B., Bazett-Jones, D. M., Esculier, J.-F., Morrissey, D., & Callaghan, M. J. (2016). 2016 patellofemoral pain consensus statement from the 4th international patellofemoral pain research retreat, manchester. part 1: Terminology, definitions, clinical examination, natural history, patellofemoral osteoarthritis and patient-reported outcome measures. *British Journal of Sports Medicine*, 50(14), 839–843.

Dadashi, F., Crettenand, F., Millet, G. P., & Aminian, K. (2012). Front-crawl instantaneous velocity estimation using a wearable inertial measurement unit. *Sensors*, 12(10), 12927–12939.

De Koning, J. J., Thomas, R., Berger, M., De Groot, G., & van Ingen Schenau, G. J. (1995). The start in speed skating: from running to gliding. *Medicine & Science in Sports & Exercise*, 27(12), 1703–1708.

de Loes, M., Dahlstedt, L. J., & Thomee, R. (2000). A 7-year study on risks and costs of knee injuries in male and female youth participants in 12 sports. *Scandinavian Journal of Medicine & Science in Sports*, 10(2), 90–97.

Díaz, S., Stephenson, J. B., & Labrador, M. A. (2020). Use of wearable sensor technology in gait, balance, and range of motion analysis. *Applied Sciences*, 10(1), 234.

D'Lima, D. D., Fregly, B. J., Patil, S., Steklov, N., & Colwell, C. W. (2012). Knee joint forces: prediction, measurement, and significance. *Proceedings of the Institution of Mechanical Engineers. Part H, Journal of Engineering in Medicine*, 226(2), 95–102.

D'Lima, D. D., Steklov, N., Patil, S., & Colwell, C. W. (2008). The mark coventry award: In vivo knee forces during recreation and exercise after knee arthroplasty. *Clinical Orthopaedics and Related Research*, 466(11), 2605–2611.

Dorschky, E., Nitschke, M., Seifer, A.-K., van den Bogert, A. J., & Eskofier, B. M. (2019). Estimation of gait kinematics and kinetics from inertial sensor data using optimal control of musculoskeletal models. *Journal of Biomechanics*, 95, 109278.

Elble, R. J. (2005). Gravitational artifact in accelerometric measurements of tremor. *Clinical Neurophysiology*, 116(7), 1638–1643.

Faber, G. S., Chang, C. C., Kingma, I., Dennerlein, J. T., & van Dieen, J. H. (2016). Estimating 3d l5/s1 moments and ground reaction forces during trunk bending using a full-body ambulatory inertial motion capture system. *Journal of Biomechanics*, 49(6), 904–912.

Faisal, A. I., Majumder, S., Mondal, T., Cowan, D., Naseh, S., & Deen, M. J. (2019). Monitoring methods of human body joints: State-of-the-art and research challenges. *Sensors*, 19(11).

Farlinger, C. M., Kruisselbrink, L. D., & Fowles, J. R. (2007). Relationships to skating performance in competitive hockey players. *Journal of Strength & Conditioning Research*, 21(3), 915–922.

Favre, J., Hayoz, M., Erhart-Hledik, J. C., & Andriacchi, T. P. (2012). A neural network model to predict knee adduction moment during walking based on ground reaction force and anthropometric measurements. *Journal of Biomechanics*, 45(4), 692–698.

Ferber, R., Osis, S. T., Hicks, J. L., & Delp, S. L. (2016). Gait biomechanics in the era of data science. *Journal of Biomechanics*, 49(16), 3759–3761.

Ferreira, G. E., Robinson, C. C., Wiebusch, M., Viero, Carolina Cabral de Mello, da Rosa, Luis Henrique Telles, & Silva, M. F. (2015). The effect of exercise therapy on knee adduction moment in individuals with knee osteoarthritis: A systematic review. *Clinical Biomechanics*, 30(6), 521–527.

Figueiredo, P., Silva, A., Sampaio, A., Vilas-Boas, J. P., & Fernandes, R. J. (2016). Front crawl sprint performance: A cluster analysis of biomechanics, energetics, coordinative, and anthropometric determinants in young swimmers. *Motor Control*, 20(3), 209–221.

Fluit, R., Andersen, M. S., Kolk, S., Verdonschot, N., & Koopman, H. F. (2014). Prediction of ground reaction forces and moments during various activities of daily living. *Journal of Biomechanics*, 47(10), 2321–2329.

Foroughi, N., Smith, R., & Vanwanseele, B. (2009). The association of external knee adduction moment with biomechanical variables in osteoarthritis: a systematic review. *The Knee*, 16(5), 303–309.

Godfrey, A., Conway, R., Meagher, D., & OLaighin, G. (2008). Direct measurement of human movement by accelerometry. *Medical Engineering & Physics*, 30(10), 1364–1386.

Guleria, P. & Sood, M. (2020). Intelligent learning analytics in healthcare sector using machine learning. In V. Jain & J. M. Chatterjee (Eds.), *Machine learning with health care perspective*, Learning and analytics in intelligent systems (pp. 39–55). Cham: Springer.

Guo, Y., Storm, F., Zhao, Y., Billings, S. A., Pavic, A., Mazzà, C., & Guo, L.-Z. (2017). A new proxy measurement algorithm with application to the estimation of vertical ground reaction forces using wearable sensors. *Sensors*, 17(10), 2181.

Gupta, S. & Sedamkar, R. R. (2020). Machine learning for healthcare: Introduction. In V. Jain & J. M. Chatterjee (Eds.), *Machine learning with health care perspective*, Learning and analytics in intelligent systems (pp. 1–25). Cham: Springer.

Gurchiek, R. D., Cheney, N., & McGinnis, R. S. (2019). Estimating biomechanical time-series with wearable sensors: A systematic review of machine learning techniques. *Sensors*, 19(23).

Hahn, M. E. & O'Keefe, K. B. (2008). A neural network model for estimation of net joint moments during normal gait. *Journal of Musculoskeletal Research*, 11(3), 117–126.

Halilaj, E., Rajagopal, A., Fiterau, M., Hicks, J. L., Hastie, T. J., & Delp, S. L. (2018). Machine learning in human movement biomechanics: Best practices, common pitfalls, and new opportunities. *Journal of Biomechanics*, 81, 1–11.

Halson, S. L. (2014). Monitoring training load to understand fatigue in athletes. *Sports Medicine*, 44(2), 139–147.

Härtel, T. & Hermsdorf, H. (2006). Biomechanical modelling and simulation of human body by means of dynamicus. *Journal of Biomechanics*, 39, 549.

Hootman, J. M., Dick, R., & Agel, J. (2007). Epidemiology of collegiate injuries for 15 sports: summary and recommendations for injury prevention initiatives. *Journal of Athletic Training*, 42(2), 311–319.

Horak, F., King, L., & Mancini, M. (2015). Role of body-worn movement monitor technology for balance and gait rehabilitation. *Physical Therapy*, 95(3), 461–470.

Horst, F., Lapuschkin, S., Samek, W., Müller, K.-R., & Schöllhorn, W. I. (2019). Explaining the unique nature of individual gait patterns with deep learning. *Scientific Reports*, 9(1), 1–13.

Hörzer, S., von Tscharner, V., Jacob, C., & Nigg, B. M. (2015). Defining functional groups based on running kinematics using self-organizing maps and support vector machines. *Journal of Biomechanics*, 48(10), 2072–2079.

Hurley, M., Scott, D., Rees, J., & Newham, D. (1997). Sensorimotor changes and functional performance in patients with knee osteoarthritis. *Annals of the Rheumatic Diseases*, 56(11), 641–648.

Ingram, J. G., Fields, S. K., Yard, E. E., & Comstock, R. D. (2008). Epidemiology of knee injuries among boys and girls in us high school athletics. *The American Journal of Sports Medicine*, 36(6), 1116–1122.

Iosa, M., Picerno, P., Paolucci, S., & Morone, G. (2016). Wearable inertial sensors for human movement analysis. *Expert Review of Medical Devices*, 13(7), 641–659.

Kaczmarczyk, K., Wit, A., Krawczyk, M., & Zaborski, J. (2009). Gait classification in post-stroke patients using artificial neural networks. *Gait & Posture*, 30(2), 207–210.

Kaila, R. (2007). Influence of modern studded and bladed soccer boots and sidestep cutting on knee loading during match play conditions. *The American Journal of Sports Medicine*, 35(9), 1528–1536.

Karatsidis, A., Bellusci, G., Schepers, H. M., de Zee, M., Andersen, M. S., & Veltink, P. H. (2017). Estimation of ground reaction forces and moments during gait using only inertial motion capture. *Sensors*, 17(1), 75.

Karatsidis, A., Richards, R. E., Konrath, J. M., van den Noort, J. C., Schepers, H. M., Bellusci, G., Harlaar, J., & Veltink, P. H. (2018). Validation of wearable visual feedback for retraining foot progression angle using inertial sensors and an augmented reality headset. *Journal of NeuroEngineering and Rehabilitation*, 15(1), 1–12.

Kavanagh, J. J. & Menz, H. B. (2008). Accelerometry: a technique for quantifying movement patterns during walking. *Gait & Posture*, 28(1), 1–15.

Kipp, K., Giordanelli, M., & Geiser, C. (2018). Predicting net joint moments during a weightlifting exercise with a neural network model. *Journal of Biomechanics*, 74, 225–229.

Konrath, J. M., Karatsidis, A., Schepers, H. M., Bellusci, G., de Zee, M., & Andersen, M. S. (2019). Estimation of the knee adduction moment and joint contact force during daily living activities using inertial motion capture. *Sensors*, 19(7), 1681.

Krafft, F. C., Eckelt, M., Kollner, A., Wehrstein, M., Stein, T., & Potthast, W. (2015). Reproducibility of spatio-temporal and dynamic parameters in various, daily occurring, turning conditions. *Gait & Posture*, 41(1), 307–312.

Krafft, F. C., Stetter, B. J., Stein, T., Ellermann, A., Flechtenmacher, J., Eberle, C., Sell, S., & Potthast, W. (2017). How does functionality proceed in acl reconstructed subjects? proceeding of functional performance from pre- to six months post-acl reconstruction. *PloS one*, 12(5), 0178430.

Kristianslund, E., Krosshaug, T., & van den Bogert, A. J. (2012). Effect of low pass filtering on joint moments from inverse dynamics: implications for injury prevention. *Journal of Biomechanics*, 45(4), 666–671.

Lafontaine, D. (2007). Three-dimensional kinematics of the knee and ankle joints for three consecutive push-offs during ice hockey skating starts. *Sports Biomechanics*, 6(3), 391–406.

LeCun, Y., Bengio, Y., & Hinton, G. (2015). Deep learning. *Nature*, 521(7553), 436–444.

Lee, J. B., Mellifont, R. B., & Burkett, B. J. (2010). The use of a single inertial sensor to identify stride, step, and stance durations of running gait. *Journal of Science and Medicine in Sport*, 13(2), 270–273.

Leporace, G., Batista, L. A., Metsavaht, L., & Nadal, J. (2015). Residual analysis of ground reaction forces simulation during gait using neural networks with different configurations. *Conference proceedings: 37th Annual International Conference of the IEEE Engineering in Medicine and Biology Society (EMBC) 2015 (Milano)*, (pp. 2812–2815).

Lieberman, D. E., Venkadesan, M., Werbel, W. A., Daoud, A. I., D'Andrea, S., Davis, I. S., Mang'Eni, R. O., & Pitsiladis, Y. (2010). Foot strike patterns and collision forces in habitually barefoot versus shod runners. *Nature*, 463(7280), 531–535.

Lim, H., Kim, B., & Park, S. (2019). Prediction of lower limb kinetics and kinematics during walking by a single imu on the lower back using machine learning. *Sensors*, 20(1).

Lin, D., Vasilakos, A. V., Tang, Y., & Yao, Y. (2016). Neural networks for computer-aided diagnosis in medicine: A review. *Neurocomputing*, 216, 700–708.

Lindinger, S. J., Göpfert, C., Stöggl, T., Müller, E., & Holmberg, H.-C. (2009). Biomechanical pole and leg characteristics during uphill diagonal roller skiing. *Sports Biomechanics*, 8(4), 318–333.

Liu, Y., Shih, S.-M., Tian, S.-L., Zhong, Y.-J., & Li, L. (2009). Lower extremity joint torque predicted by using artificial neural network during vertical jump. *Journal of Biomechanics*, 42(7), 906–911.

Lofterod, B., Terjesen, T., Skaaret, I., Huse, A.-B., & Jahnsen, R. (2007). Preoperative gait analysis has a substantial effect on orthopedic decision making in children with cerebral palsy: comparison between clinical evaluation and gait analysis in 60 patients. *Acta Orthopaedica*, 78(1), 74–80.

Luinge, H. J. & Veltink, P. H. (2005). Measuring orientation of human body segments using miniature gyroscopes and accelerometers. *Medical and Biological Engineering and Computing*, 43(2), 273–282.

Maleki, M., Arazpour, M., Joghtaei, M., Hutchins, S. W., Aboutorabi, A., & Pouyan, A. (2016). The effect of knee orthoses on gait parameters in medial knee compartment osteoarthritis: A literature review. *Prosthetics and Orthotics International*, 40(2), 193–201.

Mariani, B., Hoskovec, C., Rochat, S., Bula, C., Penders, J., & Aminian, K. (2010). 3d gait assessment in young and elderly subjects using foot-worn inertial sensors. *Journal of Biomechanics*, 43(15), 2999–3006.

Marino, G. W. (1995). Biomechanics of power skating: past research, future trends. *Proceedings of the 13th International Symposium on Biomechanics in Sports (ISBS) (1995) Thunder Bay*, (pp. 246–252).

Matić, A., Petrović Savić, S., Ristić, B., Stevanović, V. B., & Devedžić, G. (2016). Infrared assessment of knee instability in acl deficient patients. *International Orthopaedics*, 40(2), 385–391.

Matijevich, E. S., Branscombe, L. M., Scott, L. R., & Zelik, K. E. (2019). Ground reaction force metrics are not strongly correlated with tibial bone load when running across speeds and slopes: Implications for science, sport and wearable tech. *PloS one*, 14(1), e0210000.

McLean, S. G., Lipfert, S. W., & van den Bogert, A. J. (2004). Effect of gender and defensive opponent on the biomechanics of sidestep cutting. *Medicine & Science in Sports & Exercise*, 36(6), 1008–1016.

Medved, V. (2001). *Measurement of human locomotion*. Boca Raton, USA: CRC PRESS.

Mero, A., Komi, P. V., & Gregor, R. J. (1992). Biomechanics of sprint running. a review. *Sports Medicine*, 13(6), 376–392.

Mihalik, J. P., Guskiewicz, K. M., Marshall, S. W., Blackburn, J. T., Cantu, R. C., & Greenwald, R. M. (2012). Head impact biomechanics in youth hockey: comparisons across playing position, event types, and impact locations. *Annals of Biomedical Engineering*, 40(1), 141–149.

Milner, C. E. & Paquette, M. R. (2015). A kinematic method to detect foot contact during running for all foot strike patterns. *Journal of Biomechanics*, 48(12), 3502–3505.

Milner, C. E., Westlake, C. G., & Tate, J. J. (2011). Test-retest reliability of knee biomechanics during stop jump landings. *Journal of Biomechanics*, 44(9), 1814–1816.

Miyazaki, T., Wada, M., Kawahara, H., Sato, M., Baba, H., & Shimada, S. (2002). Dynamic load at baseline can predict radiographic disease progression in medial compartment knee osteoarthritis. *Annals of the Rheumatic Diseases*, 61(7), 617–622.

Molenaers, G., Desloovere, K., Fabry, G., & de Cock, P. (2006). The effects of quantitative gait assessment and botulinum toxin a on musculoskeletal surgery in children with cerebral palsy. *The Journal of Bone and Joint Surgery*, 88(1), 161–170.

Moré, J. J. (1978). The levenberg-marquardt algorithm: Implementation and theory. In G. A. Watson & J. J. Moré (Eds.), *The Levenberg-Marquardt algorithm: Implementation and theory* (pp. 105–116).: Springer Berlin Heidelberg.

Morgan, D. W., Martin, P. E., Krahenbuhl, G. S., & Baldini, F. D. (1991). Variability in running economy and mechanics among trained male runners. *Medicine & Science in Sports & Exercise*, 23(3), 378–383.

Morgenroth, D. C., Medverd, J. R., Seyedali, M., & Czerniecki, J. M. (2014). The relationship between knee joint loading rate during walking and degenerative changes on magnetic resonance imaging. *Clinical Biomechanics*, 29(6), 664–670.

Mündermann, A., Dyrby, C. O., D'Lima, D. D., Colwell, C. W., & Andriacchi, T. P. (2008). In vivo knee loading characteristics during activities of daily living as measured by an instrumented total knee replacement. *Journal of Orthopaedic Research*, 26(9), 1167–1172.

Muro-de-la Herran, A., Garcia-Zapirain, B., & Mendez-Zorrilla, A. (2014). Gait analysis methods: An overview of wearable and non-wearable systems, highlighting clinical applications. *Sensors*, 14(2), 3362–3394.

Myklebust, H., Gloersen, O., & Hallen, J. (2015). Validity of ski skating center-of-mass displacement measured by a single inertial measurement unit. *Journal of Applied Biomechanics*, 31(6), 492–498.

Myklebust, H., Losnegard, T., & Hallen, J. (2014). Differences in v1 and v2 ski skating techniques described by accelerometers. *Scandinavian Journal of Medicine & Science in Sports*, 24(6), 882–893.

Nayak, R., Jain, L. C., & Ting, B. (2001). Artificial neural networks in biomedical engineering: A review. In S. Valliappan & N. Khalili (Eds.), *Computational Mechanics* (pp. 887–892). Amsterdam and Oxford: Elsevier Science.

Neogi, T., Felson, D., Niu, J., Nevitt, M., Lewis, C. E., Aliabadi, P., Sack, B., Torner, J., Bradley, L., & Zhang, Y. (2009). Association between radiographic features of knee osteoarthritis and pain: results from two cohort studies. *BMJ*, 339, b2844.

Neptune, R. R., Wright, I. C., & van den Bogert, A. J. (1999). Muscle coordination and function during cutting movements. *Medicine & Science in Sports & Exercise*, 31(2), 294–302.

Neville, J., Wixted, A., Rowlands, D., & James, D. (2010). Accelerometers: An underutilized resource in sports monitoring. *6th International Conference on Intelligent Sensors, Sensor Networks and Information Processing (ISSNIP) (2010) Brisbane*, (pp. 287–290).

Nigg, B. M. & Herzog, W. (2007). *Biomechanics of the musculo-skeletal system*. Chichester: Wiley, third edition.

Nilsson, J., Tveit, P., & Eikrehagen, O. (2004). Effects of speed on temporal patterns in classical style and freestyle cross-country skiing. *Sports Biomechanics*, 3(1), 85–107.

Obermeyer, Z. & Emanuel, E. J. (2016). Predicting the future — big data, machine learning, and clinical medicine. *The New England Journal of Medicine*, 375(13), 1216–1219.

Oh, S. E., Choi, A., & Mun, J. H. (2013). Prediction of ground reaction forces during gait based on kinematics and a neural network model. *Journal of Biomechanics*, 46(14), 2372–2380.

Patel, S., Park, H., Bonato, P., Chan, L., & Rodgers, M. (2012). A review of wearable sensors and systems with application in rehabilitation. *Journal of NeuroEngineering and Rehabilitation*, 9(1), 1–17.

Pearsall, D., Turcotte, R., Lefebvre, R., Bateni, H., Nicolaou, M., Montgomery, D., & Chang, R. (2001). Kinematics of the foot and ankle in forward ice hockey skating. *Proceedings of the 19th International Symposium on Biomechanics in Sports (ISBS) (2001) San Francisco*, (pp. 78–81).

Pearsall, D., Turcotte, R., & Murphy, S. D. (2000). Biomechanics of ice hockey. *Exercise and Sport Science*, (pp. 675–692).

Phinyomark, A., Petri, G., Ibáñez-Marcelo, E., Osis, S. T., & Ferber, R. (2018). Analysis of big data in gait biomechanics: Current trends and future directions. *Journal of Medical and Biological Engineering*, 38(2).

Purcell, B., Channells, J., James, D., & Barrett, R. (2005). Use of accelerometers for detecting foot-ground contact time during running. *Proceedings of SPIE (2005)*, 6036, 603615.

Rampp, A., Barth, J., Schulein, S., Gassmann, K.-G., Klucken, J., & Eskofier, B. M. (2015). Inertial sensor-based stride parameter calculation from gait sequences in geriatric patients. *IEEE Transactions on Biomedical Engineering*, 62(4), 1089–1097.

Rebala, G., Ravi, A., & Churiwala, S. (2019). *An Introduction to Machine Learning*. Springer International Publishing.

Reeves, N. D. & Bowling, F. L. (2011). Conservative biomechanical strategies for knee osteoarthritis. *Nature Reviews Rheumatology*, 7(2), 113–122.

Ren, L., Jones, R. K., & Howard, D. (2008). Whole body inverse dynamics over a complete gait cycle based only on measured kinematics. *Journal of Biomechanics*, 41(12), 2750–2759.

Renaud, P. J., Robbins, S. M. K., Dixon, P. C., Shell, J. R., Turcotte, R. A., & Pearsall, D. J. (2017). Ice hockey skate starts: a comparison of high and low calibre skaters. *Sports Engineering*, 20(4), 255–266.

Richards, R., van den Noort, J. C., Dekker, J., & Harlaar, J. (2017). Gait retraining with real-time biofeedback to reduce knee adduction moment: Systematic review of effects and methods used. *Archives of Physical Medicine and Rehabilitation*, 98(1), 137–150.

Robertson, D. G. (2014). Body segment parameters. In D. G. Robertson, G. E. Caldwell, J. Hamill, G. Kamen, & S. N. Whittlesey (Eds.), *Research Methods in Biomechanics* (pp. 63–78). Champaign, IL: Human Kinetics.

Roetenberg, D., Luinge, H., & Slycke, P. J. (2009). Xsens mvn : Full 6 dof human motion tracking using miniature inertial sensors. *Xsens Motion Technologies BV, Tech. Rep.*, 1, 1–7.

Rowlands, A. V., Mirkes, E. M., Yates, T., Clemes, S., Davies, M. J., Khunti, K., & Edwardson, C. L. (2017). Accelerometer-assessed physical activity in epidemiology: Are monitors equivalent? *Medicine & Science in Sports & Exercise*, 50, 257–265.

Rozumalski, A. & Schwartz, M. H. (2009). Crouch gait patterns defined using k-means cluster analysis are related to underlying clinical pathology. *Gait & Posture*, 30(2), 155–160.

Salarian, A., Russmann, H., Vingerhoets, F. J. G., Dehollain, C., Blanc, Y., Burkhard, P. R., & Aminian, K. (2004). Gait assessment in parkinson's disease: toward an ambulatory system for long-term monitoring. *IEEE Transactions on Biomedical Engineering*, 51(8), 1434–1443.

Sarzi-Puttini, P., Cimmino, M. A., Scarpa, R., Caporali, R., Parazzini, F., Zaninelli, A., Atzeni, F., & Canesi, B. (2005). Osteoarthritis: an overview of the disease and its treatment strategies. *Seminars in Arthritis and Rheumatism*, 35(1 Suppl 1), 1–10.

Schmidt, M., Wille, S., Rheinländer, C., Wehn, N., & Jaitner, T. (2017). A wearable flexible sensor network platform for the analysis of different sport movements. *International Conference on Applied Human Factors and Ergonomics, Los Angeles, USA*, 608, 3–14.

Schmidt, R. A. & Lee, T. D. (2011). *Motor control and learning: A behavioral emphasis*. Champaign, Ill.: Human Kinetics, fifth edition.

Schöllhorn, W. I. (2004). Applications of artificial neural nets in clinical biomechanics. *Clinical Biomechanics*, 19(9), 876–898.

Seel, T., Raisch, J., & Schauer, T. (2014). Imu-based joint angle measurement for gait analysis. *Sensors*, 14(4), 6891–6909.

Sell, T. C., Ferris, C. M., Abt, J. P., Tsai, Y.-S., Myers, J. B., Fu, F. H., & Lephart, S. M. (2006). The effect of direction and reaction on the neuromuscular and biomechanical characteristics of the knee during tasks that simulate the noncontact anterior cruciate ligament injury mechanism. *The American Journal of Sports Medicine*, 34(1), 43–54.

Shahabpoor, E. & Pavic, A. (2018). Estimation of vertical walking ground reaction force in real-life environments using single imu sensor. *Journal of Biomechanics*, 79, 181–190.

Sharma, L., Hurwitz, D. E., Thonar, E. J., Sum, J. A., Lenz, M. E., Dunlop, D. D., Schnitzer, T. J., Kirwan-Mellis, G., & Andriacchi, T. P. (1998). Knee adduction moment, serum hyaluronan level, and disease severity in medial tibiofemoral osteoarthritis. *Arthritis and Rheumatism*, 41(7), 1233–1240.

Shaw, K. E., Charlton, J. M., Perry, C. K. L., de Vries, C. M., Redekopp, M. J., White, J. A., & Hunt, M. A. (2018). The effects of shoe-worn insoles on gait biomechanics in people with knee osteoarthritis: a systematic review and meta-analysis. *British Journal of Sports Medicine*, 52(4), 238–253.

Shelburne, K. B., Torry, M. R., & Pandy, M. G. (2006). Contributions of muscles, ligaments, and the ground–reaction force to tibiofemoral joint loading during normal gait. *Journal of Orthopaedic Research*, 24(10), 1983–1990.

Shull, P. B., Jirattigalachote, W., Hunt, M. A., Cutkosky, M. R., & Delp, S. L. (2014). Quantified self and human movement: a review on the clinical impact of wearable sensing and feedback for gait analysis and intervention. *Gait & Posture*, 40(1), 11–19.

Sivakumar, S., Gopalai, A. A., Gouwanda, D., & Hann, L. K. (2016). Ann for gait estimations: A review on current trends and future applications. *IEEE-EMBS Conferences on Biomedical Engineering and Sciences, 4-8 December 2016, Kuala Lumpur*, (pp. 311–316).

Stetter, B. J., Buckeridge, E., Nigg, S. R., Sell, S., & Stein, T. (2019a). Towards a wearable monitoring tool for in-field ice hockey skating performance analysis. *European Journal of Sport Science*, 19(7), 893–901.

Stetter, B. J., Buckeridge, E., von Tscharner, V., Nigg, S. R., & Nigg, B. M. (2016). A novel approach to determine strides, ice contact, and swing phases during ice hockey skating using a single accelerometer. *Journal of Applied Biomechanics*, 32(1), 101–106.

Stetter, B. J., Krafft, F. C., Ringhof, S., Stein, T., & Sell, S. (2020). A machine learning and wearable sensor based approach to estimate external knee flexion and adduction moments during various locomotion tasks. *Frontiers in Bioengineering and Biotechnology*, 8, 9.

Stetter, B. J., Ringhof, S., Krafft, F. C., Sell, S., & Stein, T. (2019b). Estimation of knee joint forces in sport movements using wearable sensors and machine learning. *Sensors*, 19(17).

Stidwill, T. J., Turcotte, R. A., Dixon, P., & Pearsall, D. J. (2009). Force transducer system for measurement of ice hockey skating force. *Sports Engineering*, 12(2), 63–68.

Stidwill, T. J., Turcotte, R. A., Dixon, P., & Pearsall, D. J. (2010). Force transducer system for measurement of ice hockey skating force. *Sports Engineering*, 12(2), 63–68.

Stief, F., Kleindienst, F. I., Wiemeyer, J., Wedel, F., Campe, S., & Krabbe, B. (2008). Inverse dynamic analysis of the lower extremities during nordic walking, walking, and running. *Journal of Applied Biomechanics*, 24(4), 351–359.

Strohrmann, C., Harms, H., Kappeler-Setz, C., & Troster, G. (2012). Monitoring kinematic changes with fatigue in running using body-worn sensors. *IEEE Transactions on Information Technology in Biomedicine*, 16(5), 983–990.

Tao, W., Liu, T., Zheng, R., & Feng, H. (2012). Gait analysis using wearable sensors. *Sensors*, 12(2), 2255–2283.

Taunton, J. E., Ryan, M. B., Clement, D. B., McKenzie, D. C., Lloyd-Smith, D. R., & Zumbo, B. D. (2002). A retrospective case-control analysis of 2002 running injuries. *British Journal of Sports Medicine*, 36(2), 95–101.

Taylor, R. (1990). Interpretation of the correlation coefficient: A basic review. *Journal of Diagnostic Medical Sonography*, 6(1), 35–39.

Teng, H.-L., MacLeod, T. D., Link, T. M., Majumdar, S., & Souza, R. B. (2015). Higher knee flexion moment during the second half of the stance phase of gait is associated with the progression of osteoarthritis of the patellofemoral joint on magnetic resonance imaging. *The Journal of Orthopaedic and Sports Physical Therapy*, 45(9), 656–664.

Umberger, B. R. & Caldwell, G. E. (2014). Musculoskeletal modeling. In D. G. Robertson, G. E. Caldwell, J. Hamill, G. Kamen, & S. N. Whittlesey (Eds.), *Research Methods in Biomechanics* (pp. 247–276). Champaign, IL: Human Kinetics.

Upjohn, T., Turcotte, R., Pearsall, D. J., & Loh, J. (2008). Three-dimensional kinematics of the lower limbs during forward ice hockey skating. *Sports Biomechanics*, 7(2), 206–221.

van den Noort, J., van der Esch, M., Steultjens, M. P., Dekker, J., Schepers, M., Veltink, P. H., & Harlaar, J. (2011). Influence of the instrumented force shoe on gait pattern in patients with osteoarthritis of the knee. *Medical & Biological Engineering & Computing*, 49(12), 1381–1392.

van den Noort, J. J., van der Esch, M., Steultjens, M. P. M., Dekker, J., Schepers, M. H. M., Veltink, P. H., & Harlaar, J. (2013). Ambulatory measurement of the knee adduction moment in patients with osteoarthritis of the knee. *Journal of Biomechanics*, 46(1), 43–49.

van der Kruk, E., Schwab, A. L., van der Helm, F., & Veeger, H. (2016). Getting the angles straight in speed skating: A validation study on an imu filter design to measure the lean angle of the skate on the straights. *Procedia Engineering*, 147, 590–595.

Vanrenterghem, J., Nedergaard, N. J., Robinson, M. A., & Drust, B. (2017). Training load monitoring in team sports: A novel framework separating physiological and biomechanical load-adaptation pathways. *Sports Medicine*, 47(11), 2135–2142.

Verheul, J., Nedergaard, N. J., Vanrenterghem, J., & Robinson, M. A. (2020). Measuring biomechanical loads in team sports – from lab to field. *Science and Medicine in Football*, 2, 1–7.

Verlaan, L., Bolink, S A A N, van Laarhoven, S. N., Lipperts, M., Heyligers, I. C., Grimm, B., & Senden, R. (2015). Accelerometer-based physical activity monitoring in patients with knee osteoarthritis: Objective and ambulatory assessment of actual physical activity during daily life circumstances. *The Open Biomedical Engineering Journal*, 9, 157–163.

von Tscharner, V. (2000). Intensity analysis in time-frequency space of surface myoelectric signals by wavelets of specified resolution. *Journal of Electromyography and Kinesiology*, 10(6), 433–445.

Walter, J. P., D'Lima, D. D., Colwell, JR, C. W., & Fregly, B. J. (2010). Decreased knee adduction moment does not guarantee decreased medial contact force during gait. *Journal of Orthopaedic Research*, 28(10), 1348–1354.

Wang, S. & Summers, R. M. (2012). Machine learning and radiology. *Medical Image Analysis*, 16(5), 933–951.

Weiss, K. & Whatman, C. (2015). Biomechanics associated with patellofemoral pain and acl injuries in sports. *Sports Medicine*, 45(9), 1325–1337.

Whittle, M. W. (1996). Clinical gait analysis: A review. *Human Movement Science*, 15(3), 369–387.

Whittlesey, S. & Robertson, D. (2014). Two-dimentional inverse dynamics. In D. G. Robertson, G. E. Caldwell, J. Hamill, G. Kamen, & S. N. Whittlesey (Eds.), *Research Methods in Biomechanics* (pp. 103–123). Champaign, IL: Human Kinetics.

Willwacher, S., Funken, J., Heinrich, K., Muller, R., Hobara, H., Grabowski, A. M., Bruggemann, G.-P., & Potthast, W. (2017). Elite long jumpers with below the knee prostheses approach the board slower, but take-off more effectively than non-amputee athletes. *Scientific Reports*, 7(1), 16058.

Wixted, A. J., Thiel, D. V., Hahn, A. G., Gore, C. J., Pyne, D. B., & James, D. A. (2007). Measurement of energy expenditure in elite athletes using mems-based triaxial accelerometers. *IEEE Sensors Journal*, 7(4), 481–488.

Wong, C., Zhang, Z., Lo, B. P. L., & Yang, G.-Z. (2015). Wearable sensing for solid biomechanics. *IEEE Sensors Journal*, 15(5), 2747–2760.

Wouda, F. J., Giuberti, M., Bellusci, G., Maartens, E., Reenalda, J., van Beijnum, B.-J. F., & Veltink, P. H. (2018). Estimation of vertical ground reaction forces and sagittal knee kinematics during running using three inertial sensors. *Frontiers in Physiology*, 9, 218.

Yang, C.-C. & Hsu, Y.-L. (2010). A review of accelerometry-based wearable motion detectors for physical activity monitoring. *Sensors*, 10(8), 7772–7788.

Yang, E. C.-Y. & Mao, M.-H. (2015). 3d analysis system for estimating intersegmental forces and moments exerted on human lower limbs during walking motion. *Measurement*, 73, 171–179.

Zajac, F. E., Neptune, R. R., & Kautz, S. A. (2002). Biomechanics and muscle coordination of human walking: Part i: Introduction to concepts, power transfer, dynamics and simulations. *Gait & Posture*, 16(3), 215–232.

Zernicke, R. & Whiting, W. C. (2000). Mechanisms of musculoskeletal injury. In V. M. Zaciorskij (Ed.), *Biomechanics in Sport* (pp. 507–522). Oxford: Blackwell Science Ltd.

Supplementary material

S1: Knee joint forces (KJF) time series of all movements.

r = Pearson's correlation coefficient; *rRMSE* = relative Root Mean Squared Errror; mean (standard deviation)

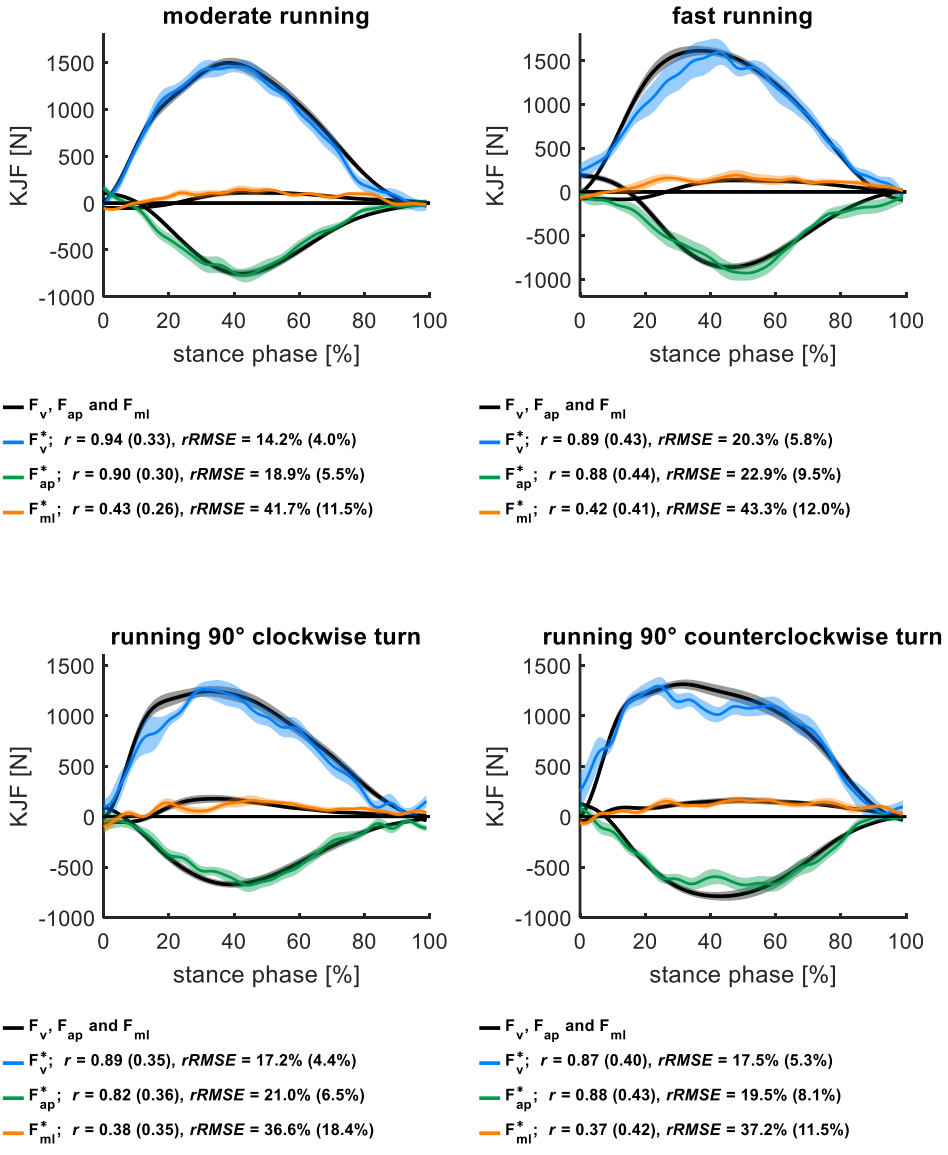

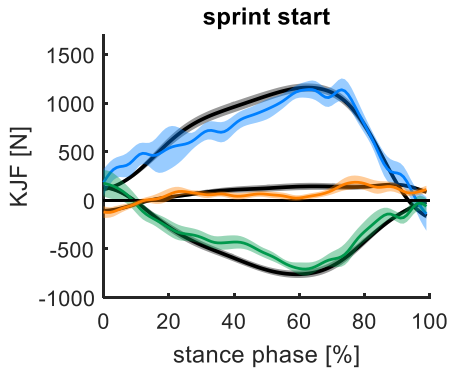

F_v, F_{ap} and F_{ml}
F^*_v; r = 0.73 (0.45), *rRMSE* = 25.9% (8.8%)
F^*_{ap}; r = 0.76 (0.40), *rRMSE* = 25.8% (9.3%)
F^*_{ml}; r = 0.31 (0.29), *rRMSE* = 43.3% (10.0%)

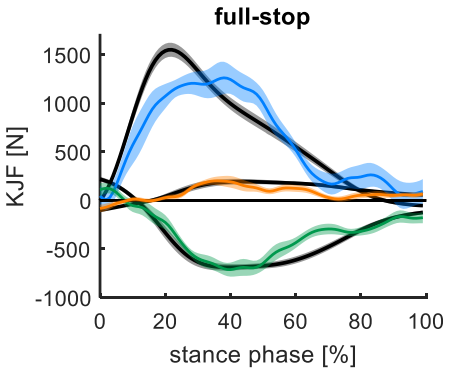

F_v, F_{ap} and F_{ml}
F^*_v; r = 0.78 (0.45), *rRMSE* = 24.7% (7.2%)
F^*_{ap}; r = 0.80 (0.34), *rRMSE* = 21.8% (7.5%)
F^*_{ml}; r = 0.45 (0.29), *rRMSE* = 37.7% (9.0%)

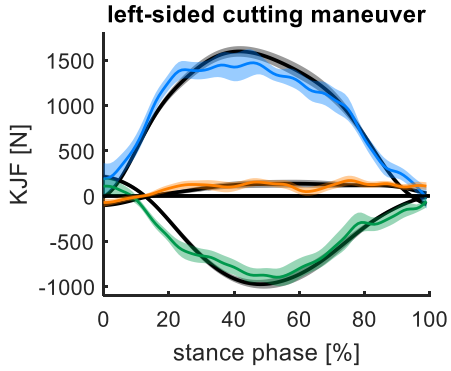

F_v, F_{ap} and F_{ml}
F^*_v; r = 0.86 (0.44), *rRMSE* = 19.4% (6.6%)
F^*_{ap}; r = 0.86 (0.41), *rRMSE* = 22.0% (7.3%)
F^*_{ml}; r = 0.30 (0.42), *rRMSE* = 44.8% (13.0%)

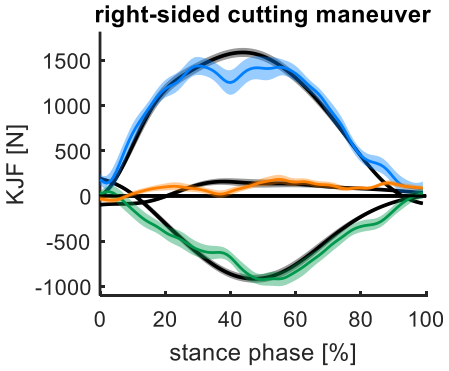

F_v, F_{ap} and F_{ml}
F^*_v; r = 0.86 (0.39), *rRMSE* = 19.0% (5.4%)
F^*_{ap}; r = 0.84 (0.35), *rRMSE* = 21.4% (5.2%)
F^*_{ml}; r = 0.25 (0.39), *rRMSE* = 45.7% (9.0%)

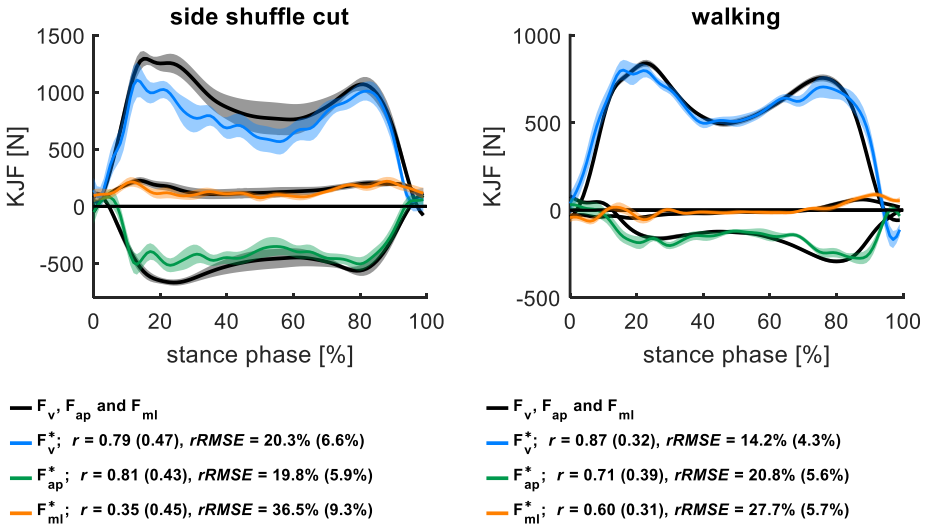
side shuffle cut
KJF [N]
stance phase [%]
F_v, F_{ap} and F_{ml}
F^*_v; r = 0.79 (0.47), rRMSE = 20.3% (6.6%)
F^*_{ap}; r = 0.81 (0.43), rRMSE = 19.8% (5.9%)
F^*_{ml}; r = 0.35 (0.45), rRMSE = 36.5% (9.3%)
walking
KJF [N]
stance phase [%]
F_v, F_{ap} and F_{ml}
F^*_v; r = 0.87 (0.32), rRMSE = 14.2% (4.3%)
F^*_{ap}; r = 0.71 (0.39), rRMSE = 20.8% (5.6%)
F^*_{ml}; r = 0.60 (0.31), rRMSE = 27.7% (5.7%)
walking 90° clockwise turn
KJF [N]
stance phase [%]
F_v, F_{ap} and F_{ml}
F^*_v; r = 0.81 (0.27), rRMSE = 16.9% (4.5%)
F^*_{ap}; r = 0.65 (0.31), rRMSE = 23.0% (6.2%)
F^*_{ml}; r = 0.31 (0.20), rRMSE = 34.1% (8.1%)
walking 90° counterclockwise turn
KJF [N]
stance phase [%]
F_v, F_{ap} and F_{ml}
F^*_v; r = 0.83 (0.29), rRMSE = 15.3% (4.0%)
F^*_{ap}; r = 0.64 (0.30), rRMSE = 22.7% (5.8%)
F^*_{ml}; r = 0.48 (0.34), rRMSE = 29.1% (6.0%)

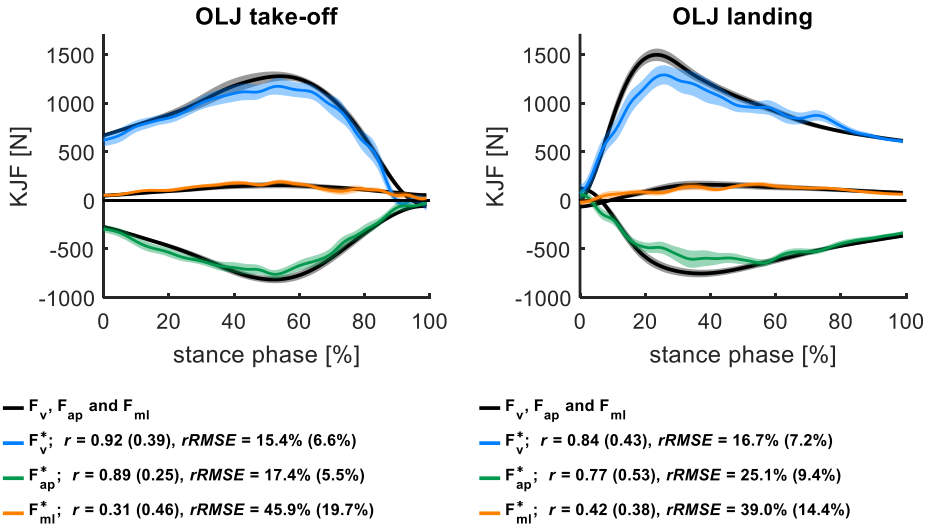
OLJ take-off
KJF [N]
stance phase [%]
F_v, F_{ap} and F_{ml}
F^*_v; r = 0.92 (0.39), rRMSE = 15.4% (6.6%)
F^*_{ap}; r = 0.89 (0.25), rRMSE = 17.4% (5.5%)
F^*_{ml}; r = 0.31 (0.46), rRMSE = 45.9% (19.7%)
OLJ landing
KJF [N]
stance phase [%]
F_v, F_{ap} and F_{ml}
F^*_v; r = 0.84 (0.43), rRMSE = 16.7% (7.2%)
F^*_{ap}; r = 0.77 (0.53), rRMSE = 25.1% (9.4%)
F^*_{ml}; r = 0.42 (0.38), rRMSE = 39.0% (14.4%)

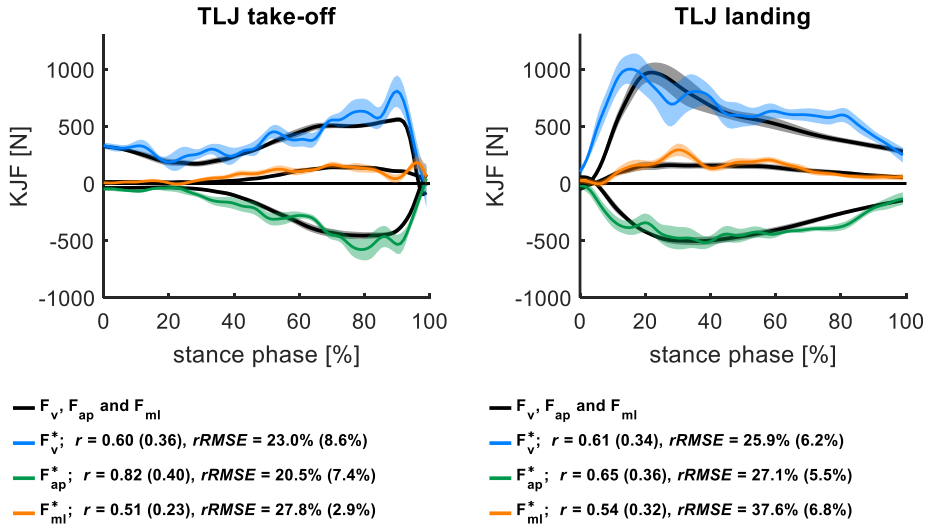
TLJ take-off
KJF [N]
stance phase [%]
F_v, F_{ap} and F_{ml}
F^*_v; r = 0.60 (0.36), rRMSE = 23.0% (8.6%)
F^*_{ap}; r = 0.82 (0.40), rRMSE = 20.5% (7.4%)
F^*_{ml}; r = 0.51 (0.23), rRMSE = 27.8% (2.9%)
TLJ landing
KJF [N]
stance phase [%]
F_v, F_{ap} and F_{ml}
F^*_v; r = 0.61 (0.34), rRMSE = 25.9% (6.2%)
F^*_{ap}; r = 0.65 (0.36), rRMSE = 27.1% (5.5%)
F^*_{ml}; r = 0.54 (0.32), rRMSE = 37.6% (6.8%)

Statutory declaration

Hiermit erkläre ich, dass ich die vorliegende Dissertation mit dem Titel

' Wearable Sensors and Machine Learning based Human Movement Analysis – Applications in Sports and Medicine – '

selbständig angefertigt habe und keine anderen als die angegebenen Hilfsmittel benutzt sowie die wörtlich oder inhaltlich übernommenen Stellen als solche kenntlich gemacht und die Satzung des Karlsruher Instituts für Technologie (KIT) zur Sicherung guter wissenschaftlicher Praxis beachtet habe. Diese Arbeit wurde nicht bereits anderweitig als Prüfungsarbeit verwendet.

Karlsruhe, 01. Juli 2020 _____